Charles University

Faculty of Science

Study programme: Cell and Developmental Biology

Branch of study: Cell Physiology

Bc. Květa Trávníčková

Mechanism of regulation of EGF receptor ligand activation via the intramembrane pseudoprotease iRhom and cell surface metalloprotease ADAM17

Mechanismus regulace aktivace ligandů EGF receptoru prostřednictvím intramembránové pseudoproteasy iRhom a metaloproteasy ADAM17

Diploma thesis

Supervisor: Ing. Kvido Stříšovský, PhD.

Prague, 2019

Prohlášení

Prohlašuji, že jsem závěrečnou práci zpracovala samostatně a že jsem uvedla všechny použité informační zdroje a literaturu. Tato práce ani podstatná její část nebyla předložena k získání jiného nebo stejného akademického titulu.

V Praze, 12.8.2019

Podpis

Acknowledgements/Poděkování

In the first place, I would like to thank my supervisor Kvido, who gave me the opportunity to complete my diploma project in his lab. It was his ethusiasm and fruitful discussions we had about the results, that stimulated my experimental effort. I am eternally grateful for the almost endless patience he had with me when I was stumbling over obstacles that I had unconsciously laid in front of my feet. Kvido, I apologise for completing the thesis at the last minute and for any sleepless night you had due to the unusual pace of my work!

In the second first place I would like to thank Blanka Collis, a colleague of mine equally engulfed by the mysterious beauty of iRhoms, for her ceaseless support and valuable advice about both the experimental and the theoretical part of the work. She was the key person who witnessed all my successes along with all my unsuccessful experiments, always ready to share my joy or to comfort my broken heart. And last but not least I owe her immense thanks for the language corrections!

My special thanks belong to Nick Johnson under whose supervision I could start diving into the excitements of laboratory work and who during my bachelor studies laid down the basis on which I could build up the practical realisation of my diploma project. I also appreciate he provided me with the DNA constructs I needed, and I am very grateful for his language corrections.

My many thanks belong to all my other colleagues from the lab who supported me across the stages of the thesis completion and did not hesitate to give me a helping hand when they found me in trouble. Namely: Anežka Tichá, without whom I would probably never ever have started writing; o;ur technitian Petra Rampírová for her help with cloning and her words of encouragement; Šárka Boháčová for her kind multilateral support; Kubo Began for the introduction into the work with the LI-COR software; Jan Šugar for his first-class 12% gels; Edita Poláchová, Lucka Polovinkin, Monika Fliegl and Markéta Bařinková for their encouragement; and last but not least Jano Kuzmík for sharing with me the burden of the thesis completion (a shared burden, half the burden…).

Very special thanks also belong to Michal Svoboda for help with my preliminary proteasome inhibition experiments as well as for original suggestions about possible future directions of the work.

I would also like to acknowledge Miguel Cavadas from the laboratory of Colin Adrain in Lisbon for providing me with the double knock-out HEKs.

Mé vřelé díky náležejí také dvěma lidem, bez jejichž podpory bych se při psaní diplomové práce, ale i v životě vůbec, neobešla: mámě a tátovi. Dále také všem mým přátelům, kteří mne bez ustání povzbuzovali a všemožně mne ubezpečovali o tom, že na tu dřinu nejsem sama.

Abstract

Signalling through the EGF receptor is subject to a complex and multilayered regulation. One such mode of regulation is through control of ligand production which plays an important role in fine-tuning EGF receptor activation. In mammals, the production of soluble, biologically active forms of EGF receptor ligands relies on ADAM metalloproteases, predominantly ADAM10 and ADAM17. Recently, a pseudoprotease from the rhomboid-like family of intramembrane proteases, iRhom, emerged as a key positive regulator of ADAM17. However, Drosophila iRhom has also been implicated in the negative regulation of EGF receptor signalling by promoting the degradation of precursors of its ligands. Cell culture based assays suggest that mammalian iRhoms might also be involved in a similar process. In this thesis, the effect of mammalian iRhom overexpression on the levels of EGF receptor ligands has been investigated. Contrary to previous findings, the data presented in this thesis suggest that the observed effect might not be entirely iRhom specific, for the inactive mutants of rhomboid proteases also diminish the levels of EGF receptor ligands. Nor do we find the effect to be specific to EGF receptor ligands, as unrelated transmembrane proteins were also depleted by iRhom overexpression. The coexpression of ADAM17 was able to prevent the depletion of EGF receptor ligands by iRhom overexpression but only in HEK cells lacking endogenous iRhom protein. The loss of EGF receptor ligands does not appear to be caused by canonical degradation pathways, for neither lysosomal nor ERAD pathway inhibitors reversed the effect of iRhom overexpression.

Key words: regulation of EGF receptor signalling, iRhom, ADAM17, quantitative immunoblotting

Abstrakt

Signalisace skrz receptor pro epidermální růstový faktor (EGF receptor, EGFR) podléhá propracované a mnohovrstevné regulaci. Jedním ze způsobů vylaďování signalisace zprostředkované tímto receptorem je kontrola produkce jeho ligandů. U savců za uvolňování solubilních, biologicky aktivních forem ligandů EGF receptoru zodpovídají především metaloproteasy ADAM10 a ADAM17. Pseudoprotease iRhom z rodiny rhomboid-like proteinů byla nedávno připsána úloha klíčového positivního regulátora ADAM17. U drosofily však je iRhom spjat s negativní regulací EGF receptoru, a to prostřednictvím degradace prekursorů jeho ligandů. Experimenty prováděné v savčích buněčných kulturách ovšem naznačují, že podobná funkce by mohla být zachována i u savčích iRhomů. V této diplomové práci byl studován vliv overexprese iRhomu na expresní úroveň ligandů EGF receptoru. Na rozdíl od dřívějších publikací však nebylo potvrzeno, že by pozorovaný efekt bylo možno vysvětlit výlučně přítomností iRhomu, neboť neaktivní mutanti rhomboidních proteas jej působili rovněž. Také nebylo prokázáno, že by iRhom takto ovlivňoval pouze ligandy EGF receptoru – strukturně podobné, avšak ligandům EGF receptoru nepříbuzné proteiny v přítomnosti iRhomu taktéž podléhaly depleci. Koexprese ADAM17 mizení ligandů EGF receptoru zamezila, avšak pouze v buněčné linii bez endogenního iRhomu. Jelikož negativní dopad overexprese iRhomu na množství ligandů EGF receptoru nezvrátila ani inhibice lysosomů ani inhibice ERAD dráhy, je možno spekulovat, že za tímto fenoménem stojí zvýšená degradace klientských proteinů iRhomu prostřednictvím nekanonické dráhy.

Klíčová slova: regulace signalisace skrz EGF receptor, iRhom, ADAM17, kvantitativní immunoblotting

Table of contents

Abbreviations

ADAM = a disintegrin and metalloprotease
ADAM10 = ADAM metallopeptidase domain 10, a. k. a. RAK; kuz; AD10; AD18; MADM; CD156c; CDw156
ADAM17 = ADAM metallopeptidase domain 17, a. k. a. CSVP; TACE; NISBD; ADAM18; CD156B; NISBD1
APS = ammonium persulfate
AREG = amphiregulin
BCAM = basal cell adhesion molecule, a. k. a. AU; LU; CD239; MSK19
BSG = basigin, a. k. a. 5F7; CD147; EMMPRIN; EMPRIN; OK; SLC7A11; TCSF
BTC = betacellulin
CANDIS = Conserved Adam seventeeN Dynamic Interaction Sequence
c-Fos = transcriptional regulator Fos, a. k. a. p55; AP-1; C-FOS
c-Jun = transcriptional regulator, a. k. a. AP1; p39; AP-1; cJUN
c-Myc = transcriptional regulator Myc
COS7 = CV-1 in Origin with SV40 genes cells
cub = "curly bare"
DKO = double knock-out
DKO HEKs = HEK cells with iRhom1 and 2 knocked out
DMEM = Dulbecco's Modified Eagle's Medium
EGAD = endosome and Golgi-associated degradation
EGF = epidermal growth factor
EGFR = epidermal growth factor receptor
EPGN = epigen (epithelial mitogen)
ER = endoplasmic reticulum
ERAD = endoplasmic reticulum-associated degradation
EREG = epiregulin
ERK = extracellular regulated MAP kinase
FBS = fetal bovine serum
FGF = fibroblast growth factor
FGFR = fibroblast growth factor receptor
FRMD8 = FERM domain containing 8, a. k. a. FKSG44; iTAP
GA = Golgi apparatus
GPCR = G protein-coupled receptor
Grb2 = growth factor receptor bound protein 2, a. k. a. ASH; Grb3-3; MST084; NCKAP2; MSTP084
HEK = human embryonic kidney cells
ICAM-1 = intercellular adhesion molecule, a. k. a. BB2; CD54; P3.58
IL-6 = interleukin 6
IL-6R = receptor for interleukin 6
iNOS = inducible nitric oxide synthase
IRF3 = interferon regulatory factor 3, a. k. a. IIAE7
IRHD = iRhom homology domain
iRhom = inactive Rhomboid-like protein
Jak = Janus kinase
JNK = c-Jun N-terminal kinase
KO = knock-out
LiDS = lithium dodecyl sulfate
LIN-3 = ligand of *C. elegans* EGFR
MARCH5 = membrane-associated ring finger 5, a. k. a. MARCH-V; MITOL; Marchv; Rnf153
mEFs = mouse embryonic fibroblasts
M-CSFR = macrophage colony stimulating factor receptor

NP-40 = nonyl phenoxypolyethoxylethanol
p38 = mitogen-activated protein kinase 14, a. k. a. PRKM14; RK; CSBP; EXIP; Mxi2; PRKM15; SAPK2A
PBS = phosphate buffered saline
PDI = protein disulphide isomerase
PKB = protein kinase B, a. k. a. Akt; CWS6; PRKBA; RAC; RAC-ALPHA
PKC = protein kinase C
PKG = protein kinase G
PLK-2 = Polo-like kinase 2
PNGase = peptide:N-glycosidase
qPCR = quantitative PCR
RNF5 = ring finger protein 5, a. k. a. RING5; RMA1
ROM-1 = retinal outer segment membrane protein 1, a. k. a. ROM; RP7; ROSP1; TSPAN23
RSK6 = ribosomal protein S6 kinase
SDS = sodium dodecyl sulfate
SDS-PAGE = sodium dodecyl sulfate-polyacrylamide gel electrophoresis
SFM = serum-free medium
Shc = SHC adaptor protein, a. k. a. SHCA
SPINT1 = serine peptidase inhibitor, Kunitz type 1, a. k. a. HAI, HAI1, MANSC2
STAT = signal transducer and activator of transcription
STING = transmembrane protein 173, a. k. a. TMEM173; ERIS; MITA; MPYS; SAVI; NET23; hMITA
TBK1 = TANK binding kinase 1, a. k. a. NAK; T2K; IIAE8; FTDALS4
TBS = Tris-buffered saline
TBS-T = Tris-buffered saline with Tween
TEMED = tetramethylethylenediamine
TGFα = transforming growth factor α
TGFβ = transforming growth factor β
TGFβR = receptor for transforming growth factor β
TMD = transmembrane domain
TNFR = receptor for tumour necrosis factor α
TNFα = tumour necrosis factor α
TOC = tylosis wih oesophageal cancer
TRAPβ = signal sequence receptor subunit 2, a. k. a. SSR2; TLAP; HSD25; TRAPB; TRAP-BETA
Tris = trisaminomethane
Ubac = Ubiquitin-associated domain-containing protein 2, a. k. a. PHGDHL1
Unc93B = unc-93 homolog B1, TLR signaling regulator, a. k. a. IIAE1; UNC93; UNC93B; Unc-93B1
Uncv = “uncovered“
UPR = unfolded protein response
VCP = valosin containing protein, a. k. a. p97; TERA; CDC48
VISA = mitochondrial antiviral signaling protein, a. k. a. MAVS; CARDIF; IPS-1; IPS1; VISA
WNT3 = Wnt family member 3, a. k. a. INT4; TETAMS
WT = wild type

1 Introduction

1.1 Epidermal growth factor receptor—a prelude

Every cell needs to sense its environment and respond to its changes. One of the possible ways of doing this is to "read" molecules in the cell's surroundings. Many of these molecules are not able to cross the plasma membrane, which is why a plethora of membrane-spanning proteins called receptors decorates the surface of every living cell. One such protein is the epidermal growth factor receptor (EGFR). It receives signals from the environment in the form of peptide molecules produced by other cells[1] and transduces the signal into the cytoplasm. Signalling cascades leading to increased cell proliferation, growth and migration can be activated by the EGFR (reviewed in Oda *et al.*, 2005). It is therefore no surprise that such an important receptor is subject to a complex, multilayered regulation (reviewed in Yarden and Sliwkowski, 2001; Citri and Yarden, 2006). This thesis aims to cast a bit more light on how the metalloprotease ADAM17 and the pseudoprotease iRhom2 contribute to the EGFR regulation network.

1.1.1 EGF receptor domain architecture

The EGF receptor is classified as a type I transmembrane protein, meaning that it has a signal peptide, its N-terminus is extracellular, and its C-terminus is oriented into the cytosol (Higy, Junne and Spiess, 2004). Apart from the signal peptide, the extracellular (or N-terminal) part of EGFR is formed by two leucine-rich and two cysteine-rich domains (**Figure 1.1A**; Ogiso *et al.*, 2002; Ferguson *et al.*, 2003). The transmembrane segment is followed by a tyrosine kinase domain and a C-terminal tail, which contains several phosphorylatable tyrosine residues (Ullrich *et al.*, 1984; Margolis *et al.*, 1989)

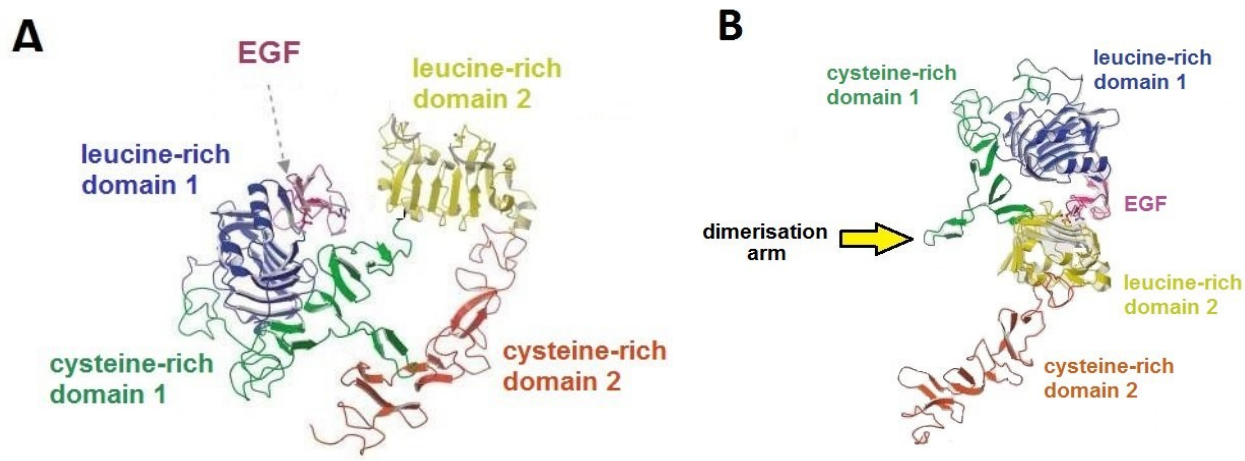

Figure 1.1: Structure of the extracellular part (ectodomain) of EGF receptor in the inactive (**A**) and the active (**B**) state. Adapted from Ferguson *et al.* 2003.

[1] Autocrine signalling, when the EGF receptor is activated by a molecule produced by the same cell as the one on whose surface it resides, can occur as well (Dong *et al.*, 1999).

1.1.2 Mechanism of EGF receptor activation

As mentioned in the previous paragraph, a tyrosine kinase domain is present in the cytosolic part of EGFR (Ullrich *et al.*, 1984). Therefore, the EGF receptor belongs to the group of receptor tyrosine kinases, together with other growth factor receptors such as insulin growth factor receptor I or fibroblast growth factor receptor (reviewed in Schlessinger, 2000). However, the process of EGF receptor activation differs slightly from other tyrosine kinases. Upon ligand binding, EGFR undergoes a conformational change leading to an extension of the "dimerisation arm" (**Figure 1.1B**). A ligand-preactivated receptor is then ready to bind another EGFR monomer with the extended dimerisation arm. The dimer of pre-activated EGF receptors then autophosphorylates the tyrosine residues in its C-terminal tail, leading to full activation of the receptor (Bertics and Gill, 1985).

The phosphorylated tyrosines in the EGFR cytosolic tail serve as docking sites for adaptor proteins such as Grb2 or Shc, which in turn recruit signal-transducing kinases, for example Ras, Raf and others (Schulze, Deng and Mann, 2005). EGF receptor activation is mainly associated with MAP kinase module signalling, however, the signal from EGFR ligands can also flow into other pro-proliferative and pro-survival pathways (*e. g.* PKB or Jak/STAT signalling; reviewed in Oda *et al.*, 2005). As a result, transcription factors, such as c-Myc, c-Jun or c-Fos, which have a large portfolio of target genes, are deinhibited or their production is enhanced (Alvarez *et al.*, 1991; De Cesare *et al.*, 1998). Hence the overall balance in the cell is tipped towards survival and/or proliferation and/or growth (Li, Liu and Cai, 2015). However, EGF receptor activation can also lead to cell differentiation or even contribute to proapoptotic signalling (Freeman, 1996; Jiang and Wu, 2014). The "context matters" principle therefore applies even in the case of signalling through the EGF receptor, precluding us from making too generalised conclusions.

1.1.3 Mechanisms of EGF receptor signalling regulation

Signalling through the EGF receptor is regulated at many levels: transcriptionally, by RNA splicing of the ligands and the receptors, by receptor localisation, by ligand production, by ligand binding, by receptor dimerisation[2], by cleavage of the extracellular part of the receptor, by phosphorylation of the tyrosine residues in the EGFR cytoplasmic tail and also through other signalling cascades (reviewed in Trávníčková, 2017). For this thesis, the regulation of EGFR signalling via the production of EGFR ligands is the most important one and will be introduced briefly in the following paragraphs. Since this thesis is focused on the regulation of mammalian EGFR signalling and most of the knowledge about this topic has been assessed in mouse or human tissue culture models, only human and murine EGFR ligands will be discussed in detail.

[2] This mechanism of regulation applies only in the organisms with more than one type of EGF receptor. For example, in humans, four EGF receptors with different affinities for the ligands are present and can form homo- and heterodimers with different signalling properties (Pinkas-Kramarski *et al.*, 1996; Tzahar *et al.*, 1996).

Almost all known EGF receptor ligands are synthesised in the form of transmembrane precursors (reviewed in Harris, Chung and Coffey, 2003). The biologically active, soluble forms of the ligands are produced by proteolytic cleavage on the plasma membrane or even in the late compartments of the secretory pathway (Lee *et al.*, 2001; Sahin *et al.*, 2004). In *Caenorhabditis elegans*, only one EGF receptor ligand, LIN-3, is present. Its membrane-tethered splicing variant LIN-3L is activated (cleaved off the membrane) by the rhomboid intramembrane protease ROM-1 (Dutt *et al.*, 2004). Rhomboid-mediated cleavage is responsible for EGF receptor ligand production even in *Drosophila melanogaster*, where three of the four known EGFR ligands, namely Spitz, Keren and Gurken, are synthesised as transmembrane precursors (Urban, Lee and Freeman, 2002). Interestingly, the rhomboid pseudoprotease iRhom has the opposite effect on EGFR signalling, for it targets the EGFR ligand precursors to a degradation pathway (Zettl *et al.*, 2011). However, vertebrate EGF receptor ligand production largely relies on a different class of proteases, the metalloproteases from the A Disinegrin And Metalloprotease family (ADAM; Sahin *et al.*, 2004; Sahin and Blobel, 2007). Interestingly, it has been reported that in addition to ADAM-mediated cleavage, some EGFR ligands are also processed by the rhomboid proteases (Adrain *et al.*, 2011). In addition, the rhomboid-like pseudoproteases iRhoms emerged as key regulators of ADAM17, one of the two major EGFR ligand producing enzymes in mice and humans. The association of the rhomboid-like family of proteins with the regulation of EGF receptor signalling across diverse taxa has captured attention of many scientists including the author of this thesis, who aims to contribute to further elucidation of this phenomenon.

In humans and mice, eleven EGFR ligands have been described to date: EGF, TGFα, heparin-binding EGF (HB-EGF), betacellulin (BTC), amphiregulin (AREG), epiregulin (EREG), neuregulin1-4 and epigen (EPGN) (reviewed in Singh and Coffey, 2014). They are all produced in the form of transmembrane precursors, except for some splice variants of neuregulins (Holmes *et al.*, 1992). Several ADAM metalloproteases are involved in the production of the soluble forms of EGFR ligands, a process also termed as “ectodomain shedding” (**Table 1.1**). However, only two key ADAM proteases are responsible for the majority of the EGFR ligand activation, namely ADAM10 and ADAM17 (reviewed in Weber and Saftig, 2012; Sahin *et al.*, 2004). These two proteases differ in their substrate specificity. ADAM17 is responsible for the shedding of TGFα, HB-EGF, AREG, EREG, EPGN and the neuregulins, whereas prominent ADAM10 substrates are EGF and BTC (**Table 1.1**; Sahin *et al.*, 2004; Sahin and Blobel, 2007).

Table 1.1: Ectodomains of EGF receptor ligand precursors are shed off by several ADAM metalloproteases. Adapted from Edwards, Handsley and Pennington, 2008.

ADAM9	HB-EGF, EGF
ADAM10	BTC, EGF
ADAM12	HB-EGF
ADAM15	AREG, HB-EGF
ADAM17	AREG, EREG, EPGN, HB-EGF, neuregulins, TGFα
ADAM19	Neuregulin-1

1.1.4 Diseases associated with EGF receptor dysregulation

EGF receptor dysregulation is implicated in many diseases, mainly those associated with altered cell proliferation or migration. Hyperactivation of EGF receptor signalling has been reported in a number of malignancies, including a plethora of tumours, but also in psoriasis (reviewed in Arteaga and Engelman, 2014; Mishra, Hanker and Garrett, 2017; Wang *et al.*, 2019). Certain cardiovascular disorders are linked to decreased neuregulin production, whereas its overproduction is associated with the development of schizophrenia (Silberberg *et al.*, 2006; Lemmens, Doggen and De Keulenaer, 2007; Banerjee *et al.*, 2010). The scrutiny of EGF receptor signalling regulation therefore represents a clinically relevant field.

1.2 ADAM17—a brief introduction

The metalloprotease ADAM17 belongs to the ADAM ("a disintegrin and metalloprotease") family of transmembrane proteins, widespread across metazoans (Wen, Metzstein and Greenwald, 1997; Huxley-Jones *et al.*, 2007). In spite of the family name, not all of its members possess proteolytic activity (Edwards, Handsley and Pennington, 2008). Those that lack the protease active site, as well as the active proteases, are involved in interactions with the extracellular matrix and cell surface molecules of neighbouring cells (reviewed in Arribas, Bech-Serra and Santiago-Josefat, 2006). Many proteolytically inactive ADAMs play a vital role during fertilisation (Yuan, Primakoff and Myles, 1997; Cho *et al.*, 1998). The active ADAM proteases, on the other hand, are crucial for successful development of an embryo (reviewed in Weber and Saftig, 2012). ADAM17 has a prominent position among the ADAM proteases for it is an enzyme central for cytokine and growth factor signalling (reviewed in Gooz, 2010). In my thesis, I will focus on the current knowledge about mammalian ADAM17, which has been studied mainly in murine models and human tissue cultures.

1.2.1 ADAM17 domain architecture

ADAM17 is a type I transmembrane protein, meaning that its C-terminus is oriented towards the cytoplasm (Black *et al.*, 1997). Like its relatives, ADAM17 shares their modular structure (**Figure 1.2**). At the very N-terminus of ADAM17, the ER-targeting signal peptide is followed by the prodomain, which ensures no premature activation of the protease domain will occur and also helps to fold the remainder of ADAM17 (Schlöndorff, Becherer and Blobel, 2000; Leonard, Lin and Milla, 2005). Next is the metalloprotease domain with a zinc cation in its active site, coordinated by three histidine residues (Bode, Gomis-Rüth and Stöckler, 1993). The polypeptide chain continues with a disintegrin-like domain, which can interact with cell surface molecules (*e. g.* integrins; Bax *et al.*, 2004; Huang, Bridges and White, 2005). C-terminal to the disintegrin domain is the membrane-proximal domain. It is also referred to as the cysteine-rich or the EGF-like domain, for two different domains, the cysteine-rich and the EGF-like domains, are found at this position in other ADAMs (Edwards, Handsley and Pennington, 2008; Düsterhoft *et al.*, 2013)[3]. The juxtamembrane part of ADAM17 forms a sequentially conserved motif termed CANDIS (Conserved Adam seventeeN Dynamic Interaction Sequence). As its name indicates, it is found solely in ADAM17 (Düsterhöft *et al.*, 2014). CANDIS has been suggested to play a role in substrate recognition and in the regulation of ADAM17 activity through binding to negatively charged phospholipids, namely phosphatidylserine, via the basic residues on one side of the amphipatic helix it forms (Düsterhöft *et al.*, 2015). The most C-terminal part of ADAM17

[3] The only exception is ADAM10, the closest relative of ADAM17, where the disintegrin-like domain is also folllowed by a single domain (Janes *et al.*, 2005; Seegar *et al.*, 2017). Thanks to this structural uniqueness, ADAM10 and 17 together represent a special subgroup of ADAM metalloproteases (Black and White, 1998; Düsterhöft *et al.*, 2014).

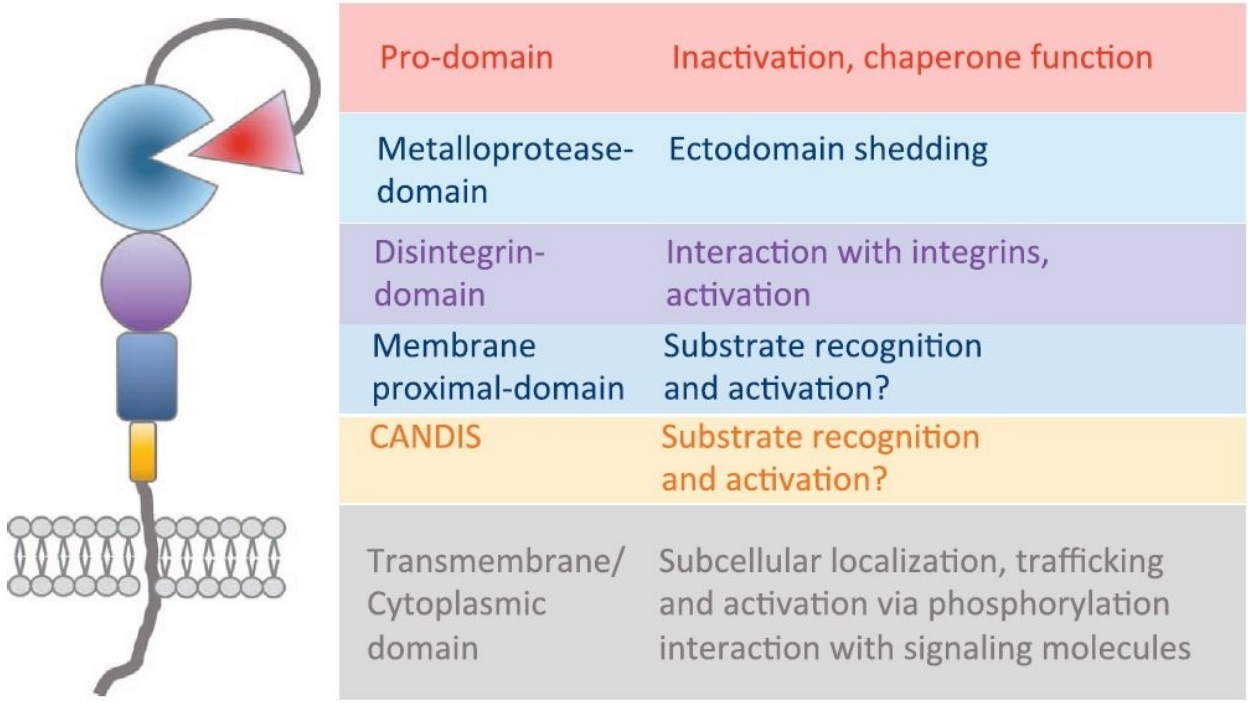

Figure 1.2: Schematic representation of ADAM17 modular structure. Adapted from Zunke *et al.,* 2017.

comprises the transmembrane domain, crucial for stimulated activity of the metalloprotease, and the cytosolic domain, important for ADAM17 dimerisation and probably also for regulation of its activity through phosphorylation (Xu and Derynck, 2010; Xu *et al.*, 2012).

To date, only the metalloprotease domain and the membrane-proximal domain structure has been solved (**Figure 1.3A,B**; Ingram *et al.*, 2006; Düsterhoft *et al.*, 2013). It therefore remains unclear how all of the ADAM17 domains are arranged with respect to each other. However, a general idea of how they are spatially arranged can be based on the structure of PII snake venom metalloproteases, enzymes with a domain architecture similar to that of the ADAMs (Kini and Evans, 1992; Takeda *et al.*, 2006). Moreover, the structure of the extracellular part of ADAM10, the closest ADAM17 relative, has been solved and can provide an even truer picture of what ADAM17 might look like (**Figure 1.3C,D**; Seegar *et al.*, 2017).

1.2.2 ADAM17 and its life cycle

Similar to other membrane proteins, ADAM17 begins its journey in the endoplasmic reticulum (ER) as a full-length immature protein. It is then transported into the Golgi apparatus (GA), where the prodomain hitherto protecting the peptidase site is removed by furin proprotein convertase (Schlöndorff, Becherer and Blobel, 2000). Mature ADAM17 with the metalloprotease domain freed from the prodomain's grasp then continues to the plasma membrane. Once at the cell surface, ADAM17 acts on its substrates, cleaving off their extracellular part (Liu *et al.*, 2009; Le Gall *et al.*, 2010). When ADAM17 is not needed any further, it is internalised into the endosomes and degraded in the lysosomes (Lorenzen *et al.*, 2016; Künzel *et al.*, 2018). A small pool of

ADAM17 can also be trafficked into the exosomes and release signal molecules from their surface (Groth *et al.*, 2016). It should be stressed that successful transit of ADAM17 through the secretory pathway absolutely depends on iRhoms, the pseudoproteases from the rhomboid-like family of proteins (Adrain *et al.*, 2012; McIlwain *et al.*, 2012). The iRhoms associate tightly with ADAM17 throughout its life cycle and can therefore be regarded as ADAM17's trafficking cofactors. In addition, iRhoms are also required for the stimulated activity of ADAM17 (Maretzky *et al.*, 2013). The iRhom-ADAM17 interaction is discussed in detail in **section 1.3.3.2**.

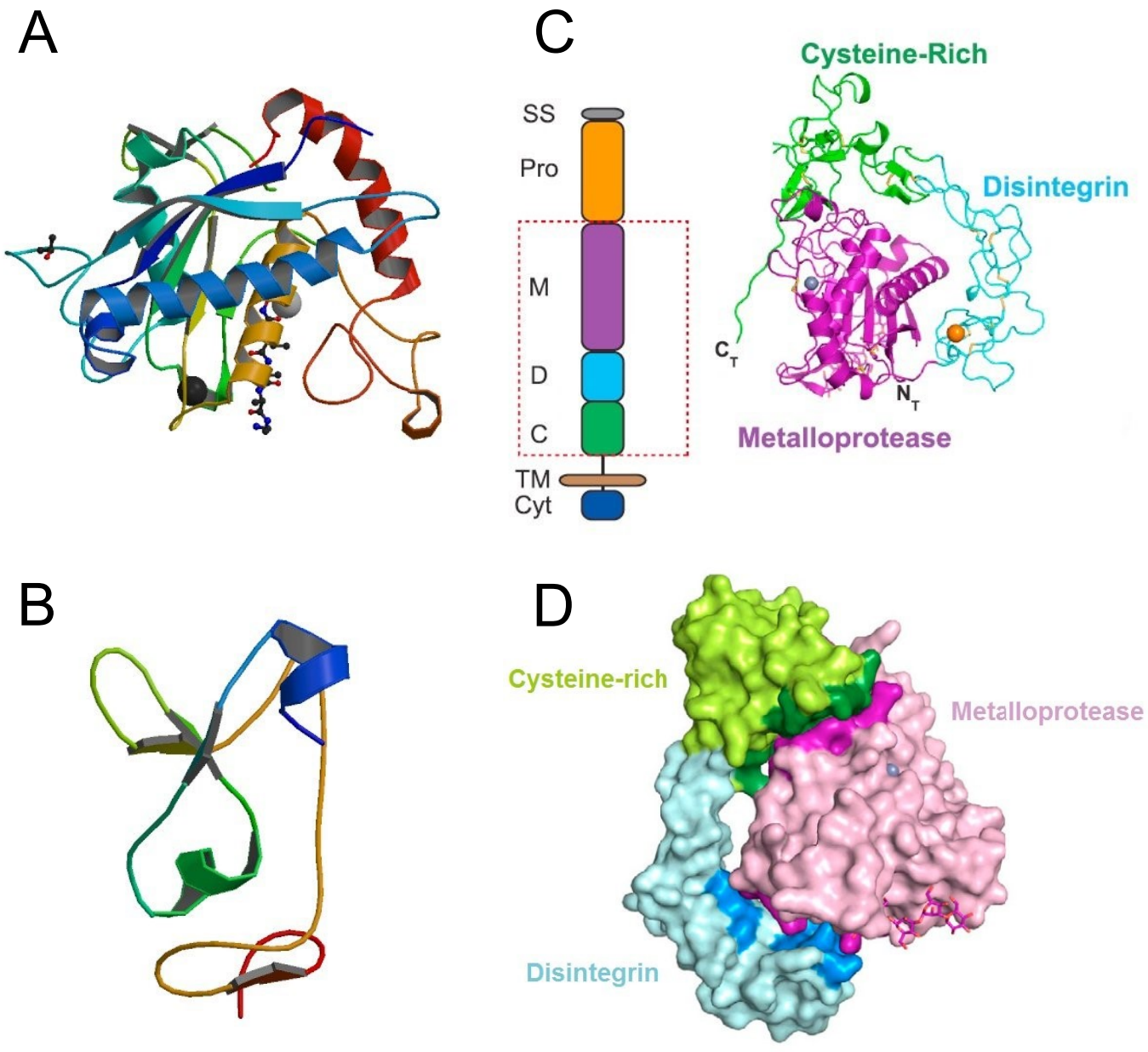

Figure 1.3: A – Structure of ADAM17 metalloprotease domain. PDB code: 2DDF. **B** – Structure of ADAM17 membrane-proximal domain. PDB code: 2M2F. **C** – A schematic representation of ADAM10 domain architecture. SS, signal sequence; Pro, prodomain; M, metalloprotease; D, disintegrin; C, cysteine-rich; TM,transmembrane; Cyt, cytoplasmic tail. On the right, an X-ray structure of the boxed region is shown. The catalytic Zn^{2+} is in grey. **D** – Space-filling model of ADAM10 ectodomain. **C** and **D** adapted from Seegar *et al.*, 2017.

1.2.3 ADAM17 and its substrates/physiological role

Once the ADAM17 metalloprotease (or, more precisely, the iRhom-ADAM17 complex) reaches the plasma membrane, its main task is to cleave off extracellular part of its clients, in a process called ectodomain shedding (Hayashida *et al.*, 2010). ADAM17 substrates can be classified into several groups (**Table 1.2**). Firstly, ADAM17 is the prominent producer of TNFα, IL-6 and several other cytokines involved in the regulation of the immune response and tissue repair . Interestingly, the receptors of ADAM17-produced cytokines are also shed by this metalloprotease (IL-6R, M-CSFR, TNFR and others; Black *et al.*, 1997; Moss *et al.*, 1997; Chalaris *et al.*, 2007; Horiuchi, Miyamoto, *et al.*, 2007; Maney *et al.*, 2015; Cavadas *et al.*, 2017). Therefore, ADAM17 participates not only in cytokine production, but also in the attenuation of the signal by negative feedback regulation (Maney *et al.*, 2015). Secondly, the production of the majority of EGFR ligands, namely that of TGFα, HB-EGF, AREG, EREG and EPGN, is almost exclusively dependent on ADAM17 (Sahin *et al.*, 2004; Sahin and Blobel, 2007). The remaining two EGFR ligands, EGF and BTC, are released by ADAM10, however, Rhomboid2 significantly contributes to the shedding of EGF (Sahin *et al.*, 2004; Adrain *et al.*, 2011). Thirdly, cleavage of molecules involved in cell adhesion and recognition, such as L-selectin or ICAM-1, is also catalysed by ADAM17 (Peschon *et al.*, 1998; Tsakadze *et al.*, 2006).

In addition to the steady-state, constitutive shedding, ADAM17 activity can be rapidly upregulated by various stimuli. To date, molecules such as lipopolysaccharide (an activator of the innate immune response), thrombin (a G-protein coupled receptor (GPCR) agonist), FGF, EGF or TNFα were described as transactivators of ADAM17 (Robertshaw and Brennan, 2005; Le Gall *et al.*, 2010; Maretzky *et al.*, 2011). In such conditions, ADAM17 is involved in a process called the triple membrane-passing signal (**Figure 1.4**). Here, a signal in the form of an agonist of a plasma membrane-resident receptor, be it a GPCR or a growth factor receptor, activates its receptor. The receptor then passes the signal inside the cell, activating the respective signalling cascade. A branch of the cascade targets mature ADAM17 at the plasma membrane, rapidly enhancing its shedding activity. ADAM17 then produces other signal molecules, which represent transformation of the initial signal and which then activate their respective receptors either on itself or on a neighbouring cell (Daub *et al.*, 1996; Fischer *et al.*, 2003; Hart *et al.*, 2005; Maretzky *et al.*, 2011s; ADAM17 transactivation via GPCRs is reviewed in Ohtsu, Dempsey and Eguchi, 2006). It is not yet fully understood what the branch of the signalling cascades leading to ADAM17 transactivation looks like, however, considerable amount of experimental data suggests that iRhoms play a crucial role in the process (Maretzky *et al.*, 2013; Cavadas *et al.*, 2017; Grieve *et al.*, 2017).

Table 1.2: Substrates of ADAM17. Adapted from Zunke *et al.,* 2017.

Immune system	Development, differentiation	Cell adhesion	Others
$IL\text{-}1R_{II}$	TGFα	ALCAM	ACE-2
IL-6R	Hb-EGF	CD44	APP
IL-15R	AREG	CD62L (L-selectin)	APP-like protein2
CX3CL1 (fractalkine)	Epigen	Collagen XVII	Carbonic hydrolase 9
M-CSFR	EREG	Desmoglein 2	Prion protein
$TNF\text{-}R_I$	NRG1	EpCam	Ebola virus glycoprotein
$TNF\text{-}R_{II}$	FLT-3L	ICAM-1	EPCR
LDL-R	KL-1	JAM-A	GPIba
SORL1	KL-2	L1-CAM	GPV
SORT1	Jagged	NCAM	GPVI
SORCS1	DLL1	Nectin-4	Klotho
SORCS3	Notch1	SynCAM1	Muc-1
TNFα	GH-R	VACM-1	NPR
Lymphotoxin α	IGF2-R		Pre-adipocyte factor
RANKL (TRANCE)	HER4 (ErbB4)		Ptprz
CSF-1	TrkA		
TIM-1	VEGF-R2		
TIM-3	LYPD3		
TIM-4	PMEL17		
MIC-A	PTP-LAR		
MIC-B	SEMA4D		
LAG-3	Syndecan1		
CD16	Syndecan4		
CD30 (TNFRSF8)	TEMEFF2		
CD36	Vasorin		
CD40 (TNFRSF5)			
CD89			
CD91 (APOER)			
CD163			
ICOS-L			

Altogether these findings highlight ADAM17's key role in cell to cell communication, with the metalloprotease regulating processes such as embryonic development, tissue homeostasis, maintenance of epithelial polarity or the immune response (reviewed in Gooz, 2010; Zunke and Rose-John, 2017). There is no doubt that further investigation of its physiological functions deserves special attention.

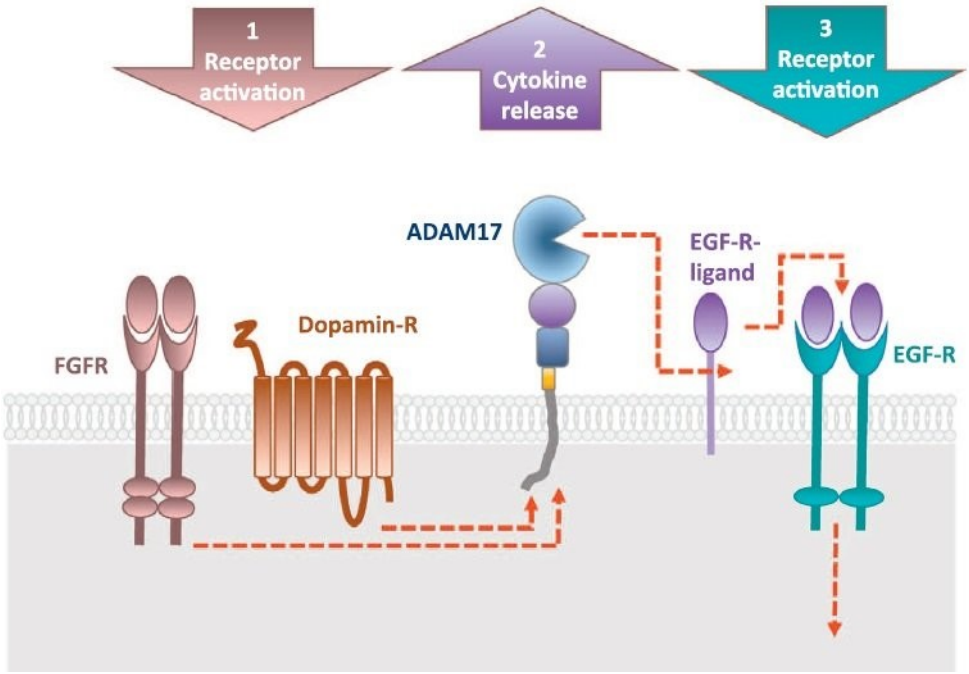

Figure 1.4: ADAM17 transactivation occurs through a process called triple membrane-passing signal. After stimulation of cell surface receptors (in this case fibroblast growth factor receptor, FGFR, and Dopamin receptor), ADAM17 is activated via the signalling cascades triggered inside the cell. Shedding of ADAM17 substrates leads to production of soluble signal molecules, which bind to and activate other receptors (EGFR in this case). By this mechanism, the original signal has been passed through the plasma membrane three times. Adapted from Zunke and Rose-John, 2017.

1.2.4 Posttranslational regulation of ADAM17 activity

As already mentioned above, the most important trafficking and activatory cofactors of ADAM17 are the iRhoms, whose relationship with ADAM17 is discussed in **section 1.3.3.2**. Here, ways of regulating ADAM17 activity other than through iRhoms will be introduced briefly. For more detailed information see Gooz, 2010 and Düsterhöft *et al.*, 2019.

In the secretory pathway, premature proteolytic activity of ADAM17 is prevented by the presence of its prodomain (Schlöndorff, Becherer and Blobel, 2000). Upon its cleavage by furin, it binds weakly to the metalloprotease domain and is eventually degraded (Milla *et al.*, 1999; Li *et al.*, 2009). The capability of the prodomain to block the ADAM17 active site served as the basis for the development of potent ADAM17 inhibitors (Wong *et al.*, 2016). At the cell surface, ADAM17 activity is influenced both by its lipid environment and by its interactions with other proteins. It was suggested that before activation, ADAM17 clusters into cholesterol-rich microdomains (Matthews *et al.*, 2003; Tellier *et al.*, 2006). However, in the presence of stimuli activating cell-surface receptors, phosphatidylserine transiently appears in the outer leaflet of the plasma membrane, allowing for interaction with the basic residues of the CANDIS motif (de Jong *et al.*, 2002; Harper and Poole, 2011; Düsterhöft *et al.*, 2015). It was suggested that this interaction might lead to a conformational change leading to appropriate positioning of the metalloprotease active site to perform shedding (Düsterhöft *et al.*, 2015). Another means of regulating ADAM17 activity is its dimerisation, most

likely via the cytosolic tail (Xu *et al.*, 2012). This interaction is a prerequisite for TIMP3 inhibitor binding into the active site of both (dimerised) ADAM17s (Xu *et al.*, 2012). This inhibition is reversible by phosphorylation of ADAM17 at T735, which disrupts the dimers (Xu *et al.*, 2012). Although the cytosolic domain is not necessary for the trafficking or transactivation of ADAM17, it was suggested that its phosphorylation by signal-transducing kinases such as ERK, p38, PLK-2 or PKC might fine-tune ADAM17 shedding activity (Xu and Derynck, 2010). The disintegrin domain negatively regulates ADAM17 activity, for by binding to integrins, it sterically blocks access to the peptidase site (Gooz *et al.*, 2012; Trad *et al.*, 2013). Tetraspanin (CD9) acts as a more specific inhibitor, for by binding to ADAM17 it downregulates exclusively the cleavage of ICAM1 and TNFα (Gutiérrez-López *et al.*, 2011). Another factor modulating ADAM17 activity are the extracellular protein disulfide isomerases (PDIs). It has been proposed that disulfide bridge remodelling turns the membrane-proximal domain of ADAM17 into a more rigid conformation, less favourable for performing substrate cleavage (Düsterhoft *et al.*, 2013). However, to fully elucidate the role of PDIs in eliciting ADAM17 conformational changes and how this is linked to the regulation of ADAM17 proteolytic activity, more experimental data need to be collected.

1.2.5 Diseases associated with dysregulation of ADAM17

Given the prominent role ADAM17 plays in cell signalling, it is no surprise that a vast number of pathologies are linked to its dysregulation. Since ADAM17 is involved in inflammatory signalling, its upregulation is associated with many inflammatory conditions such as rheumatoid arthritis (Issuree *et al.*, 2013), inflammatory bowel disease (reviewed in Papadakis and Targan, 2000), psoriasis (Kawaguchi, Mitsuhashi and Kondo, 2005), multiple sclerosis (Seifert *et al.*, 2002) or endotoxin shock (Horiuchi, Kimura, *et al.*, 2007). In addition, dysregulation of ADAM17 is implicated in the development of Alzheimer's disease, one of its substrates being the potentially amyloidogenic APP protein (Buxbaum *et al.*, 1998). Excessive production of EGFR ligands by ADAM17 has been observed in many types of cancer and is usually correlated with poor prognosis (reviewed in Duffy *et al.*, 2009). Overproduction of TGFα and HB-EGF is associated with several kidney diseases, for example the polycystic kidney disease (Richards *et al.*, 1998).

It is beyond the scope of this thesis to discuss the ADAM17 contribution to all of the pathologies in detail. To gain a deeper insight into the topic, a review from (Gooz, 2010) is recommended for further reading.

1.3 iRhoms and their kin

iRhoms are members of the rhomboid-like superfamily of proteins (**Figure 1.5**). The hallmark of this protein group is a hydrophobic core of six membrane-embedded helices (Wang, Zhang and Ha, 2006; Lemberg and Freeman, 2007). Hence the whole life cycle of these molecules from their biogenesis to their degradation is tightly coupled with cellular membranes. The first rhomboid-like proteins to be discovered were the proteolytically active ones, the rhomboid proteases (Urban, Lee and Freeman, 2001). Their active site being buried in the phospholipid bilayer (Wang, Zhang and Ha, 2006), rhomboids represent one of the four mechanistically distinct groups of intramembrane proteases described to date and are also the most widespread one (reviewed in Beard *et al.*, 2019). However, as shown by bioinformatic analysis, many members of this remarkable family of proteins have lost their proteolytic activity during evolution (Lemberg and Freeman, 2007). Pseudoenzymes are a common phenomenon among other enzyme families, as discussed in (Adrain and Freeman, 2012). The proteolytically inactive rhomboid family members fall into two categories based on their sequence conservation: the inactive rhomboid-like proteins, which are sequentially very distinct from the

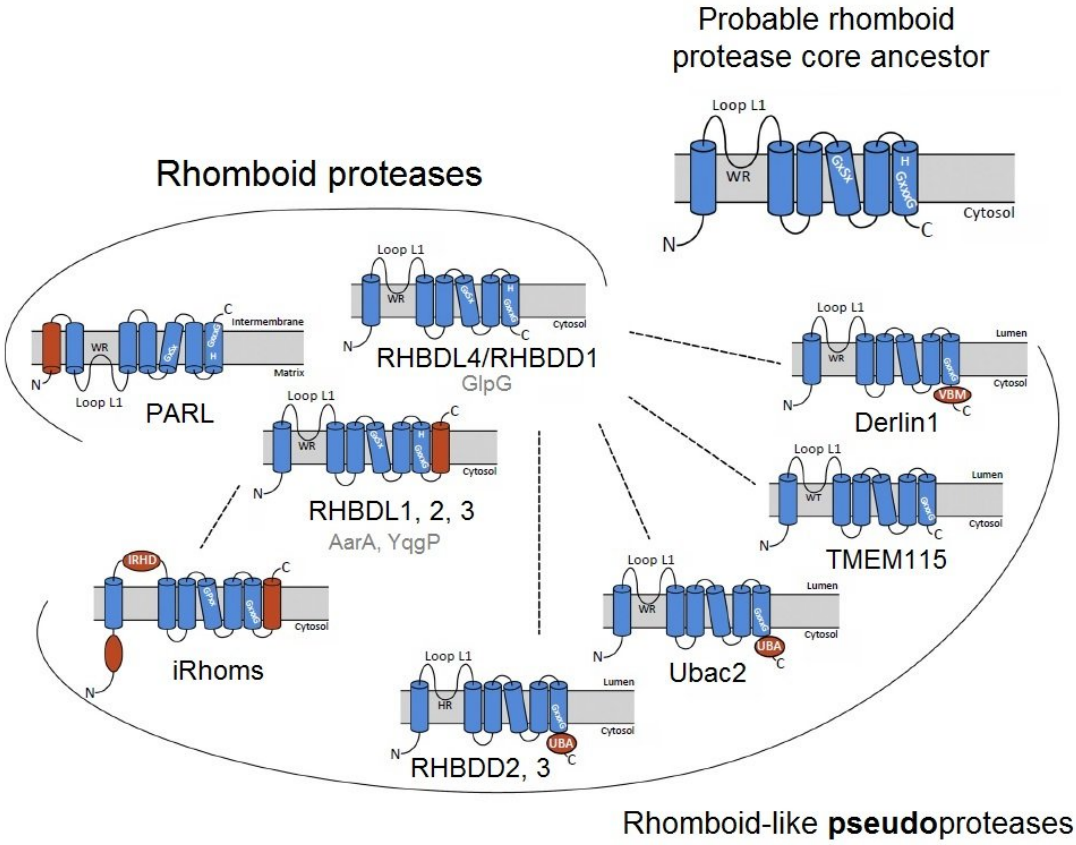

Figure 1.5: Schematic topological models of the rhomboid superfamily proteins. The rhomboid core domain is shown in blue, with additional features specific to a particular subclass indicated in red. Typical representatives of each subgroup are named (the prokaryotic ones are in grey). Broken lines indicate probable evolutionary relationships. Among all the rhomboid-like pseudoproteases, iRhoms are the ones most closely related to the so-called secretase A type of rhomboid proteases with the 6 + 1 TMD topology (represented by the RHBDL1, 2, 3 subgroup). Abbreviations: IRHD, iRhom homology domain; UBA, ubiquitin-associated domain; VBM, VCP(p97)-binding motif. Adapted from Tichá, Collis and Strisovsky, 2018.

active proteases, and the iRhoms (Lemberg and Freeman, 2007; Tichá, Collis and Strisovsky, 2018). Since rhomboid proteases are conserved across all the three branches of living organisms (Koonin *et al.*, 2003; Lemberg and Freeman, 2007), it is tempting to speculate that a proteolytically active rhomboid represents the common ancestor of the rhomboid-like family tree and that all its proteolytically inactive members arose later in evolution (Adrain and Freeman, 2012). There also exists an alternative hypothesis, which attempts to explain the large evolutionary distance of non-iRhom inactive rhomboid-like proteins from the rhomboid proteases. It suggests that an ancestor of all the rhomboid-like family existed in the last universal common ancestor, whose function was to recognise transmembrane domains of other proteins. The intramembrane proteolytic activity evolved later in the rhomboid branch of the family and was lost again in the iRhoms, which are present only in metazoan genomes (Lemberg and Freeman, 2007; Adrain and Freeman, 2012). The non-iRhom inactive members of the rhomboid-like superfamily therefore did not evolve from active rhomboids but represent something more like the original common ancestor (Adrain and Freeman, 2012).

iRhoms were first described based on *in silico* analysis of rhomboid-related sequences (Lemberg and Freeman, 2007). Although predicted and then confirmed experimentally to be proteolytically inactive (Lemberg and Freeman, 2007; Zettl *et al.*, 2011), the surprisingly high degree of their sequence conservation enabled them to be clustered into a special group, its hallmark being the well-conserved loop between the first two transmembrane helices (Lemberg and Freeman, 2007). The high degree of sequence conservation between iRhoms also indicates that their protein products occupy an important niche in the organisms (Lemberg and Freeman, 2007).

The reason for classifying iRhoms as proteolytically inactive lies in the sequence motif in their putative active site. The GxSx sequence—the S being the key catalytic residue and an alanine or a serine usually found at the first "x" position—conserved in transmembrane helix 4 of active rhomboids is invariantly replaced by GPxx in iRhoms (Lemberg and Freeman, 2007). The proline residue is thought to disrupt the geometry of the putative active site in such a way that it is no longer favourable for substrate cleavage. Indeed, this is exactly what happens if the residue at the "x" position before the catalytical serine is replaced with proline in rhomboids (Lemberg and Freeman, 2007; Zettl *et al.*, 2011; Adrain and Freeman, 2012). This hypothesis about the causes of iRhom catalytic inactivity also nicely explains why there is such a diversity in the catalytic dyad[4] conservation among the iRhoms. Once the peptidase active site has been disabled by proline introduction, the pressure for catalytic residue conservation ceased to exist, leading to some iRhoms having lost the catalytic serine only (human and mouse iRhoms), some the catalytic histidine only (fruit fly iRhom) and some both serine and histidine (*Anopheles gambiae* iRhom; Lemberg and Freeman, 2007). The *C. elegans* iRhoms represent a special case with both potentially catalytic residues preserved, further supporting the aforementioned hypothesis (Lemberg and Freeman, 2007).

[4] In contrast to soluble serine proteases, rhomboids perform peptide bond cleavage using only two residues, the serine in transmembrane domain (TMD) 4 and the histidine in TMD6 (Wang, Zhang and Ha, 2006).

1.3.1 iRhom domain architecture

Based on *in silico* analysis, iRhoms are predicted to possess a hydrophobic core consisting of six transmembrane helices, most likely structurally similar to that of rhomboid proteases (**Figure 1.6**; Lemberg and Freeman, 2007). Compared to the rhomboid core architecture, another transmembrane helix is present at the C-terminus of iRhoms (**Figure 1.5**). The very N-terminus forms a large cytosolic domain spanning several hundreds of amino acids. This is in contrast with active rhomboids, whose N-terminal part is formed only by several tens of amino acids or completely absent (Koonin *et al.*, 2003). Being oriented into the cytosol, the iRhom N-terminal domain was shown to play a role in regulating iRhom, and through it ADAM17 activity (see **section 1.3.3.2** for details). Posttranslational modifications, namely phosphorylation and ubiquitinylation, were also shown to take place on the N-terminal domain and to influence iRhom-mediated regulation of ADAM17 activity (Chanthaphavong *et al.*, 2012; Cavadas *et al.*, 2017; Grieve *et al.*, 2017; Zhang *et al.*, 2018).

The most conserved and at the same time the least well characterised part of the iRhoms is the extracellular loop between transmembrane helices 1 and 2 (Lemberg and Freeman, 2007). It forms a domain called the iRhom homology domain (IRHD; Lemberg and Freeman, 2007). Since its sequence is dissimilar to any known fold, prediction of its structure is extremely challenging. Interestingly, it contains sixteen conserved

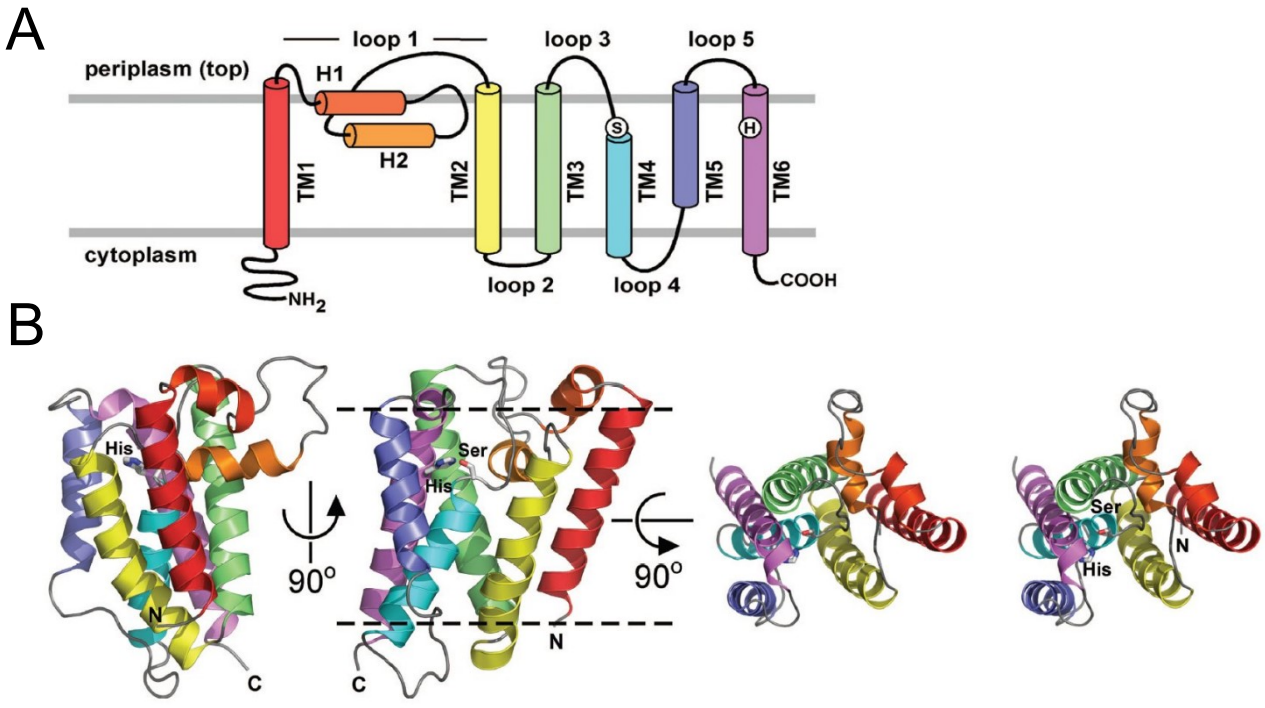

Figure 1.6: Schematic representation (**A**) and ribbon diagram of the crystal structure (**B**) of GlpG, a bacterial rhomboid protease. In **B**, three GlpG orientations are shown with helices color-coded as in **A**; the top view is shown in stereo. Adapted from Ben-Shem, Fass and Bibi, 2007.

cysteine residues (Lemberg and Freeman, 2007). Up to eight disulfide bridges can therefore be formed, which makes the structural predictions even more difficult (Lemberg and Freeman, 2007). In the IRHD of iRhom1, one N-glycosylation site has been predicted and confirmed experimentally (Nakagawa *et al.*, 2005).

1.3.2 iRhoms and cellular localisation

The predominant localisation of endogenous iRhom is on the plasma membrane, as shown by microscopy of human keratinocytes and by quantitative mass spectrometry of HeLa cells (Blaydon *et al.*, 2012; Itzhak *et al.*, 2016). However, overexpressed iRhoms localise mainly to the ER, as visualised by confocal microscopy (Nakagawa *et al.*, 2005; Zettl *et al.*, 2011; Maney *et al.*, 2015; Künzel *et al.*, 2018; Oikonomidi *et al.*, 2018). Smaller pools of overexpressed iRhom proteins can be found also in the GA (Oikonomidi *et al.*, 2018) and on the plasma membrane (Blaydon *et al.*, 2012; Maney *et al.*, 2015; Cavadas *et al.*, 2017; Oikonomidi *et al.*, 2018), corresponding with iRhom involvement in cytokine and EGFR signalling. Once not needed at the cell surface, iRhom is internalised into lysosomes (Künzel *et al.*, 2018; Oikonomidi *et al.*, 2018). Specifically for innate immunity, upon DNA virus infection, iRhom2 with its client STING travels from the ER to the GA, finishing its route in the perinuclear microsomes of immune cells (Luo *et al.*, 2016). Interestingly, iRhom2 has also been detected in the mitochondria-associated ER-membranes as well as in the mitochondrial membrane itself (Luo *et al.*, 2017), raising questions about possible mechanisms of intermembrane transport and interactions.

1.3.3 iRhom functions known to date

1.3.3.1 Protein quality control

The first function ever ascribed to an iRhom is that of a negative regulator of EGF receptor signalling in the fruit fly (Zettl *et al.*, 2011). Here, iRhom promotes the degradation of EGF receptor ligands‘ precursors in the ER, most likely via the ERAD pathway (Zettl *et al.*, 2011). In the same paper, it was suggested that this transmembrane protein-destabilizing effect might be conserved in mammalian iRhoms too, based on the experimental evidence from *in vitro* cultured cells (Zettl *et al.*, 2011). In another study, iRhom1 has been shown to participate in the response to ER-stress by facilitating the dimerisation of PAC1/PAC2 proteins and by recruiting the proteasomes to the clients intended for disposal (Lee *et al.*, 2015). It is also worth pointing out that other proteolytically inactive proteins from the rhomboid-like superfamily such as derlins or Ubac2 are associated with ER-quality control mechanisms (Oda *et al.*, 2006; Christianson *et al.*, 2011).

1.3.3.2 Regulation of EGFR signalling through ADAM17 maturation and activation

The scrutiny of mammalian iRhom function began by creating mouse knock-outs (KO; Adrain *et al.*, 2012; Christova *et al.*, 2013). Two mammalian iRhom genes exist, *Rhbdf1* and *Rhbdf2* (Lemberg and Freeman, 2007). Their protein products, iRhom1 and iRhom2, respectively, share significant sequence similarity (**Figure 1.7**; Lemberg and Freeman, 2007; Düsterhöft *et al.*, 2019) but differ in tissue expression profiles.

A

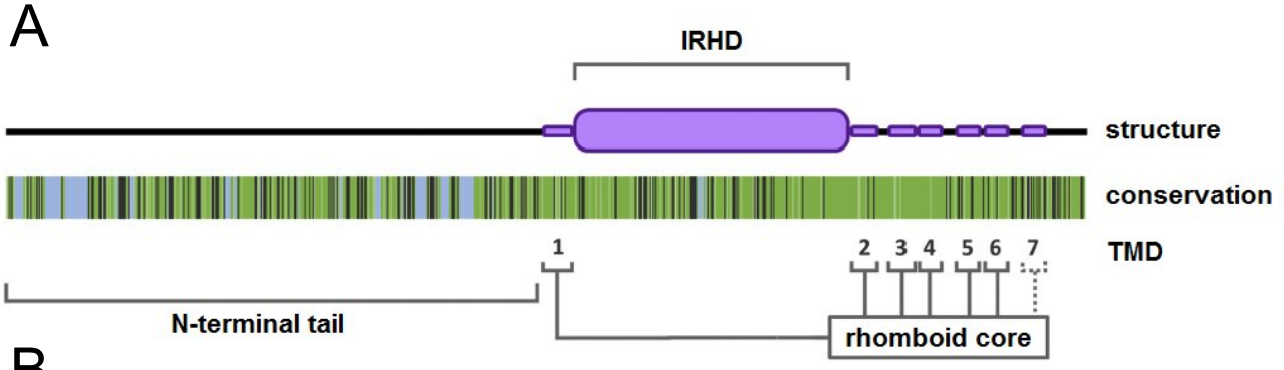

B

structural unit	N-terminal tail	IRHD	TMD1	TMD2	TMD3	TMD4	TMD5	TMD6	TMD7
identity [%]	42.2	66.7	72.4	78.3	85.7	94.1	70.0	76.2	37.5
similarity [%]	54.9	77.9	89.7	91.3	100.0	100.0	75.0	90.5	58.3

Figure 1.7: Conservation between human iRhom1 and iRhom2. **A** – Conservation between human iRhom1 and iRhom2 is represented as colour code: dark green = conservation; light green = amino acid residues with similar properties; blue = deletions/extensions; dark grey = no conservation. **B** – Overview of the identity and similarity of structural units in human iRhom1 and iRhom2 is presented. Adapted from Düsterhöft et al., 2019.

Whereas iRhom1 is expressed at significant levels throughout many tissues, iRhom2 expression is much less prominent except for the myeloid cells (Siggs *et al.*, 2012; Christova *et al.*, 2013). This was, together with their partial redundancy, indeed reflected by the single knock-outs: while iRhom1 KO mice died within six weeks after birth[5], iRhom2 KO mice survived until adulthood, were fertile and had no obvious defects except when the immune response was stimulated (Adrain *et al.*, 2012; Christova *et al.*, 2013). However, double knock-out mice died either at the embryonic stage or perinatally, indicating that iRhom proteins are indispensable for the development and the survival of an adult organism (Christova *et al.*, 2013; Li *et al.*, 2015). It should be remarked that phenotypically the iRhom 1 and 2 double knock-out mice strongly ressemble the ADAM17 KO and EGFR KO strains in that they have open eyes at birth, enlarged heart valves and prolonged growth plates in the bones (Li *et al.*, 2015).

Indeed, it is ADAM17 that is the key to the mystery. It has been revealed that macrophages of otherwise normally looking iRhom2 KO mice are impaired in the production of soluble TNFα, the major mediator of the inflammatory response (Adrain *et al.*, 2012; McIlwain *et al.*, 2012). Upon further investigation, it was shown that the lack of mature, plasma membrane-resident ADAM17 accounts for this phenotype (Adrain *et al.*, 2012). Without either iRhom, trafficking of ADAM17 from the ER to the GA is suspended, thereby preventing its prodomain removal by the furin protease (Adrain *et al.*, 2012; Christova *et al.*, 2013). Coimmunoprecipitation and crosslinking experiments suggest that the iRhom-ADAM17 interacton is likely

[5] There was another iRhom1 KO mouse strain reported, the animals being viable and fertile with no evident pathological phenotypes (Li *et al.*, 2015). This phenotypic discrepancy may be caused by different genetic backgrounds of the mutated mice as well as by different exon span of the knock-outs.

direct rather than via a third protein (Adrain *et al.*, 2012; Maney *et al.*, 2015; Künzel *et al.*, 2018). Since the mature form of ADAM17 was, although less tightly, bound by iRhoms, iRhom was suggested to participate in ADAM17 transactivation at the cell surface. Experimental data indeed favour these ideas, for in the cells devoid of iRhoms the stimulated shedding activity of ADAM17 is absent or significantly reduced compared to the wild type (WT; Christova *et al.*, 2013; Maretzky *et al.*, 2013; Cavadas *et al.*, 2017; Grieve *et al.*, 2017; Li *et al.*, 2017). Surprisingly, iRhoms are not only key factors for ADAM17 maturation and mediators of its transactivation, but they also influence the ADAM17 substrate repertoire (Maretzky *et al.*, 2013; Li *et al.*, 2017). Based on ADAM17 transactivation studies in iRhom2 KO mouse embryonic fibroblasts (mEFs), the substrates of ADAM17 can be divided into two groups, firstly proteins whose stimulated shedding[6] requires iRhom2 (iRhom2-dependent substrates), and secondly ADAM17 clients whose stimulated shedding by ADAM17 occurs even in the absence of iRhom2 (iRhom2-independent substrates; **Table 1.3**; Maretzky *et al.*, 2013). It is worth noting that the interaction between iRhoms and ADAM17 is very specific, for any other transmembrane clients of the iRhom pseudoproteases have been identified neither among other ADAM metalloproteases, nor among cell surface receptors and precursors of their ligands (Christova *et al.*, 2013).

Table 1.3: iRhom2 substrate selectivity in mEFs. Adapted from Maretzky *et al.*, 2013.

iRhom2-dependent substrates	iRhom2-independent substrates
Amphiregulin	TGFα
Epiregulin	ICAM
HB-EGF	L-selectin
Ephrin B4	
KitL2	
Tie2	

When considering the long-lived and multilateral relationship between iRhom and ADAM17, a question arises about how they interact and how this is linked to iRhom's domain architecture (summarised in **Figure 1.8**). Many experiments have been performed to elucidate the problem. The most important domain required for fruitful interaction of the two partners seems to be the transmembrane domain of ADAM17 and the first transmembrane helix of iRhom (Cavadas *et al.*, 2017; Li *et al.*, 2017). If the transmembrane domain (TMD) of ADAM17 is exchanged for the TMD of its closest homologue, the ADAM10, no interaction between the chimera and iRhom is detected (Cavadas *et al.*, 2017). The importance of transmembrane domain interaction

[6] Constitutive shedding of all ADAM17 substrates in the iRhom2 KO cells remained comparable with the wild type levels (Maretzky *et al.*, 2013).

is further underlined by the finding that the rapid stimulation of ADAM17 at the cell surface depends on its TMD in the first place, which paved the way for a membrane-spanning regulator of this enzyme, the iRhom, to be discovered (Le Gall *et al.*, 2010; Adrain *et al.*, 2012; McIlwain *et al.*, 2012). In addition, certain point mutations introduced into the ADAM17 transmembrane domain reduced its ability to respond to transactivating stimuli, although its iRhom2 binding ability was not compromised (Li *et al.*, 2017). Conversely, a point mutation in the middle of the first transmembrane helix of iRhom2 leads to impaired stimulated activity of ADAM17 (Li *et al.*, 2017). The intramembrane interaction seems to influence the substrate repertoir as well, the hypothesis being supported by the fact that the ADAM17 TMD point mutants mentioned above showed less stimulated activity towards iRhom2-dependent substrates while their ability to perform stimulated cleavage of TGFα, an ambiguous substrate (cleavage is stimulated by both iRhom1 and 2, **Table 1.3**.) of the metalloprotease, was not affected (Li *et al.*, 2017). This phenomenon can be explained easily by iRhom1 substituting for iRhom2, most likely because it interacts with ADAM17 TMD in a different way (Li *et al.*, 2017). However, all these conclusions are based on a single published study and would benefit from further confirmation.

The IRHD appeared to be indispensable for ADAM17 maturation by binding to immature ADAM17, however, nothing beyond this is known about the underlying mechanism (Grieve *et al.*, 2017). Contrary to that, the N-terminal domain received much attention and its involvement in the regulation of iRhom-ADAM17 still causes some controversies. While being dispensable for ADAM17 trafficking from the ER to the GA, the N-terminal domain of iRhom seems to play a crucial role once the iRhom-ADAM17 complex reaches the plasma membrane (Grieve *et al.*, 2017). Firstly, it protects the complex from internalisation into the lysosomes (Grieve *et al.*, 2017). Secondly, it negatively regulates constitutive ADAM17 proteolytic activity, for iRhom N-terminal domain removal results in increased production of soluble forms of ADAM17 targets (Maney *et al.*, 2015). Thirdly, the iRhom2 N-terminal domain is involved in regulation of TNFα-induced ADAM17 maturation (Zhang *et al.*, 2018). Upon TNFR stimulation, the E2-E3 ubiquitin ligase complex Uev1A-Ubc13 is recruited to iRhom2 and performs K63 polyubiquitinylation of its N-terminal domain (Zhang *et al.*, 2018). This leads to enhanced ADAM17 maturation and hence increased ADAM17-mediated TNFR cleavage, resulting in the attenuation of TNFα signalling by a negative feedback loop (Zhang *et al.*, 2018).

Fourthly, the N-terminal domain of iRhom is vital for mediating the response to ADAM17 transactivating stimuli (Maretzky *et al.*, 2013; Maney *et al.*, 2015; Cavadas *et al.*, 2017; Grieve *et al.*, 2017). The presence of phosphorylatable residues, mainly those located to the first 200 amino acids of the N-terminal domain, is necessary for this function of iRhom (Cavadas *et al.*, 2017; Grieve *et al.*, 2017). Several signal-transducing kinases have been identified to act on these sites, namely ERK1/2, p38, JNK, RSK6 or iNOS-induced PKG, thus enabling the iRhom to be viewed as a hub on which signals from various pathways are integrated (Chanthaphavong *et al.*, 2012; Cavadas *et al.*, 2017; Grieve *et al.*, 2017). Phosphorylated residues in the N-terminal domain then serve as binding sites for 14-3-3 proteins, key components of stimulated ADAM17

shedding response (Cavadas *et al.*, 2017; Grieve *et al.*, 2017). This was confirmed by concurrent introduction of the constitutive 14-3-3 binding motif, the R18 peptide, into the cytosolic domain of iRhom, and the mutation of all putative phosphorylatable amino acids to alanine, when rescued stimulated activity of ADAM17 was observed (Cavadas *et al.*, 2017; Grieve *et al.*, 2017). However, the interaction of iRhom2 with ADAM17 was weakened by the 14-3-3 protein binding, revealing an N-terminal domain paradox: on the one hand, the iRhom-ADAM17 complex is stabilised at the cell surface and protected from lysosomal degradation, and on the other the recruitment of 14-3-3 proteins releases ADAM17 from iRhom's embrace and promotes its proteolytic activity (Cavadas *et al.*, 2017; Grieve *et al.*, 2017).

These ambiguous observations are further reflected in the debate about naturally occuring mutations in the iRhom cytosolic domain. In the case of tylosis with oesophageal cancer syndrome (TOC) there is a consensus that the point mutants associated with this pathology are gain-of-function mutations (Brooke *et al.*, 2014). However, in the case of the mouse *cub* mutant (for "curly bare" phenotype; Johnson *et al.*, 2003) where iRhom2 lacks the first 268 amino acids (Siggs *et al.*, 2014) it is still unclear if excessive ADAM17 activity towards its substrate amphiregulin or rather ADAM17's lack of proteolytic processing activity accounts for the phenotype (Hosur *et al.*, 2014; Siggs *et al.*, 2014). Another layer of complexity of the *cub* mutant problem is added by the observation that inhibition of proteasomes results in iRhom protein accumulation in the cells, an effect significantly more pronounced in the case of wild-type iRhom compared to that of the *cub* mutant (Hosur *et al.*, 2014). It may therefore mean that although the degradation of iRhom-ADAM17 complex occurs in lysosomes, there is a pool of iRhom that succumbs to proteasomal degradation, which would imply a K48 ubiquitinylation should occur on its cytosolic domain. Alternatively, the *cub* mutant is much more resistant to the ubiquitinylation-conditioned proteasomal degradation, thereby supporting ADAM17 activity more readily (Hosur *et al.*, 2014). However, in another mouse iRhom2 mutant, the *Uncv* (from *uncovered*—the mice homozygous for *Uncv* are bare), the 118—191 spanning deletion in the N-terminal domain is linked to defective ADAM17 maturation (Yang *et al.*, 2014). It is therefore currently impossible to draw any general simplifying conclusions about the role of the iRhom cytosolic domain in ADAM17 regulation.

Apart from the kinases, 14-3-3 proteins and ubiquitin ligases, the iRhom N-terminal domain interacts with another partner, the FRMD8 (iTAP) protein (Künzel *et al.*, 2018; Oikonomidi *et al.*, 2018). FRMD8 remains bound to iRhom during its odyssey through the secretory pathway, the site of interaction lying between residues 191 and 271 of mouse iRhom2 and between residues 200 and 300 of human iRhom2 (Künzel *et al.*, 2018; Oikonomidi *et al.*, 2018). While being dispensable for iRhom trafficking from the ER to the GA, FRMD8 is needed for iRhom-ADAM17 complex stabilisation in the distal compartments of the secretory pathway (trans-Golgi network, plasma membrane; Künzel *et al.*, 2018; Oikonomidi *et al.*, 2018). The presence of FRMD8 has also been established as a premise for ADAM17 activity (Künzel *et al.*, 2018; Oikonomidi *et al.*, 2018).

1.3.3.3 iRhom and antiviral response

In addition to protein quality control and cytokine signalling, iRhom2 is indispensable for the innate immunity response to DNA and RNA viruses (Luo *et al.*, 2016, 2017). Upon infection by a DNA virus, iRhom2 facilitates trafficking of the adaptor protein STING from the ER to the perinuclear microsomes by recruiting the translocon TRAPβ to its vicinity[7]; during the journey, proteins IRF3 and TBK1 associate with STING and trigger type 1 interferon production (Luo *et al.*, 2016). iRhom2 also associates with the EIF3S5 deubiquitinase, hence protecting its client STING from proteasomal degradation (Luo *et al.*, 2016). Interestingly, these two iRhom2 antiviral activities are independent of each other (Luo *et al.*, 2016).

The immune response to RNA virus infection is mediated through polymerisation of the mitochondrial membrane-resident adaptor protein VISA (also known as MAVS, IPS-1 and Cardif; Hou *et al.*, 2011). iRhom2 has been identified as a stabilising factor of VISA, acting on different E3-ubiquitin ligases depending on the stage of infection (Luo *et al.*, 2017). In un-infected cells and in the early phase of RNA virus infection, iRhom2 prevents ERAD of VISA by disabling the RNF5 E3 ubiquitin ligase, which usually marks VISA for degradation, by promoting its self-association and autoubiquitinylation (Luo *et al.*, 2017). In the late stage of infection, iRhom2 protects VISA from the E3-ubiquitin ligase MARCH5 by facilitating the destruction of MARCH5 in proteasomes (Luo *et al.*, 2017). As with ADAM17, STING and TRAPβ, the iRhom2-VISA interaction occurs via the first transmembrane helix of iRhom2 (Luo *et al.*, 2017).

1.3.4 iRhom and diseases

As mentioned earlier, iRhoms are vital for the development of an organism and for maintaining the homeostasis of adult tissues. It is therefore not surprising that alteration of its normal function or dysregulation leads to pathological conditions (reviewed in Dulloo, Muliyil and Freeman, 2019). The majority of such diseases stems from the tight relationship between iRhom and ADAM17-dependent signalling. This is indeed the case of the tylosis with oesophageal cancer (TOC) hereditary syndrome, described in a few families around the world (Ellis *et al.*, 1994; Stevens *et al.*, 1996; Varela *et al.*, 2011; Saarinen *et al.*, 2012). Point mutations in a restricted area of the iRhom2 N-terminal domain were identified as causative for the phenotype – hyperkeratotic lesions on palms and feet and increased risk of oesophageal cancer development (Blaydon *et al.*, 2012; Saarinen *et al.*, 2012; Ellis *et al.*, 2015). This was rationalised by suggesting that the iRhom2 mutations are gain-of-function ones, leading to ADAM17 hyperactivity and therefore production of pro-proliferative cytokines (Blaydon *et al.*, 2012; Brooke *et al.*, 2014).

Apart from this rare syndrome, both iRhoms were confirmed to contribute to several types of cancer. iRhom1-mediated proliferative signalling has been associated with breast and head-and-neck carcinoma (Yan *et al.*, 2008), probably through enhancing EGFR signalling transactivation via the GPCRs (Zou *et al.*, 2009). The

[7] As in the case of ADAM17, the first transmembrane domain of iRhom2 is involved in the interaction both with STING and with TRAPβ (Luo *et al.*, 2016).

epitelo-mesenchymal transition of colorectal carcinoma cells is most likely supported by iRhom1, which in this case upregulates the Wnt/β-catenin signalling pathway (Yuan *et al.*, 2018). Increased expression of iRhom2 was detected in the cancer-associated fibroblasts isolated from the gastric tumour and shown to be connected with their enhanced migration potential (Ishimoto *et al.*, 2017). As an underlying mechanism the regulation of non-canonical TGFβ signalling via excessive TGFβR cleavage by ADAM17 has been proposed (Ishimoto *et al.*, 2017).

Thanks to the unique association of iRhom2 with TNFα-mediated proinflammatory signalling, many iRhom2-dependent inflammatory pathologies were described. iRhom2-mediated ADAM17 upregulation has been shown to play a role in inflammatory arthritis (Issuree *et al.*, 2013), in haemophilia A (Haxaire *et al.*, 2018) and in the development of lupus nephritis (Qing *et al.*, 2018). Interestingly, iRhom2-dependent proinflammatory signalling in macrophages mediates the tissue-damaging inflammatory response to a myocardial infarction as well as the tissue reparation process in the later stages (Lu *et al.*, 2017; Barnette *et al.*, 2018).

Moreover, differential methylation of the *Rhbdf2* gene and hence potentially altered gene expression was identified as one of the many probable contributors to the onset of Alzheimer's disease (De Jager *et al.*, 2014). This might be related to the high iRhom2 expression in microglia compared to the other brain tissue cell types (Li *et al.*, 2015).

Last but not least, functional iRhom2 is indispensable for an appropriate innate immunity response to pathogens. In the absence if iRhom2, the organism is susceptible to bacterial (McIlwain *et al.*, 2012) as well as DNA- and RNA-viral infections (Luo *et al.*, 2016, 2017).

Taken together, all these observations make both iRhoms, and especially innate-immunity related iRhom2, promising targets for drug development.

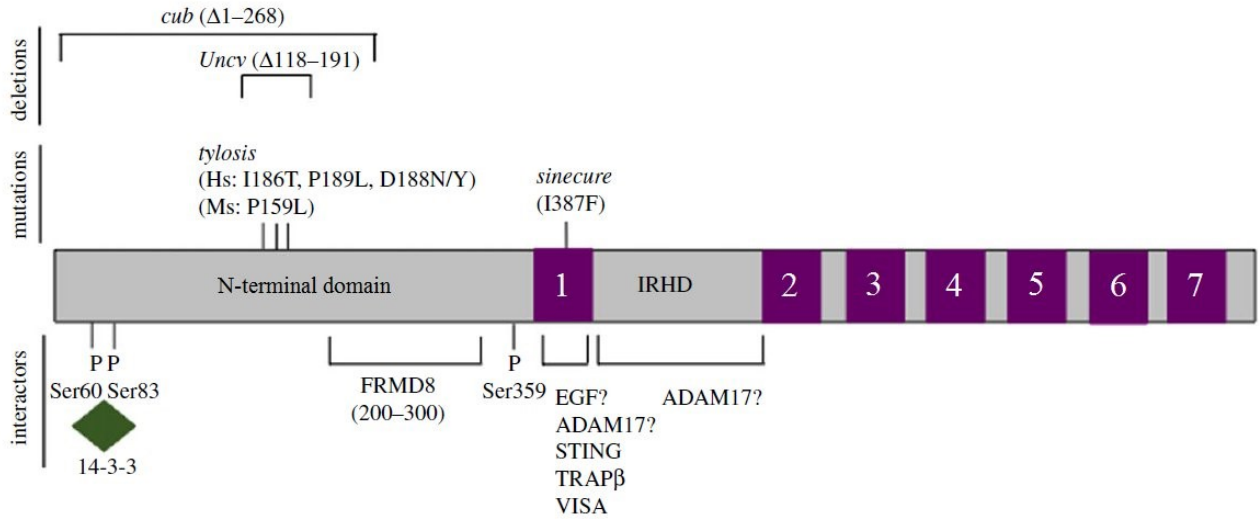

Figure 1.8: Schematic summarisation of iRhom mutants and interactors. Adapted from Dulloo, Muliyil and Freeman, 2019.

2 Aims of the thesis

2.1 Intellectual background

As outlined in the previous chapter, the involvement of iRhom in EGF receptor signalling regulation is a fascinating field of research. However, a concept that would fit all, or at least some, of the diverse roles of iRhom in mammalian cells described to date is still missing. In this thesis, I attempt to reconcile iRhom2 involvement in the negative regulation of EGF receptor signalling with the positive impact of iRhom2 on EGFR ligand production by iRhom2 interaction with ADAM17.

2.2 Questions to be answered

Based on the findings of (Zettl *et al.*, 2011), I aimed to confirm the experiments which suggest that mammalian iRhom overexpression causes a decrease in the protein levels of EGF receptor ligands precursors. My next questions were whether this effect is iRhom specific and if EGF receptor ligands are the only client proteins affected. Furthermore, I wanted to explore how ADAM17 overexpression influences this iRhom-triggered effect on its clients. Finally, I aimed to confirm that the observed effect of iRhom overexpression on EGFR ligands is caused by enhanced degradation of iRhom client proteins.

2.3 Methodological approach

In order to explore the interactions of proteins of interest, tagged proteins were overexpressed in HEK cells. Cell lysates were then collected into a sample buffer and the levels of proteins of interest were analysed by quantitative immunoblotting (see **section 3.5** for details). The overexpression system approach was chosen due to its robustness and adaptability. HEK cells were used because of their good transfection efficiency. Quantitative immunoblotting using the LI-COR Odyssey near-infrared fluorescence detection system was the method of choice for its wide linear detection range (4—5 orders of magnitude) and low background. Moreover, this approach allows for detecting two proteins of interest in two separate channels on one membrane, increasing the precision of subsequent quantification.

2.4 Questions to be answered—a detailed description

2.4.1.1 Does increasing expression of human iRhom2 have an effect on protein levels of EGF receptor ligand precursors?

Rationale: In the study of (Zettl *et al.*, 2011), overexpressed human iRhom1 and mouse iRhom2 were reported to diminish the levels of various EGF receptor ligands. However, the concentration-dependence of this effect was shown only for EGF. The aim therefore was to explore whether human iRhom2 affects EGFR ligands in the same, concentration-dependent way. Two EGFR ligands, EGF and TGFα, were tested in this thesis.

2.4.1.2 Is the observed effect of human iRhom2 overexpression iRhom2-specific?

Rationale: The effect of iRhom2 overexpression in diminishing EGFR ligands could be a consequence of an overload of the ER with an overexpressed polytopic membrane protein, for an overexpressed iRhom2 localises predominantly to the ER (see **section 1.3.2**). Therefore, other ER-resident proteins structurally similar to iRhom2 were tested. In the Zettl *et al.*, 2011 study, the inactive KDEL-tagged mutant of Rhomboid2 (Rhomboid2-SA-KDEL) and a polytopic rhomboid-like family unrelated protein, Unc93B, were shown to have no effect on EGF protein levels. The aim was to scrutinise a wider repertoire of ER-resident polytopic membrane proteins. In addition to Rhomboid2-SA-KDEL and Unc93B, both the active and the inactive mutant of the ER-resident protease Rhomboid4 were assessed in this thesis.

2.4.1.3 Is the effect of human iRhom2 overexpression specific towards EGFR ligands?

Rationale: The effect of iRhom2 overexpression might not be restricted to EGF receptor ligands, but might also present with other ER-resident, type I transmembrane proteins. In the work of Zettl *et al.*, 2011, the levels of WNT3 and Delta, both type I transmembrane proteins, were shown to be unaffected by increasing iRhom concentration. In this thesis, other topologically similar proteins were tested, namely basal cell adhesion molecule (BCAM), serine peptidase inhibitor Kunitz type 1 (SPINT1) and basigin (BSG).

2.4.1.4 Is the effect of human iRhom2 overexpression influenced by ADAM17 coexpression?

Rationale: iRhom2 in complex with ADAM17 positively regulates EGF receptor signalling by promoting ADAM17 trafficking through the secretory pathway and by mediating rapid activation of ADAM17 at the plasma membrane (see **section 1.3.3.2**). I therefore speculated that upon high levels of ADAM17, the effect of overexpressed iRhom2 in diminishing EGFR ligands might be reduced. This hypothesis would ensure that when ADAM17 is expressed, the production of EGFR ligands, many of which are ADAM17 substrates, is not suspended. However, upon low levels of ADAM17, which could be sensed by ER-resident, uncomplexed iRhom2, the levels of EGFR ligands would be downregulated by iRhom2 in order to prevent the accumulation of EGFR ligand precursors at the plasma membrane and hence potentially harmful auto- or juxtacrine EGFR signalling (**Figure 2.1**). To see whether the disappearance of EGF in the presence of overexpressed iRhom2 would be rescued by ADAM17 overexpression, ADAM17 was coexpressed with increasing concentration of iRhom2. The impact of ADAM17 overexpression on the EGF protein levels upon iRhom2 overexpression was studied in wild-type as well as in the iRhom1 and 2 double knock-out (DKO) HEKs.

2.4.1.5 Is the effect of human iRhom2 overexpression on the levels of EGFR ligands caused by enhanced degradation of its client proteins?

Rationale: The disappearance of EGFR ligands upon iRhom2 overexpression could be due to their enhanced degradation. In principle, there are two major ways of disposal of membrane proteins, the lysosome-dependent pathway and the proteasome-dependent pathway. If overexpressed iRhom2 indeed promotes degradation of its client proteins, inhibition of either of the degradation pathways would rescue the effect. The lysosomal pathway was inhibited with 100 nM bafilomycin. However, the proteasome-dependent degradation of ER-

resident membrane proteins occurs mainly through the ERAD machinery, and fruit fly iRhom was shown to participate in this process (Zettl *et al.*, 2011). In order to avoid misfolded soluble protein accumulation and hence reduce the stress caused by the treatment, a specific inhibitor of ERAD pathway, CB-5083, was used instead of an inhibitor of proteasomes.

Figure 2.1: An illustration of the hypothesis proposed in **paragraph 2.4.1.4**. When the expression of ADAM17 is high (upper part of the scheme), iRhom is occupied by promoting its trafficking through the secretory pathway and mediates stimulated ADAM17 activation at the plasma membrane. Upon low levels of ADAM17 (lower part of the scheme), iRhom is occupied by decreasing the levels of EGFR ligands, probably through enhancing their degradation. Drawing by the author.

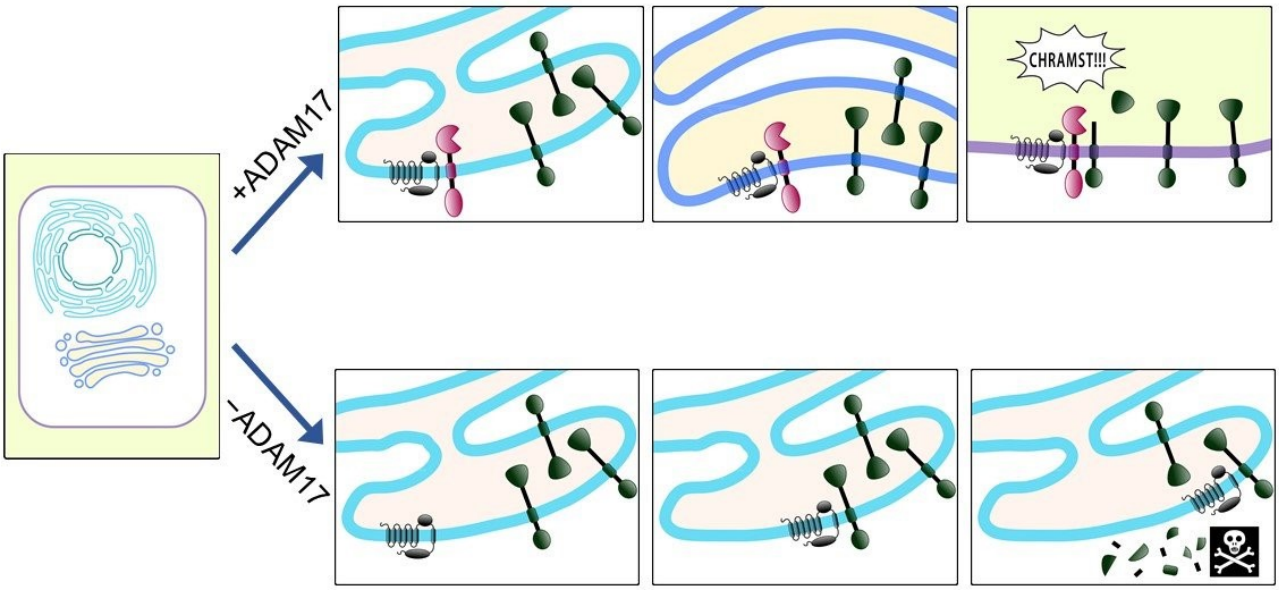

3 Materials and methods

3.1 Chemicals and media

Cell culture and transfection:

- DMEM: Gibco #2026729
- FBS: Gibco #10270106
- PBS: Gibco #70011036
- X-tremeGENE HP DNA Transfection reagent: Sigma #06366546001
- FuGENE® HD: Promega #E2692
- Bafilomycin A1: Enzo Life Sciences
- CB-5083: Cayman Chemical Company #19311

Cell lysis and protein concentration analysis

- Tris: Sigma #T1503
- SDS: BioRad #161-0302
- LiDS: Sigma #L9781
- Glycerol: Penta #56-81-5
- β-mercaptoethanol: Sigma #M3148
- Bromophenol blue: Sigma #B5525
- cOmplete™ protease inhibitors: Roche #33576900
- Pierce universal nuclease: Thermo #88701
- $MgCl_2$: NEB #B0510A

Deglycosylation:

- Glycobuffer 2: NEBioLabs #B3704S
- NP-40: NEBioLabs #B3704S
- PNGase F: NEBioLabs #P0704L

Western blotting:

- Tris: Sigma #T1503
- Glycine: Sigma #G8898
- Color protein standard: NEB #P7712
- Methanol: Sigma #67-56-1
- Immobilon®-FL: Sigma #IPVH00010
- Pierce 660 nm Protein Assay reagent: Thermo #22660
- Ionic Detergent Compatibility reagent: Thermo #22663
- Pre-diluted Protein Assay Standards: Thermo #23208
- Blocker™ Casein in TBS: Thermo #37532
- NaCl: Penta #7647-14-5
- Tween®: Sigma #1002684474
- REVERT™ Total Protein Stain: LI-COR #926-11010

Antibodies:

Primary
- HA tag: Roche #11583816001
- STREP tag: Qiagen #34850
- Myc tag: CST #2278S

- αtubulin: CST #3873S
- Rhomboid2: Proteintech #12467-1-AP
- iRhom2: Abcam #ab116139

Secondary

- Goat anti-Rat IgG (H&L) Antibody - IRDye680LT: LI-COR #925-68029
- IRDye 680RD Goat anti-Mouse IgG: LI-COR #925-68070
- IRDye 680RD Goat anti-Rabbit IgG: LI-COR #925-68071
- Donkey anti-Rabbit IgG (H+L) Cross-Adsorbed Secondary Antibody, DyLight 800: Thermo #SA5-10044
- Donkey anti-Mouse IgG (H+L) Cross Adsorbed Secondary Antibody, DyLight 800: Thermo #SA5-10172

3.2 Buffers and solutions

I. SDS-PAGE sample buffer

To make 6× concentrated solution:

- 350mM Tris pH 6.8
- 30% (v/v) Glycerol
- 10% (w/v) SDS
- 16,6% (v/v) ß-mercaptoethanol
- A pinch of bromophenol blue
- Distilled water to 10 ml

To make 1× sample buffer, 8.33 ml of the 6× buffer was dissolved in 41.8 ml of milli-Q water and one tablet of cOmplete^{TM} protease inhibitors was added.

II. LiDS sample buffer

To make 4× concentrated solution:

- 277.8mM Tris-HCl pH 6.8
- 4.4% (w/v) LiDS
- 44.4% (v/v) Glycerol
- 10% (v/v) β-mercaptoethanol
- A pinch of Bromophenol blue

III. SDS-PAGE running buffer

- 25 mM Tris
- 192 mM Glycine
- 0.1% (w/v) SDS

IV. Immunoblotting transfer buffer

- 12.5 mM Tris
- 96 mM Glycine
- 5% (v/v) Methanol
- 0.01% (w/v) SDS

V. Tris-buffered saline (TBS)

- 50 mM Tris
- 137 mM NaCl pH 7.6

VI. TBS-Tween (TBS-T)

- TBS solution with 0.1% (v/v) Tween® 20

3.3 Cell lines

HEK293ET cells (referred to as wild-type HEKs) were obtained from ATCC. The iRhom1 and 2 double knock-out HEK293 cells (referred to as DKO HEKs) were kindly provided by Miguel Cavadas from the Colin Adrain laboratory.

3.4 DNA constructs

Insert	Vector	Reference/Source
Spitz signal peptide–STREP–His mEGF	pcDNA3.1	Cloned in our laboratory
Spitz signal peptide–STREP–His–hBCAM	pcDNA3.1	Johnson *et al.*, 2017
Spitz signal peptide–STREP–His–hSPINT1	pcDNA3.1	Johnson *et al.*, 2017
Spitz signal peptide–STREP–His–hBSG	pcDNA3.1	Johnson *et al.*, 2017
hiRhom2–HA	pcDNA3.1	Cloned in our laboratory
hRhomboid2(SA)–KDEL	pcDNA3.1	Cloned in our laboratory
hRhomboid4–HA	pcDNA3.1	Cloned in our laboratory
hRhomboid4(SA)–HA	pcDNA3.1	Cloned in our laboratory
hUnc93B–HA	pcDNA3.1	Obtained from Colin Adrain laboratory
Spitz signal peptide–myc–hTGFα	pcDNA3.1	Adrain *et al.*, 2012
hADAM17–myc	pRK5	Addgene – pRK5M (Liu *et al.*, 2009)

3.5 Methods

3.5.1 Cell culture and transfection

HEK293ET cells (or the DKO HEK cells) were plated at 3×10^5 cells/well and cultured in 2.5 ml DMEM + 10 % FBS (v/v) in 6-well tissue culture plates. After 24 hours, they were transfected with Fugene6 or X-

tremeGENE HP DNA Transfection reagent in serum free DMEM according to manufacturer's protocol, using the following ratio of 2.5 µg DNA:7.5 µl of transfection reagent:250 µl of serum-free medium. After 24 hours from transfection, the medium was removed and lysosomal (bafilomycin 100 nM) or ERAD (CB-5083 1 µM) inhibitors dissolved in 2 ml serum free medium (SFM; DMEM without FBS) were added and left for either 6 (CB-5083) or 24 hours (bafilomycin).

3.5.2 Harvesting the samples

Next, 48 hours post transfection (in the case of ERAD inhibition 30 hours) the medium was removed and cell monolayers were lysed with 150 µl SDS-PAGE sample buffer containing 20 mM $MgCl_2$ and Pierce universal nuclease (1:1000). Samples were denatured for 10 minutes at 65 °C. For assays with hUnc93B, LiDS sample buffer was used, harvesting was done on ice and the denaturation step was omitted.

3.5.3 Deglycosylation

Samples containing proteins whose glycosylation prevented them from making clear bands on the membrane (Unc93B, BSG, TGFα) were deglycosylated. For each reaction, 15 µl of the sample was incubated with 2 µl of Glycobuffer2 and 2 µl of NP-40 and 1 µl of PNGase F for one hour at 37 °C.

3.5.4 Protein concentration analysis

Protein concentrations were measured using the Pierce 660nm Protein Assay protocol with Ionic Detergent Compatibility Reagent (IDCR) according to the manufacturer's protocol.

3.5.5 SDS-PAGE electrophoresis and Western blotting

Samples were separated on either 7.5 % or 12 % polyacrylamide gels for 70 minutes at 150 V at 4 °C and then transferred onto Immobilon FL membranes for 90 minutes at 80 V at room temperature with cooling.

3.5.6 Membrane immunostaining

After transfer, membranes were washed with Tris buffered saline (TBS). Membranes of interest (*i. e.*, those intended to be quantified) were stained with REVERT™ Total Protein Stain, visualized on LI-COR and destained. All membranes were then blocked in Casein blocker for 1 hour at room temperature and incubated for 16 hours at 4 °C with primary antibodies diluted 1:1000 (HA, Myc, FLAG, αtubulin, Rhomboid2, iRhom2) or 1:2000 (STREP) in Casein blocker containing 0.1 % (v/v) Tween. After three washes with TBS-T, membranes were incubated with secondary antibodies diluted in Casein blocker containing 0.1 % Tween for at least 1 hour in the dark at room temperature. After washing with TBS-T (3×) and TBS (1×), the membranes were dried and imaged using near-infrared fluorescence (Odyssey® CLx imaging system).

3.5.7 Fluorescent signal quantification

Images were quantified using Image Studio™ Lite software (LI-COR). First, the total protein signal from the REVERT-stained membrane was quantified (**Figure 3.1A**). The background, defined by the average signal from the rectangle in the upper right corner, was subtracted from each lane. Next, the signal from the bands of interest was quantified, both in the 680 nm channel (**Figure 3.1B**) and in the 800 nm channel (**Figure 3.1C**). Here, the background was defined as the median pixel intensity in the area around each band of interest.

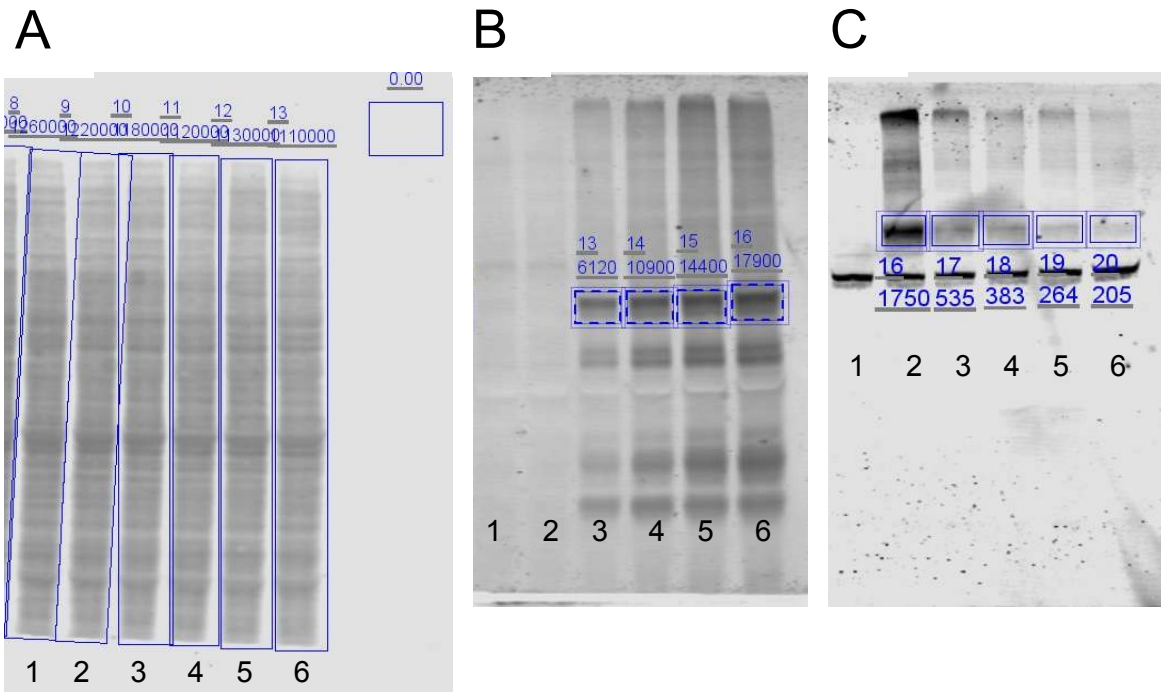

Figure 3.1: Quantification of the total protein amount (**A**) and of the bands of interest in the 680 nm channel (**B**) and the 800 nm channel (**C**). The numbering of the rectangles is different for each channel due to the different number of analysed shapes.

The signal from the 680 nm and the 800 nm channel was normalised to the total protein amount in the corresponding lane (columns 680/Revert and 800/Revert in **Table 3.1**). The signal from the 800 nm channel was then converted to the percent of the normalised signal from the lane 2 (sample where only protein detected in the 800 nm channel was transfected). The values from the 680/Revert column, corresponding to relative protein levels of the protein of interest, were then plotted on the x-axis (**Figure 3.2**). The percent values of the 800 nm signal were plotted on the left y-axis and the relative protein levels corresponding to the values in the 800/Revert column on the right y-axis. Graphs were made in GraphPad Prism software.

Table 3.1: The example values obtained by analysis in Image Studio Lite software. In the lane 2, the signal from the 680 channel was considered as zero for the construct with the protein of interest was not transfected into the cells.

Lane no.	Revert	800	800/Revert	680	680/Revert	800/Revert %
2	1221329.376	1748.734375	0.001431829	0	0	100.00
3	1183206.785	534.8457031	0.000452031	6119.625	0.005172067	31.57
4	1117027.333	383.0107422	0.000342884	10899.19531	0.009757322	23.95
5	1132918.877	263.9824219	0.000233011	14442.1875	0.012747768	16.27
6	1109351.077	205.2929688	0.000185057	17901.51953	0.016136929	12.92
			Right y-axis		x-axis	Left y-axis

Figure 3.2: An example graph where the values from the quantitative immunoblot analysis (**Table 3.1**) are plotted.

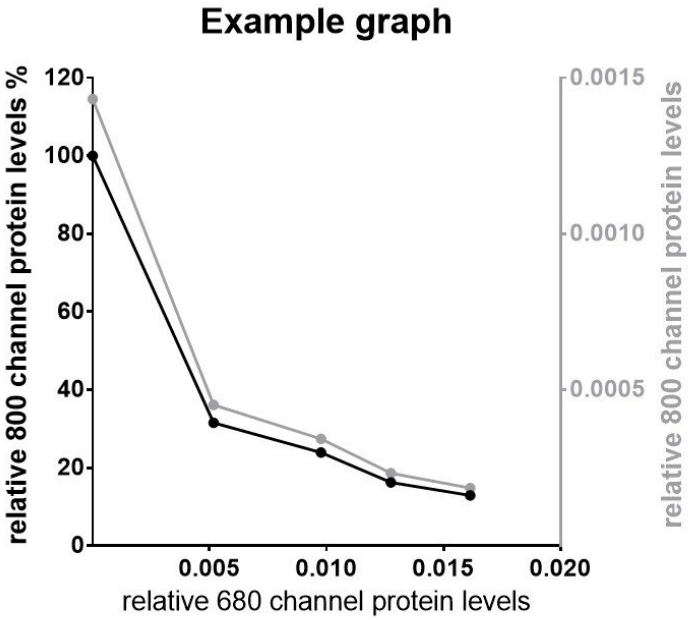

4 Results

To confirm the effect of iRhom2 overexpression on the protein levels of EGFR ligands, iRhom2 was coexpressed with EGF in HEK cells (**Figure 4.1**). In this and in all the following experiments, the amounts of transfected iRhom2 DNA ranged from 250 to 1500 ng, as indicated above the immunoblots. As shown by **Figure 4.1**, the amount of EGF decreased with increasing iRhom2 levels. Another EGFR ligand, TGFα, was tested in the same assay (**Figure 4.2**). In immunoblot **4.2A**, only the uppermost TGFα band seems to be affected by increasing concentrations of iRhom2, whereas in immunoblot **4.2B**, the levels of all the TGFα species decrease. Therefore, due to the better reproducibility of the results, EGF was used in the following experiments.

Next, the specificity of the observed effect was assessed. To see if overexpression of other polytopic ER-resident proteins reduces the levels of EGF, EGF was overexpressed either with a KDEL-tagged[8] mutant of Rhomboid2 (Rhomboid2-SA-KDEL; **Figure 4.3**), with wild-type Rhomboid4 (**Figure 4.4**), with the Rhomboid4 inactive mutant (Rhomboid4-SA; **Figure 4.5**) or with Unc93B (**Figure 4.6**). Both inactive mutants Rhomboid2-SA-KDEL and Rhomboid4-SA had the same effect as iRhom2, for EGF levels diminished with an increasing concentration of the mutant rhomboid proteases (**Figures 4.3** and **4.5**). Contrary to that, the overexpression of the Rhomboid4 did not cause EGF disappearance, rather, it seemed to stabilise or even upregulate EGF levels (**Figure 4.4**). In the case of Unc93B, a protein unrelated to the rhomboid-like family, EGF was poorly detectable in both immunoblots, which complicated assessment of changes of its levels (**Figure 4.6**). Based on these data, iRhom2 seems not to be the only polytopic ER-resident protein which influences the amount of EGF. At the same time, the disappearance of EGF in the presence of iRhom2 is not a general effect of the overexpression of any polytopic ER-resident protein (**Figure 4.4**).

The disappearance of EGFR ligands upon overexpression of iRhom2 was surprising and I sought to investigate the specificity of this effect. iRhom2 was coexpressed with type I transmembrane proteins, which are not EGF receptor ligands. In the case of BCAM (**Figure 4.7**), a decrease of BCAM protein levels was observed, although it was not as dramatic as with EGF (**Figure 4.1**). The amount of another potential iRhom2 client protein tested, SPINT1, was not significantly affected (**Figure 4.8A**), or rather slightly increased (**Figure 4.8B**) in the presence of overexpressed iRhom2. In the case of basigin (BSG; **Figure 4.9**), the diminishing effect of iRhom2 overexpression was also observed, however, the decrease of BSG levels was again not as pronounced as with EGF levels (**Figure 4.1**).

Next, the impact of ADAM17 overexpression on the disappearance of EGF upon increasing levels of iRhom2 was assessed. In wild-type HEKs, ADAM17 overexpression did not reverse the effect of overexpressed iRhom2 on EGF (**Figure 4.10**). However, when the same effect of EGF disappearance upon increasing

[8] The proteolytically inactive mutant was chosen in order to prevent possible EGF cleavage by Rhomboid2 (Adrain *et al.*, 2011). The KDEL tag ensures that Rhomboid2 stays in the ER and does not continue to other compartments of the secretory pathway, mimicking the cellular localisation of overexpressed iRhom2 (Matsukawa *et al.*, 2012).

concentration of iRhom2 was reproduced in iRhom1 and 2 double knock-out (DKO) HEKs (**Figure 4.11A**), which were not available in our laboratory at the time the experimental work for this thesis was started, ADAM17 coexpression rescued the EGF levels (**Figure 4.11B**). However, the DKO HEK were growing at a slower rate than the WT HEKs and were dying extensively upon transfection, which complicated the experimental work. That is why the WT HEKs were used again in the following experiments.

The last question to be answered was what mechanism underlies the disappearance effect of overexpressed iRhom2 on EGF levels. To test if EGF degradation is promoted by iRhom2, inhibition of lysosomes and the ERAD pathway was performed. Upon treatment with 100 nM bafilomycin (reported in Musiwaro *et al.*, 2013), the inhibitor of lysosomal acidification, the levels of EGF still decreased with increasing iRhom2 amount (**Figure 4.12**). The ERAD pathway was inhibited by the VCP/p97 inhibitor CB-5083, whose working concentration of 1 μM was determined in a kill curve experiment (**Figure 4.14A**). The accumulation of BSG, an ERAD substrate, was used as a read-out of successful inhibition of this degradation pathway (Tyler *et al.*, 2012). However, even CB-5083 had no effect on iRhom2 overexpression-triggered disappearance of EGF (**Figure 4.13**). The inhibition of proteasomes was not performed due to the limited time for the thesis completion.

The result of a preliminary experiment where the endogenous and transfected iRhom2 expression was compared is shown in **Figure 4.14B**. The anti iRhom2 antibody detected multiple species together with two non-specific bands, which raises doubts about its specificity. Surprisingly, the bands that could represent endogenous iRhom2, for they do not appear in the DKO HEK lysate (lane 1), have substantially different molecular weights than expected. One possible explanation might be that endogenous iRhom2 undergoes proteolytic processing or some hitherto undescribed posttranslational modifications. The other option is that the antibody binds to proteins whose expression is downregulated in the DKO HEKs. Neverthless, if the nearly 130-kDa species indeed corresponds to iRhom2, it might be concluded that the amount of endogenous and tagged iRhom2 is in the same order of magnitude (quantification in **Figure 4.14C**).

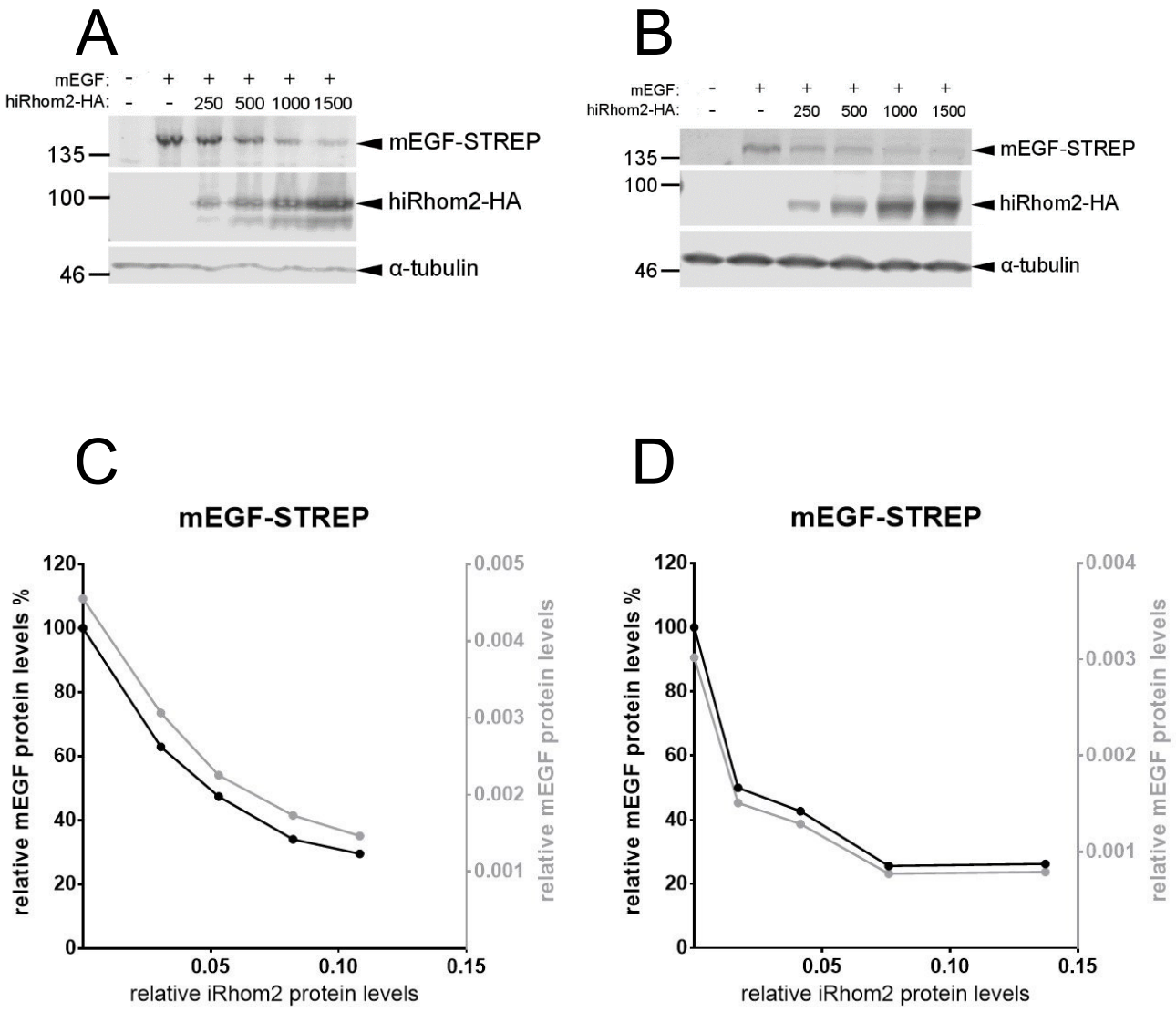

Figure 4.1: Effect of iRhom2 overexpression on mouse EGF (mEGF) in WT HEKs. (**A, B**) Immunoblots from cell lysates containing a varying amount of iRhom2. The amount of transfected human iRhom2-HA construct ranged from 250 to 1500 ng DNA. Molecular weights are indicated in kDa. (**C, D**) Quantifications of the immunofluorescent signal were performed in Image Studio™ Lite software (LI-COR). The signal from mEGF-STREP was normalised to the signal from the total protein amount in the corresponding lane and is indicated in percent, where the signal from the lane with mEGF alone is considered as 100 %. The signal from hiRhom2-HA was normalised to the total protein amount in the corresponding lane. For details see materials and methods.

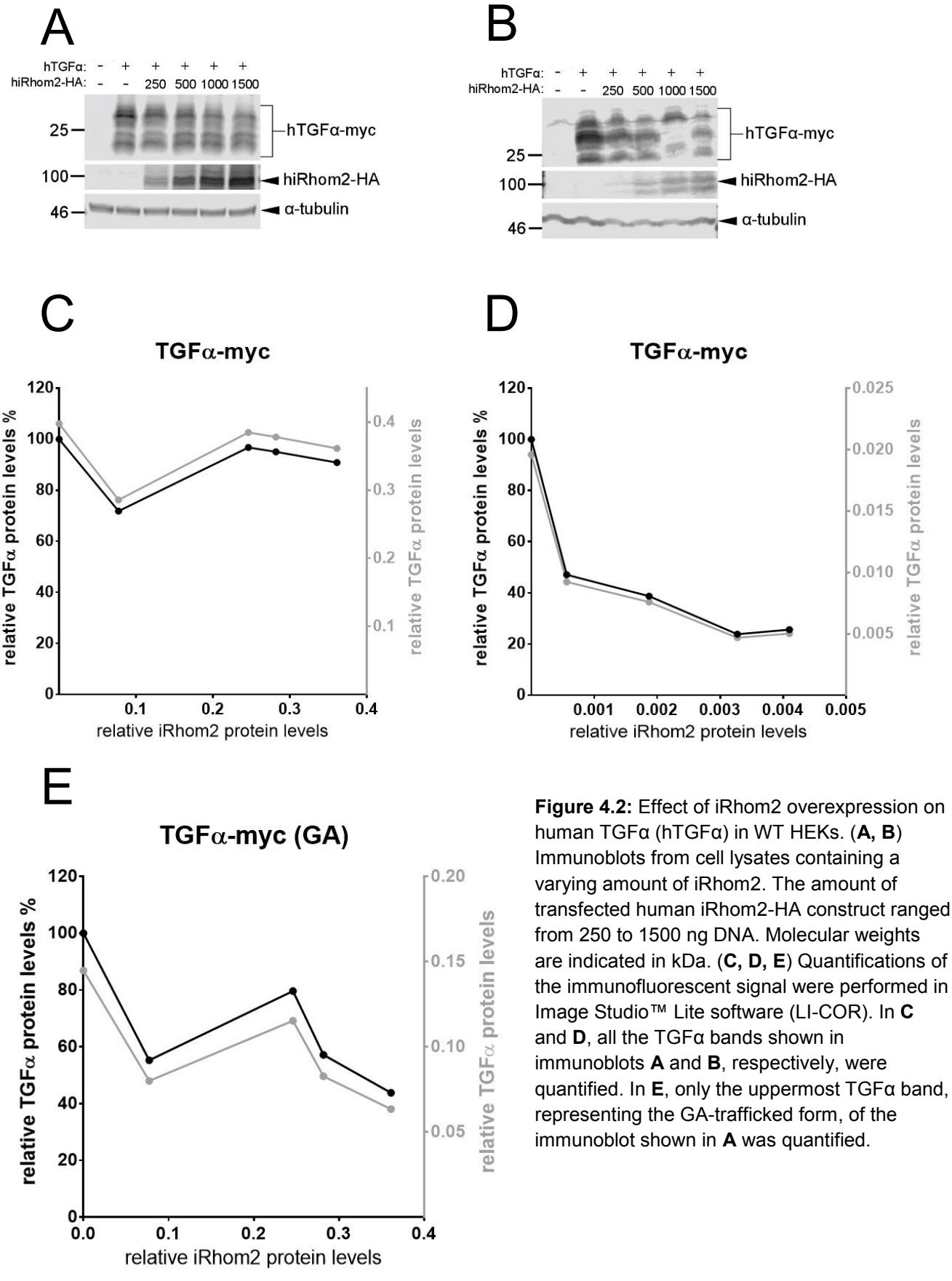

Figure 4.2: Effect of iRhom2 overexpression on human TGFα (hTGFα) in WT HEKs. (**A, B**) Immunoblots from cell lysates containing a varying amount of iRhom2. The amount of transfected human iRhom2-HA construct ranged from 250 to 1500 ng DNA. Molecular weights are indicated in kDa. (**C, D, E**) Quantifications of the immunofluorescent signal were performed in Image Studio™ Lite software (LI-COR). In **C** and **D**, all the TGFα bands shown in immunoblots **A** and **B**, respectively, were quantified. In **E**, only the uppermost TGFα band, representing the GA-trafficked form, of the immunoblot shown in **A** was quantified.

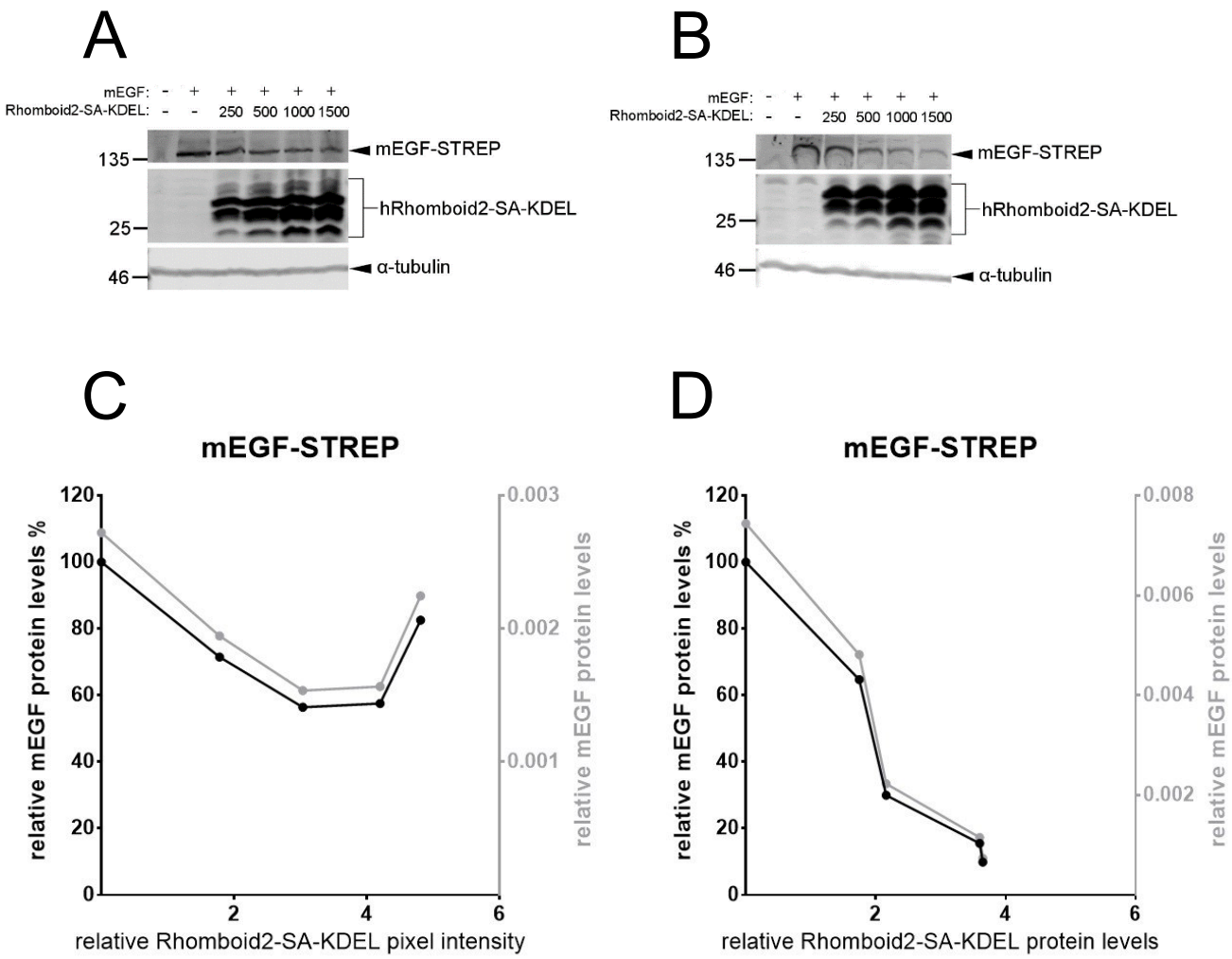

Figure 4.3: Effect of a KDEL-tagged inactive mutant of human Rhomboid2 (Rhomboid2-SA-KDEL) overexpression on mEGF in WT HEKs. (**A, B**) Immunoblots from cell lysates containing a varying amount of Rhomboid2-SA-KDEL. The amount of transfected Rhomboid2-SA-KDEL construct ranged from 250 to 1500 ng DNA. Molecular weights are indicated in kDa. (**C, D**) Quantifications of the immunofluorescent signal were performed in Image Studio™ Lite software (LI-COR).

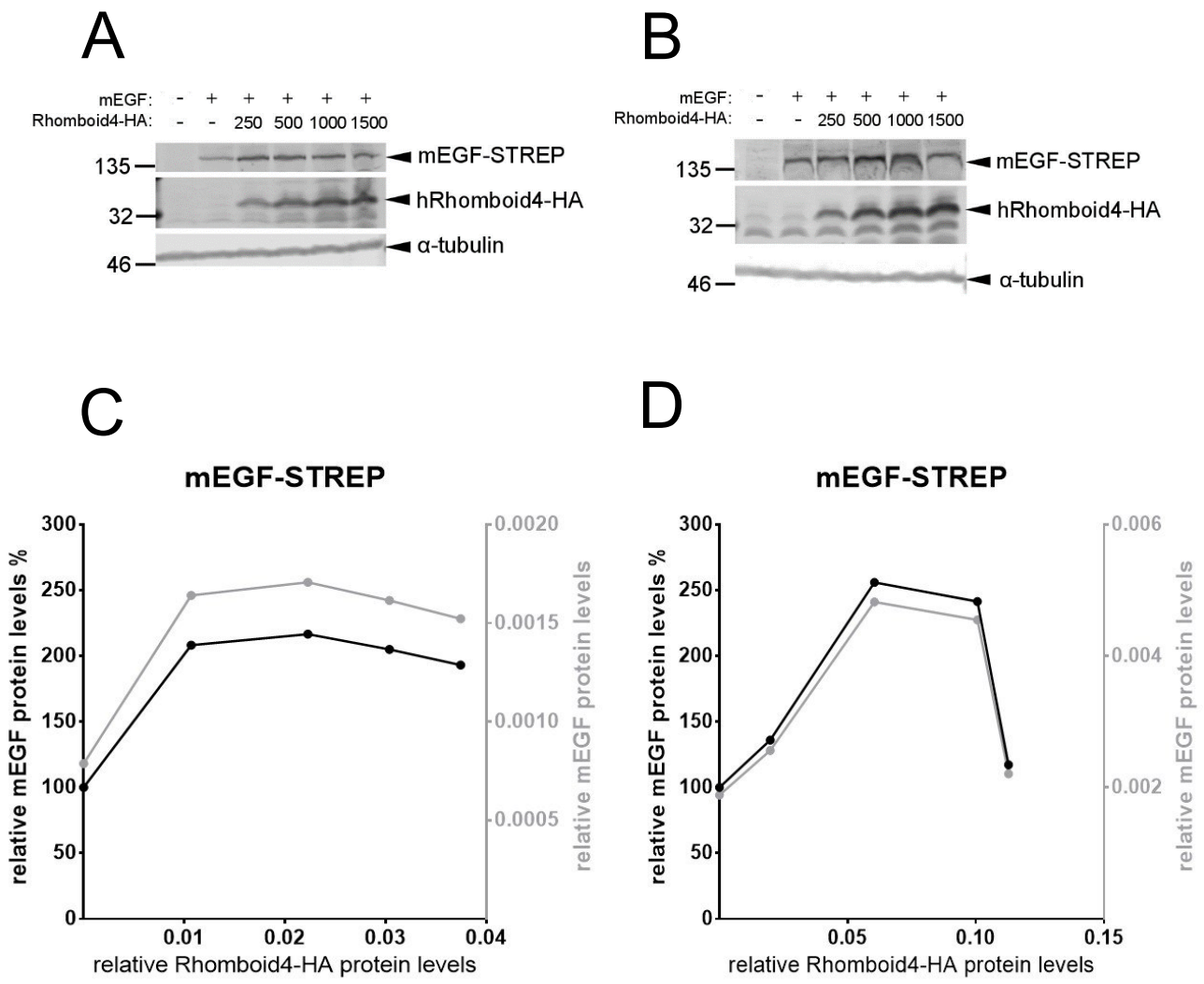

Figure 4.4: Effect of human Rhomboid4-HA overexpression on mEGF in WT HEKs. (**A, B**) Immunoblots from cell lysates containing a varying amount of Rhomboid4-HA. The amount of transfected human Rhomboid4-HA construct ranged from 250 to 1500 ng DNA. Molecular weights are indicated in kDa. (**C, D**) Quantifications of the immunofluorescent signal were performed in Image Studio™ Lite software (LI-COR).

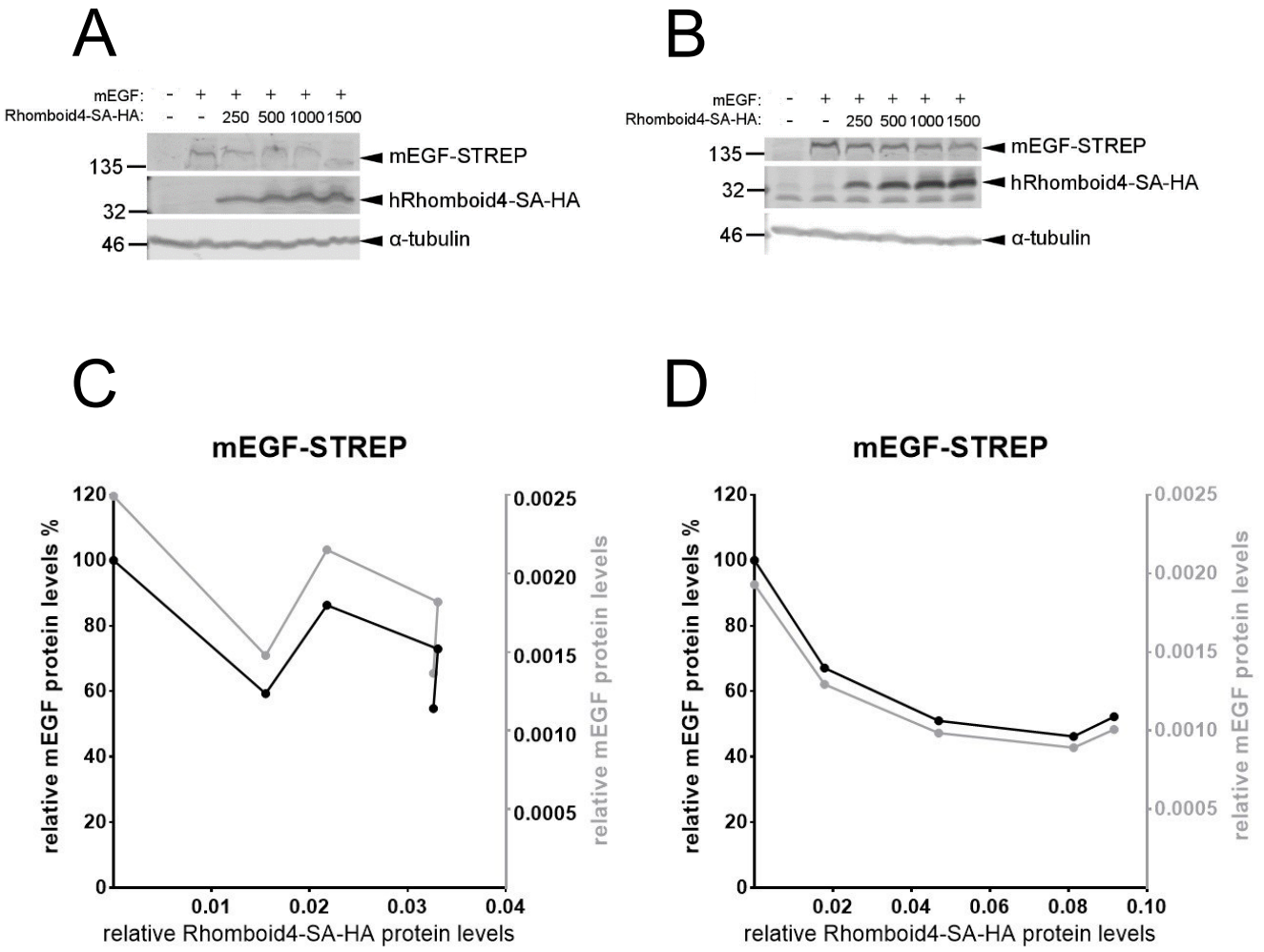

Figure 4.5: Effect of human Rhomboid4-SA-HA overexpression on mEGF in WT HEKs. (**A, B**) Immunoblots from cell lysates containing a varying amount of Rhomboid4-SA-HA. The amount of transfected human Rhomboid4-HA construct ranged from 250 to 1500 ng DNA. Molecular weights are indicated in kDa. (**C, D**) Quantifications of the immunofluorescent signal were performed in Image Studio™ Lite software (LI-COR).

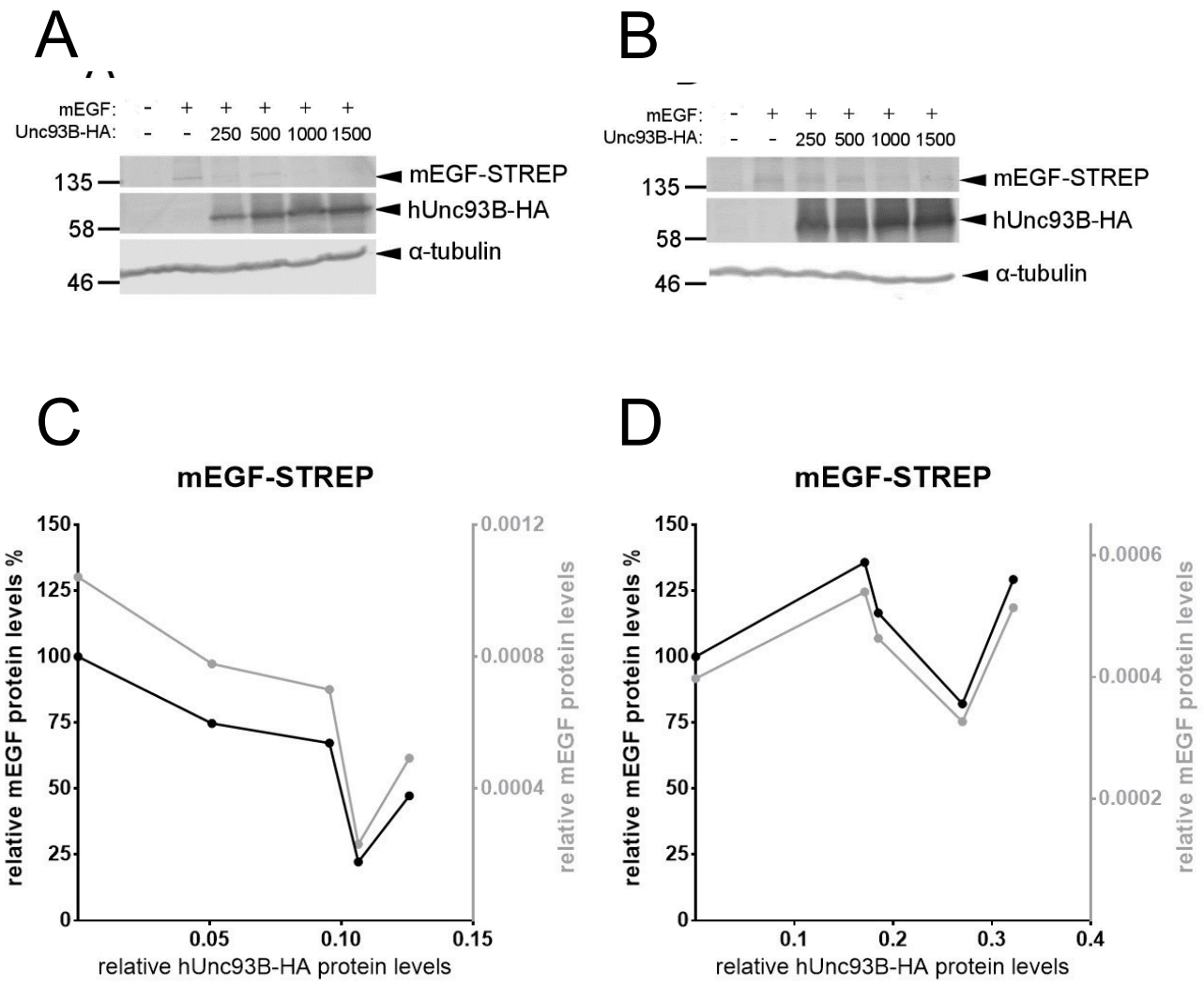

Figure 4.6: Effect of human Unc93B-HA (hUnc93B-HA) overexpression on mEGF in WT HEKs. (**A, B**) Immunoblots from cell lysates containing a varying amount of hUnc93B-HA. The amount of transfected human hUnc93B-HA construct ranged from 250 to 1500 ng DNA. Molecular weights are indicated in kDa.
(**C, D**) Quantifications of the immunofluorescent signal were performed in Image Studio™ Lite software (LI-COR).

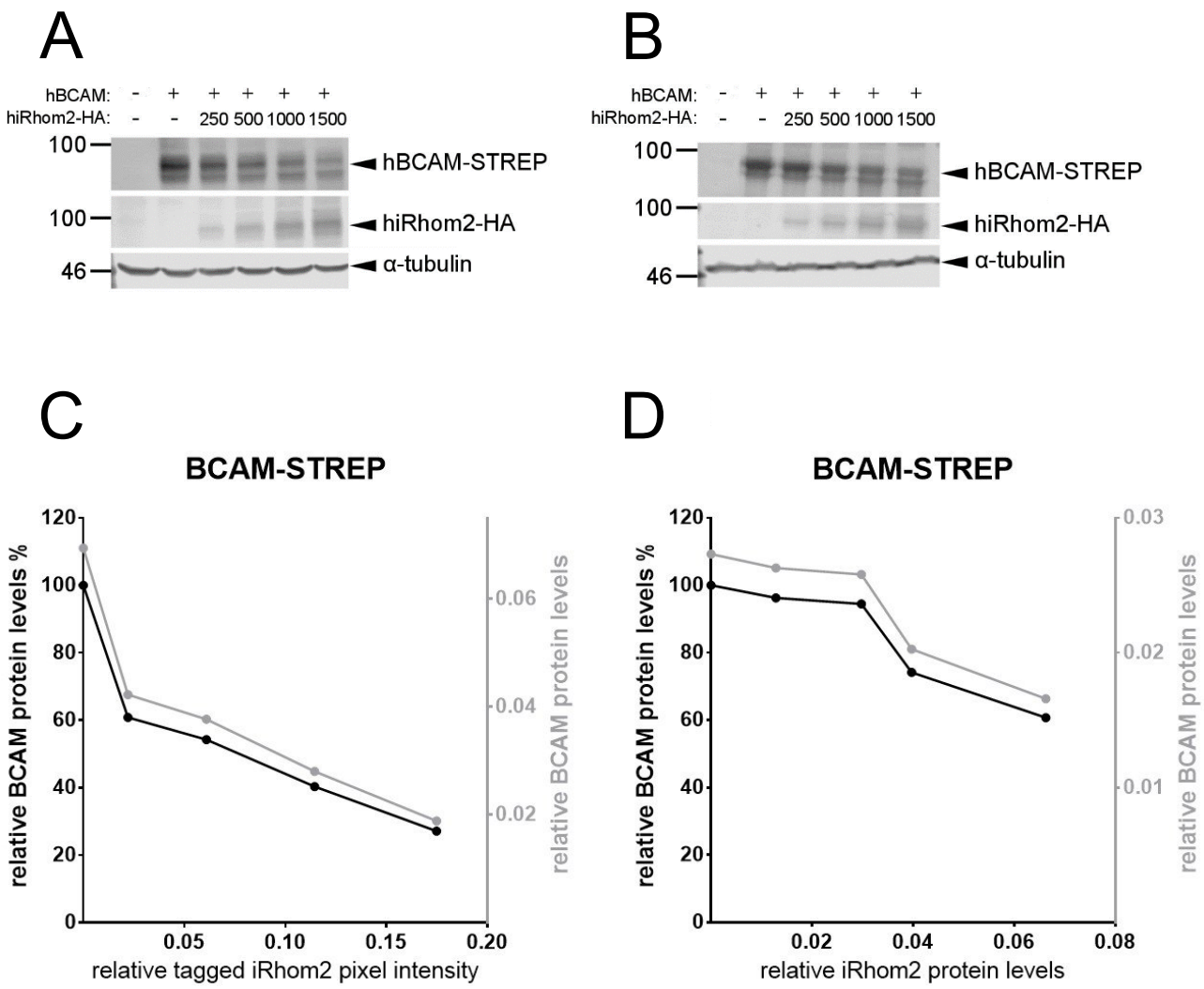

Figure 4.7: Effect of iRhom2 overexpression on human BCAM in WT HEKs. (**A, B**) Immunoblots from cell lysates containing a varying amount of iRhom2. The amount of transfected human iRhom2-HA construct ranged from 250 to 1500 ng DNA. Molecular weights are indicated in kDa. (**C, D**) Quantifications of the immunofluorescent signal were performed in Image Studio™ Lite software (LI-COR).

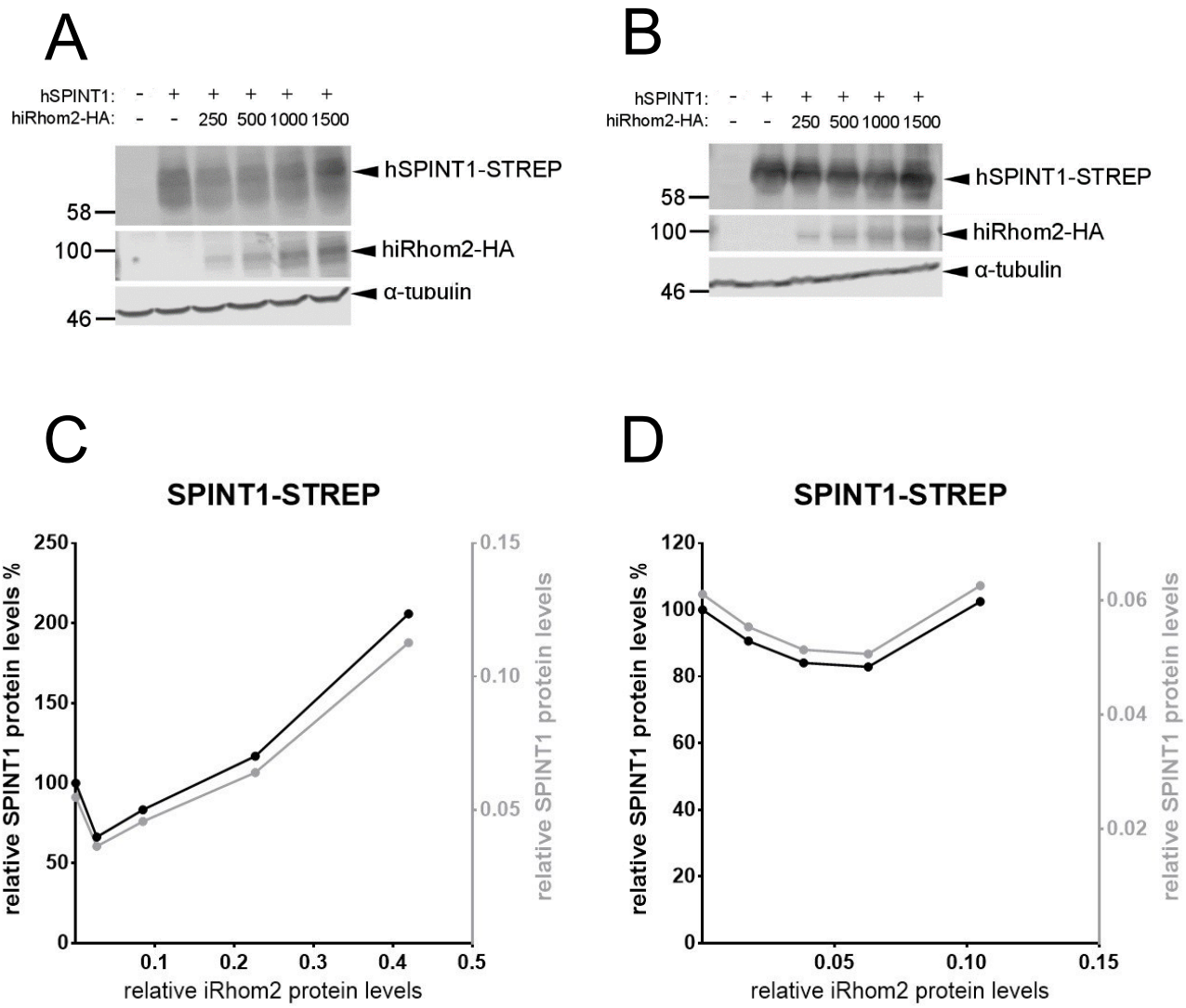

Figure 4.8: Effect of iRhom2 overexpression on human SPINT1 in WT HEKs. (**A, B**) Immunoblots from cell lysates containing a varying amount of iRhom2. The amount of transfected human iRhom2-HA construct ranged from 250 to 1500 ng DNA. Molecular weights are indicated in kDa. (**C, D**) Quantifications of the immunofluorescent signal were performed in Image Studio™ Lite software (LI-COR).

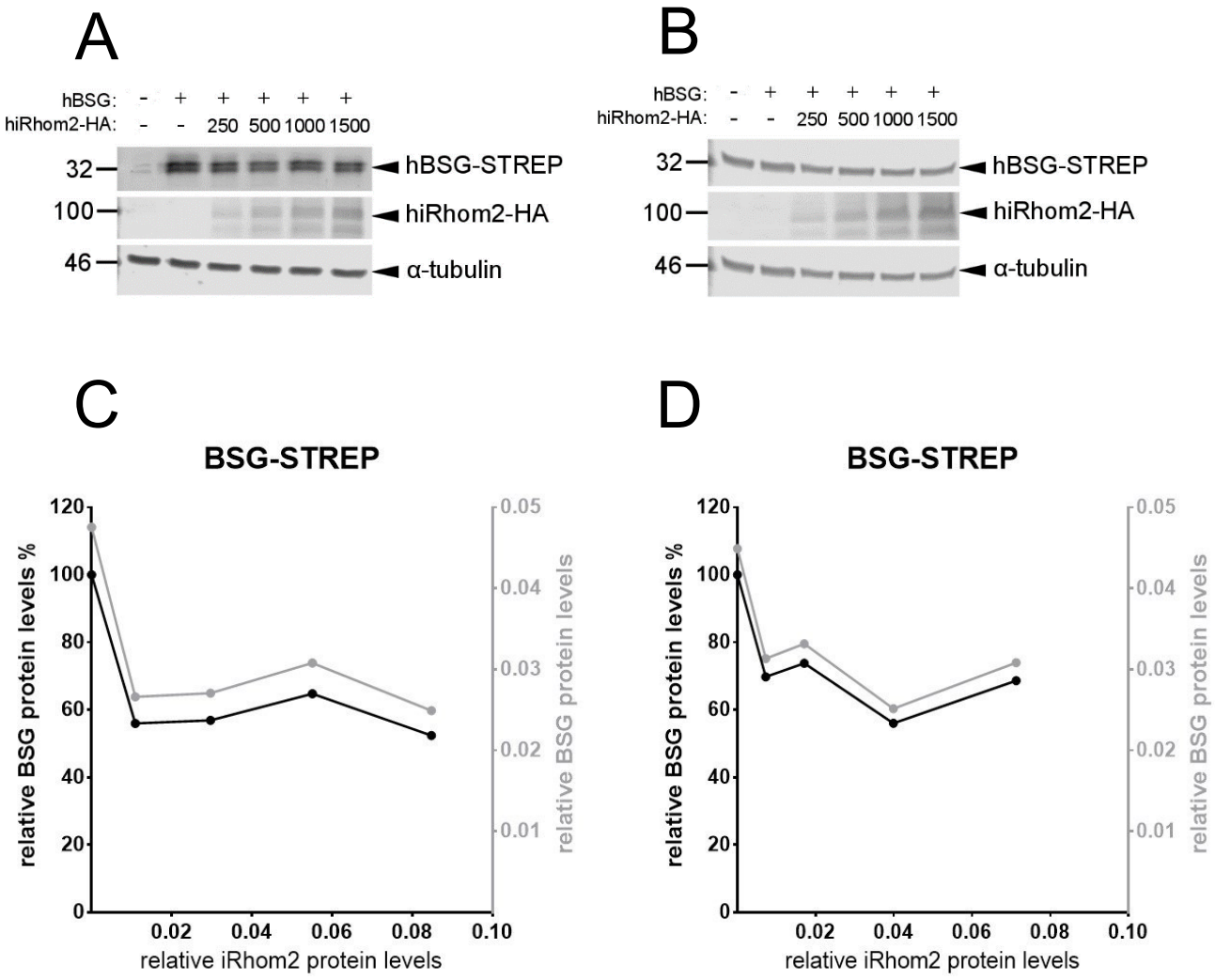

Figure 4.9: Effect of iRhom2 overexpression on human BSG in WT HEKs. (**A, B**) Immunoblots from cell lysates containing a varying amount of iRhom2. The amount of transfected human iRhom2-HA construct ranged from 250 to 1500 ng DNA. Molecular weights are indicated in kDa. (**C, D**) Quantifications of the immunofluorescent signal were performed in Image Studio™ Lite software (LI-COR).

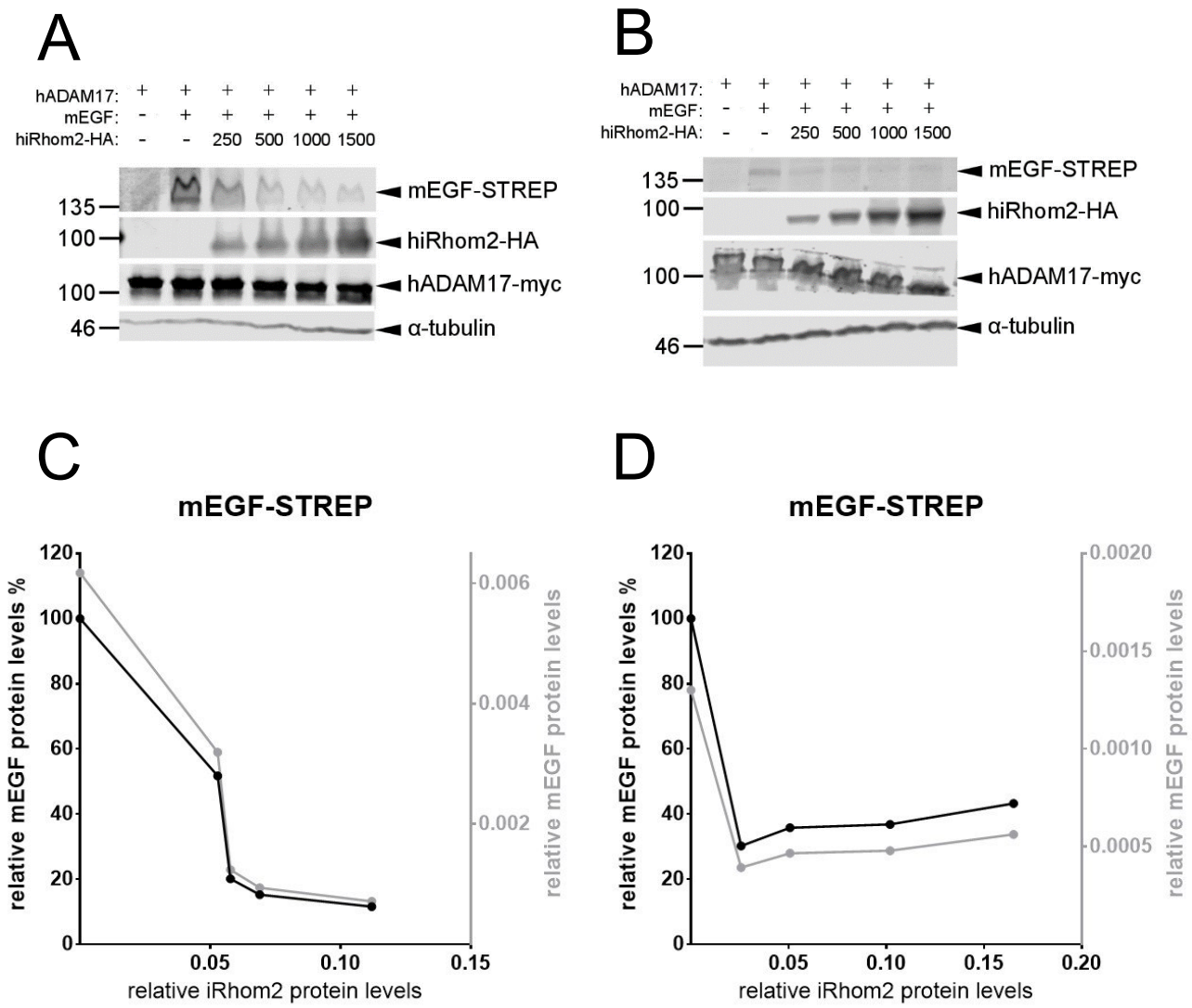

Figure 4.10: Effect of human ADAM17 coexpression on mEGF disappearance in the presence of hiRhom2-HA in WT HEKs. (**A, B**) Immunoblots from cell lysates containing a varying amount of iRhom2. The amount of transfected human iRhom2-HA construct ranged from 250 to 1500 ng DNA. Molecular weights are indicated in kDa. (**C, D**) Quantifications of the immunofluorescent signal were performed in Image Studio™ Lite software (LI-COR).

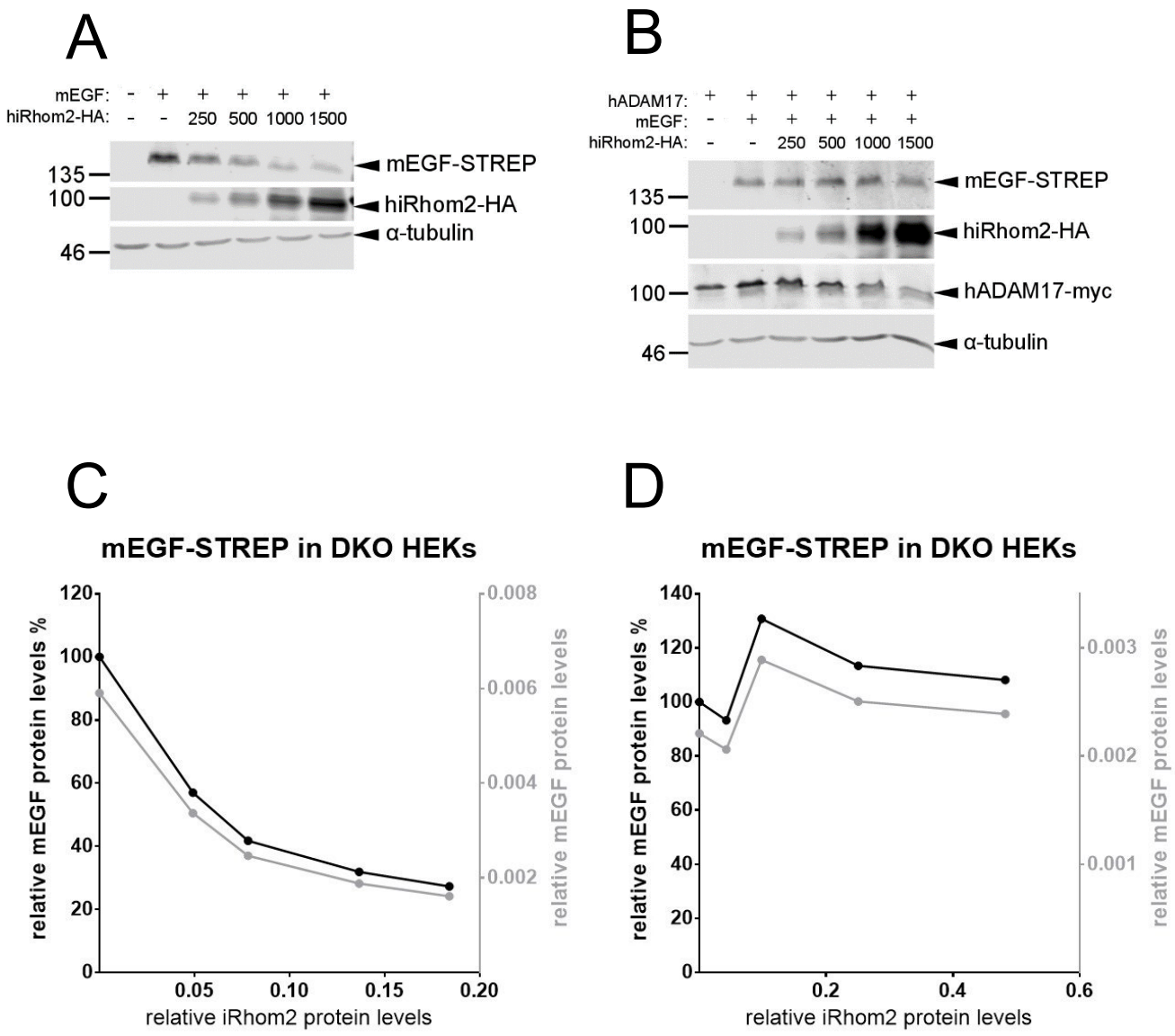

Figure 4.11: Effect of iRhom2 overexpression on mEGF in DKO HEKs (**A, C**) and the effect of human ADAM17 coexpression on mEGF disappearance in the presence of hiRhom2-HA in DKO HEKs (**B, D**). In **A** and **B,** immunoblots from cell lysates containing a varying amount of iRhom2 are shown. The amount of transfected human iRhom2-HA construct ranged from 250 to 1500 ng DNA. Molecular weights are indicated in kDa. (**C, D**) Quantifications of the immunofluorescent signal were performed in Image Studio™ Lite software (LI-COR).

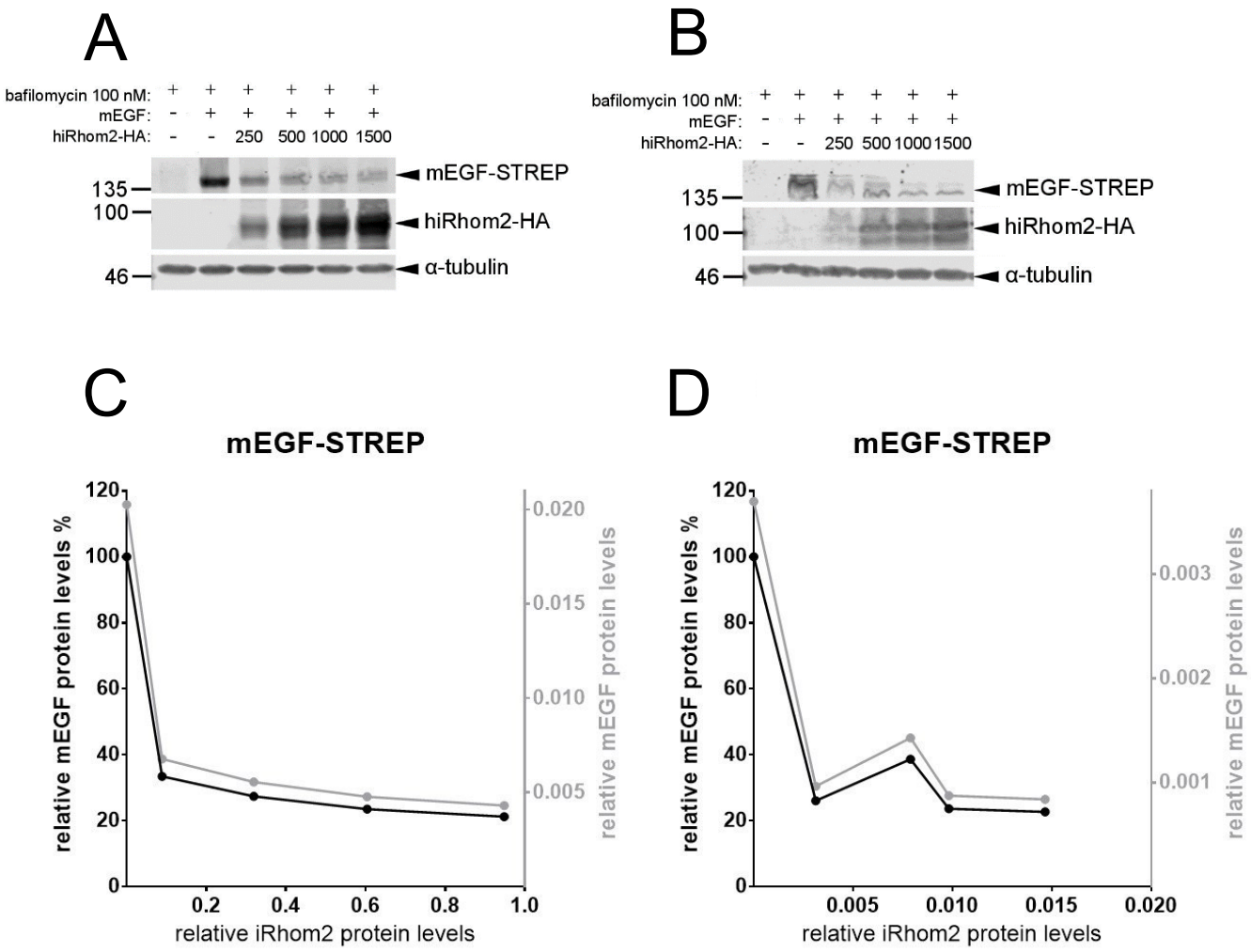

Figure 4.12: Effect of lysosomal inhibition by 100 nM bafilomycin on mEGF disappearance in the presence of hiRhom2-HA in WT HEKs. (**A, B**) Immunoblots from cell lysates containing a varying amount of iRhom2. The amount of transfected human iRhom2-HA construct ranged from 250 to 1500 ng DNA. Molecular weights are indicated in kDa. (**C, D**) Quantifications of the immunofluorescent signal were performed in Image Studio™ Lite software (LI-COR).

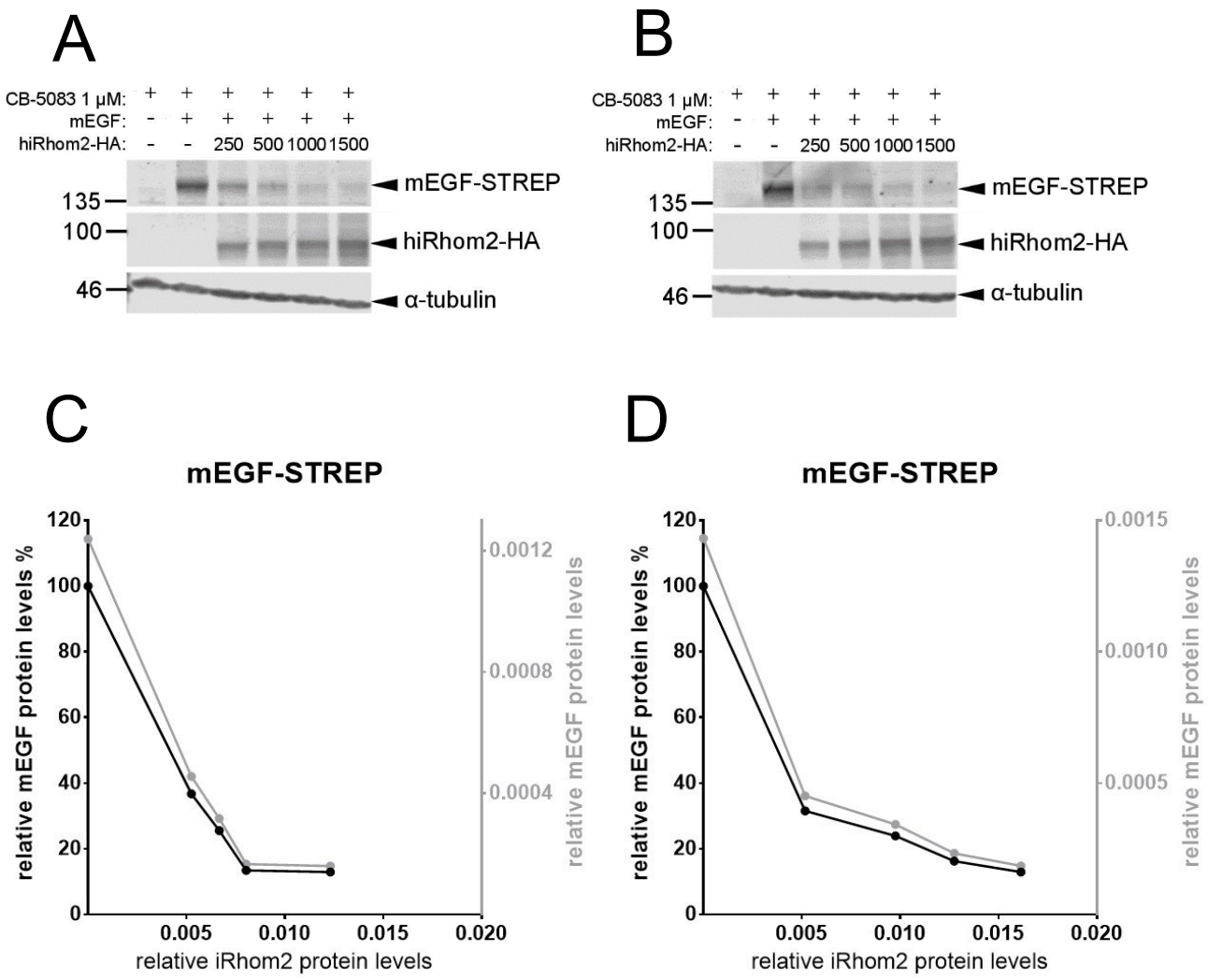

Figure 4.13: Effect of ERAD inhibition by 1 µM CB-5083 on mEGF disappearance in the presence of hiRhom2-HA in WT HEKs. (**A, B**) Immunoblots from cell lysates containing a varying amount of iRhom2. The amount of transfected human iRhom2-HA construct ranged from 250 to 1500 ng DNA. Molecular weights are indicated in kDa. (**C, D**) Quantifications of the immunofluorescent signal were performed in Image Studio™ Lite software (LI-COR).

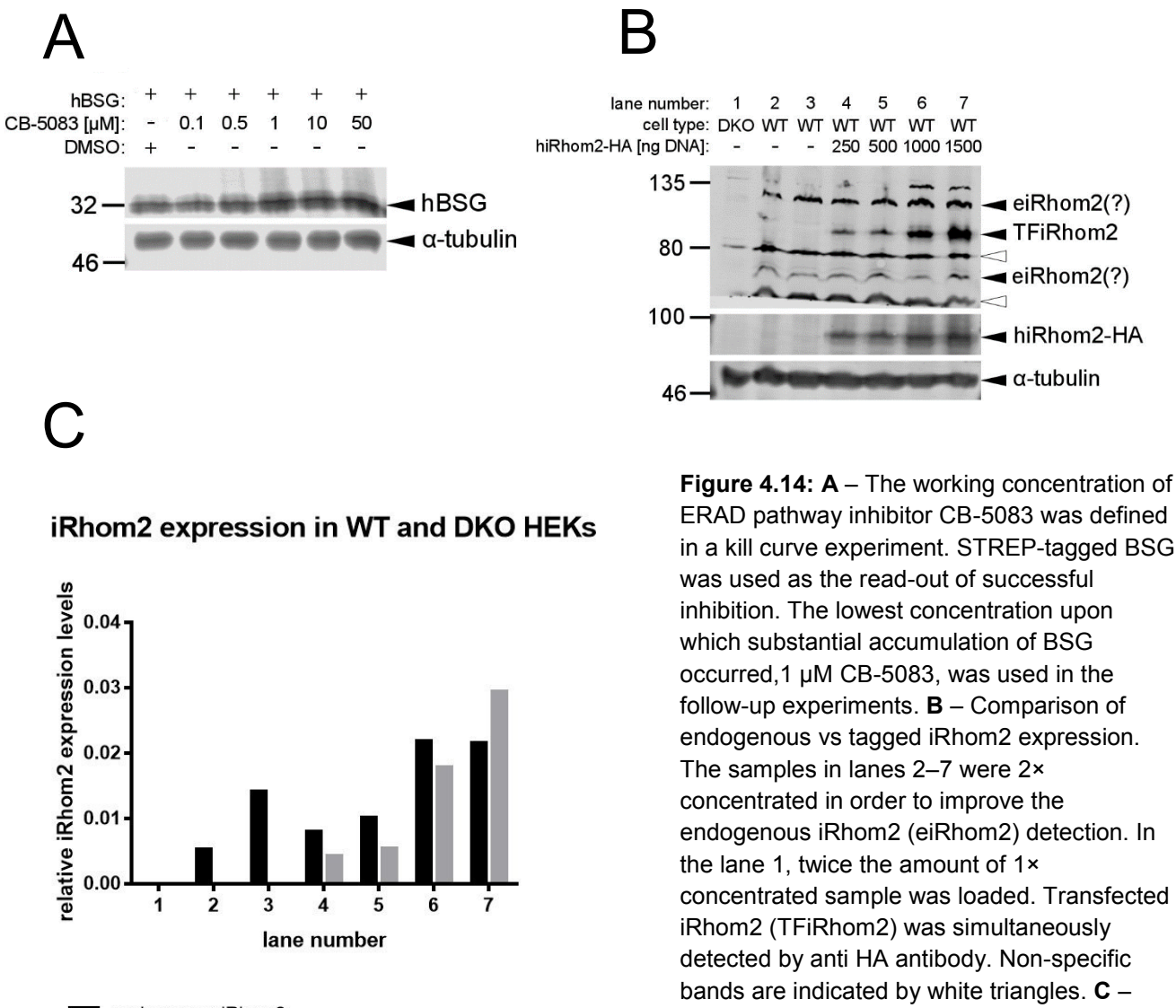

Figure 4.14: A – The working concentration of ERAD pathway inhibitor CB-5083 was defined in a kill curve experiment. STREP-tagged BSG was used as the read-out of successful inhibition. The lowest concentration upon which substantial accumulation of BSG occurred,1 μM CB-5083, was used in the follow-up experiments. **B** – Comparison of endogenous vs tagged iRhom2 expression. The samples in lanes 2–7 were 2× concentrated in order to improve the endogenous iRhom2 (eiRhom2) detection. In the lane 1, twice the amount of 1× concentrated sample was loaded. Transfected iRhom2 (TFiRhom2) was simultaneously detected by anti HA antibody. Non-specific bands are indicated by white triangles. **C** – Quantification of the signal from immunoblot shown in B, where the signal from anti iRhom2 antibody is plotted. Only the upper eiRhom2 band was quantified.

5 Discussion

In this work, the effect of iRhom2 on the production of EGFR ligands was assessed. The experimental data shown in **Figure 4.1** confirm the previous finding that an increasing concentration of overexpressed iRhom2 diminishes the levels of EGF (Zettl *et al.*, 2011). The Zettl *et al*., 2011 study also shows that TGFα succumbs to the same effect. However, the conclusions from the immunoblots shown in **Figure 4.2** are not as clear-cut. On immunoblot **4.2B**, TGFα disappearance is clearly apparent, whereas on immunoblot **4.2A** the effect is not detectable when considering the fluorescent signal from the entire spectrum of TGFα species in each lane (**Figure 4.2C**). However, if only the uppermost band is taken into account, its pixel intensity noticeably reduces with increasing levels of iRhom2 (**Figure 4.2E).** It is therefore possible that iRhom2 acts only on one form of TGFα and does not significantly influence the amount of the lower molecular weight TGFα forms. According to Wunderle *et al.*, 2016, the uppermost band should represent the form of TGFα that has been already trafficked into the GA. The disappearance of this band upon increasing levels of overexpressed iRhom2 could therefore mean that iRhom2 prevents TGFα trafficking. Another possible explanation could be that iRhom2 targets this form of TGFα into a degradation pathway. Interestingly, Zettl *et al.*, 2011 show a reversal of the EGF disappearance effect by inhibiting the proteasome. It would therefore be interesting to see if the same applies to the high molecular weight form of TGFα. Additionally and interestingly, the quantifications reveal that in the case of immunoblot **4.2B**, the ratio of the highest TGFα:highest iRhom2 levels is approximately five times higher than in the case immonoblot **4.2A**, yet the disappearance of TGFα is apparent for all of the TGFα species in **4.2B**. This might be explained by constraints of the chosen methodological approach, for every immunoblot represents a mean steady state of all the cells in a well and does not reflect the variability of transfected DNA expression in individual cells. Also, compared to the highest EGF:highest iRhom2 levels ratio in the **Figure 4.1**, TGFα is much better expressed. However, it is depleted by iRhom2 to roughly the same extent as EGF (approximately 20 %). Therefore, iRhom2 seems to be more active towards TGFα than towards EGF.

Next, we looked at whether the effect on the levels of EGFR ligands was specific to iRhom2. The question to be answered was whether the disappearance of the ligands (or, more precisely, their precursors) is caused solely by the presence of iRhom2 in the ER or whether the overexpression of any ER-resident polytopic membrane protein has the same effect. Since the iRhom2 effect was better visible and reproducible with EGF, the follow-up experiments were performed with EGF only. When the HEK cells were transfected with proteolytically inactive KDEL-tagged Rhomboid2[9] (Rhomboid2-SA-KDEL), a mild decrease in the amount of EGF was observed (**Figure 4.3A,C**). However, in the duplicate experiment, the levels of EGF decreased significantly (**Figure 4.3B,D**), speaking against the effect being iRhom2 specific. I have no idea how this discrepancy could be explained. The fact that an inactive rhomboid protease mutant overexpression can

[9] The proteolytically inactive mutant was chosen in order to prevent possible EGF cleavage by Rhomboid2 (Adrain *et al.*, 2011). The KDEL tag ensures that Rhomboid2 stays in the ER and does not continue to other compartments of the secretory pathway, mimicking the cellular localisation of overexpressed iRhom2 (Matsukawa *et al.*, 2012).

induce ER-stress (Fleig *et al.*, 2012) might play a role, for the levels of Rhomboid2-SA-KDEL protein are indeed very high. However, in the work of Zettl *et al.*, 2011 the KDEL-tagged mutant Rhomboid 2 was shown to have no effect on EGF levels. This might be due to the different expression ratio of EGF:Rhomboid2-SA-KDEL. In the Zettl *et al.*, 2011 study, Rhomboid2-SA-KDEL levels were similar to the levels of myc-tagged EGF, whereas in my experiments the Rhomboid2-SA-KDEL expression was very high. It might therefore be true that upon adjusting the expression of the mutant Rhomboid2, EGF levels would not be diminished and also more consistent results would probably be obtained. Additionally, in the work of Zettl *et al.*, 2011, a different cell line, COS7, was used in the overexpression assays, which could also contribute to the discrepancy.

Another polytopic membrane protein from the rhomboid-like family, Rhomboid4, was tested in the same assay (**Figure 4.4A,B**). In contrast to experiments with iRhom2 and Rhomboid2-SA-KDEL, no decrease of EGF levels was observed. Rather, the level of EGF rose upon Rhomboid4 overexpression. Interestingly, when proteolytically inactive mutant of Rhomboid4 was tested, a mild decrease of EGF levels was observed in both replicates (**Figure 4.5**). It must be admitted though that the immunoblot shown in **Figure 4.5A** is not very convincing, for the overall EGF amount was for some reason poorly detectable and therefore was not easy to quantify. The same applies to the experimental data obtained with Unc93B (**Figure 4.6**), an ER-resident membrane protein unrelated to the rhomboid superfamily. The signal from EGF is so weak that the quantified data is unreliable. However, Zettl *et al.*, 2011 show that even this polytopic rhomboid-like family unrelated protein has no effect on EGF levels. To confirm and move beyond their findings, the experiments should be repeated, optimising the cell harvesting protocol to solve the problem with the poor detectability of EGF.

Taken together, the data shown in **figures 4.3—4.6** suggest that iRhom2 is not the only polytopic transmembrane protein that might influence the amount of EGF receptor ligands. Interestingly, those proteins that had a similar effect on EGF levels to iRhom2 were both inactive rhomboid proteases. It is known that overexpression of such intramembrane protease mutants can induce ER stress and promote the unfolded protein response (Fleig *et al.*, 2012). Therefore, it can not be ruled out that the effect observed in the case of the inactive Rhomboid2 and Rhomboid4 is in fact general, caused by the non-physiological state of the ER, rather than specific to EGFR ligands. Contrary to that, active Rhomboid4 overexpression seemed to stabilise EGF. This observation is extremely interesting in the light of a study which reported that Rhomboid4 promotes non-canonical secretion of membrane-tethered forms of TGFα via microsomes (Wunderle *et al.*, 2016). The effect was not restricted to TGFα, for the secretion of other proteins, CD44 and a fruit fly EGFR ligand Spitz, was also shown to be enhanced by Rhomboid4 (Wunderle *et al.*, 2016). In view of this, the results in **Figure 4.4** might suggest that EGF could be another Rhomboid4 client.

The next question to be answered was whether the disappearance of EGFR ligands in the presence of iRhom2 is specific to EGFR ligands or general for any type I transmembrane proteins. To test this, three type I transmembrane proteins which are not EGFR ligands, namely BCAM, SPINT1 and BSG, were cotransfected with increasing amounts of iRhom2. In the case of BCAM, the protein levels diminish, although the effect

seems to be stronger in the immunoblot A (**Figure 4.7**). In both experiments, the ratio of highest BCAM:highest iRhom2 level is approximately equal, however, it is higher than in the case of EGF (**Figure 4.1**). It therefore appears that iRhom2 is capable of depleting BCAM to the similar extent as EGF, even when the relative BCAM levels are higher than those of EGF.

On the other hand, the amount of SPINT1 remained more or less constant upon increasing iRhom2 levels (**Figure 4.8**). In the case of immunoblot **4.8A**, SPINT1 seems to be stabilised by iRhom2, although SPINT1 levels decreased slightly in the lanes with the two lowest concentrations of transfected iRhom2 construct. The levels of the last potential iRhom2 client tested here, BSG, seem to be negatively influenced by iRhom2 overexpression (**Figure 4.9**). The amount of BSG is reduced in the lane with the lowest concentration of cotransfected iRhom2 (to approximately 55—70 % of the signal from the lane with no iRhom2 overexpression) and does not decrease to the same extent as is the case with EGF (to approximately 20 % of the signal from the lane without iRhom2 cotransfection).

Taken together, these results suggest that EGFR ligands are not the only proteins influenced by iRhom2 overexpression in a concentration-dependent manner. iRhom2 overexpression negatively regulates the levels of BCAM and of BSG (**Figures 4.7** and **4.9**). However, SPINT1 levels are not significantly influenced by iRhom2 overexpression, therefore a generalised conclusion as to the effect of iRhom2 on the disappearance of all the type I transmembrane proteins tested in this study (EGF, TGFα, BCAM, BSG aside from SPINT1) can not be really made.

Our next aim was to assess if the presence of overexpressed ADAM17 in the ER would rescue the disappearance effect of iRhom2 on EGF. The reasoning behind this question is based on the close and long-lived iRhom2-ADAM17 relationship (discussed in **section 1.3.3.2**). It might be true that when sufficient ADAM17 is present, iRhom2 is preferentially occupied with ADAM17 trafficking and hence has reduced capacity to influence the client proteins (EGF, TGFα, BCAM, BSG). This mechanism would ensure that when ADAM17 is present, its substrates are allowed to reach the plasma membrane, but when it is not, their levels are diminished by iRhom2. In such a way futile production of ADAM17 substrates would be prevented. Additionally, this would also prevent potentially harmful accumulation of precursors of EGFR ligands on the plasma membrane, which could lead to unwanted or excessive juxtacrine signalling and hence perturb the tissue homeostasis. However, the results obtained from WT HEKs did not support this scenario (**Figure 4.10**). Rather, the EGF levels decrease even in the presence of overexpressed ADAM17. Interestingly, when the same experiment was performed in iRhom1 and 2 double knock-out (DKO) HEKs (where the negative impact of iRhom2 overexpression on the EGF levels was shown as well (**Figure 4.11A**), the rescue of EGF disappearance was clearly observed (**Figure 4.11B**). This discrepancy could be a display of an overexpression system caveat. It might be true that the endogenous iRhom1 and 2 background in the WT HEKs is so high that even ADAM17 co-overexpression does not efficiently mimic the state with plenty of ADAM17 and therefore the disappearance effect of iRhom2 on EGF persists. On the other hand, I only had access to a single clone of DKO HEK cells, which means that the clonal effect might influence the results. To minimise such doubts

about the data credibility, other clones of DKO HEKs should be tested. Additionally, scaling the expression of the tagged proteins down to the endogenous levels might overcome overexpression artefacts. The result of one such preliminary experiment is shown in **Figure 4.14B**. The expression levels of endogenous iRhom2 were detected by anti iRhom2 antibody and compared to the levels of transfected HA-tagged iRhom2. However, certain doubts about the specificity of the antibody prevent me from making any clear conclusion. In the study of (Cabron *et al.*, 2018), where the same antibody was used, endogenous iRhom2 is detected as nearly 100 kDa species, whereas in my immunoblot only the tagged iRhom2 was visualised as a protein of similar molecular weight. The other potential endogenous iRhom2 bands, *i. e.* those absent in the lane with the DKO HEK sample, have different molecular weights than expected. It is therefore hard to tell if they represent posttranslationally modified forms of endogenous iRhom2 or proteins which are substantially downregulated in DKO HEK cells. Quantification of the upper eiRhom2 band in **Figure 4.14C** reveals that in each lane, the expression of endogenous and tagged iRhom2 is at the same order of magnitude. If the quantified band indeed represents endogenous iRhom2, it can be summarised that upon iRhom2 overexpression, the overall iRhom2 levels approximately doubled, which, in my opinion, is a change not dramatic enough to consider the results obtained from overexpression assays as completely unreliable. However, it should be noted that the intensity of the upper eiRhom2 band increases with increasing concentration of transfected iRhom2. One possible explanation could be that it is posttranslationally modified form of iRhom2 and its amounts rise with increasing levels of total iRhom2. It might also mean that iRhom2 positively regulates its own expression and the rate of iRhom2 synthesis increases upon higher iRhom2 levels. Another explanation might be that it is a protein upregulated by iRhom2, whose expression is therefore suspended in DKO HEKs. To scrutinise which scenario is true, the identity of the bands of interest could be revealed, for example by mass spectrometry. In order to avoid using the anti iRhom2 antibody, the detection of endogenous iRhom2 levels could also be performed by in-genome tagging and subsequent immunodetection of iRhom2 by a reliable antibody. The usage of antibodies could be circumvented by a mass spectrometry analysis of the HEK cell proteome. Such an approach would certainly be methodologically complicated and, taking the limited time for the diploma thesis to be completed into account, was therefore condemned to stay unrealised. Another, although indirect, way of determining endogenous iRhom2 expression would be by using real time qPCR.

The next question was how the disappearance effect caused by iRhom2 could be rescued. One possible explanation for the observed negative regulation of client protein levels by iRhom2 could be that iRhom2 promotes their degradation. Generally speaking, there are two major degradation pathways for transmembrane proteins in the cell: the lysosome-dependent pathway and the proteasome-dependent one (reviewed in Fonseca and Carvalho, 2019). If iRhom2 really promotes client protein degradation, then inhibition of at least one of these pathways would rescue the disappearance of EGF effected by iRhom2 overexpression. First, the lysosomal degradation pathway was inhibited by treating the cells with 100 nM bafilomycin. However, decreasing EGF protein levels upon iRhom2 overexpression were still observed in bafilomycin (**Figure 4.12**). Secondly, the inhibition of a proteasome-dependent way of ER-resident protein degradation, ERAD, was

performed. The reasoning behind this choice was that since all the iRhom2 clients are synthesised at the rough ER membrane, the only way to degrade them in the proteasomes is to retrotranslocate them into the cytoplasm. This process is indeed performed by the ERAD machinery (Ballar, Pabuccuoglu and Kose, 2011). By inhibiting specifically this degradation pathway, the impact on the proteostasis of cytosolic proteins would be prevented. In this work, the inhibitor CB-5083 was chosen. This compound inhibits the ATPase VCP, also known as p97, which is required for the retrotranslocation process (Radhakrishnan, den Besten and Deshaies, 2014; Zhou *et al.*, 2015). Based on a kill curve, the concentration of 1 μM was used (**Figure 4.14A**). However, even ERAD inhibition by CB-5083 did not rescue the EGF disappearance (**Figure 4.13**). This would implicate either an undescribed degradation route for membrane proteins, or transcriptional effects, or, perhaps most likely, a problem in membrane targeting, meaning that the client proteins would fail to reach the translocons and would be degraded by cytosolic proteasomes even before entering the ER. The last option would be consistent with the reported rescue effect of proteasomal inhibition by MG-132 (Zettl *et al.*, 2011).

5.1 Future directions

The negative impact of iRhom2 overexpression on the protein levels of EGF previously reported by Zettl *et al.*, 2011 was corroborated in this thesis. The experiments performed with another EGFR ligand, TGFα, suggest that iRhom2 also has a similar effect on TGFα, or at least on its ER-to-GA-trafficked form. However, the fact that the PNGase F sensitive form of TGFα is visible in the immunoblots (**Figure 4.2**) indicates that the deglycosylation was incomplete. For the scope of this thesis, this imperfection is not a tragedy, for bands of a sufficient sharpness were obtained without deglycosylation. Rather, it allows us to specify which TGFα form is influenced by iRhom2 overexpression. The deglycosylation step can therefore be omitted in future assays rather than prolonged, in order to preserve the information about all the detectable TGFα forms. To get an even more precise idea about the iRhom2 effect on different TGFα forms, an untagged TGFα could be used and detected by a TGFα-specific antibody as described in (Wunderle *et al.*, 2016).

It would be equally interesting to see if proteasome inhibition would rescue the disappearance of GA-trafficked TGFα, as was reported for EGF in Zettl *et al.*, 2011. However, the majority of membrane-tethered TGFα has been shown to succumb to proteasomal degradation, hence the inhibition of proteasomes leads to massive accumulation of all the TGFα forms and complicates their separation on the immunoblots (Wunderle *et al.*, 2016).

Regarding the suggestion that iRhom2 might influence only the levels of GA-trafficked form of TGFα (**Figure 4.2A**), it may be speculated that iRhom2 is involved in the Endosome-and-Golgi-Associated Degradation (EGAD) pathway. EGAD is a proteasome-dependent way of disposal of proteins that have been already trafficked from the ER. The membrane components of the EGAD machinery functionally correspond to those of the ERAD pathway and are also structurally homologous to them (reviewed in Fonseca and Carvalho, 2019). However, its components and mechanism of action have been scrutinised only in yeast (Schmidt *et al.*, 2019). Interestingly, a homologue of human rhomboid-like pseudoprotease Ubac2 was

identified among proteins crucial for this degradation mechanism (Schmidt *et al.*, 2019). Given that iRhom2 passes through the GA on the way to the plasma membrane and that the rhomboid-like pseudoprotease Derlin1 participates in ERAD substrate recognition (Mehnert, Sommer and Jarosch, 2014; Neal *et al.*, 2018), speculating that another rhomboid-like pseudoprotease (iRhom) is involved in a proteasome-dependent degradation pathway is not too far-fetched.

The disappearance of the GA-trafficked form of TGFα could alternatively be explained by negative regulation of its trafficking by iRhom2. This possibility could be assessed by a pulse-chase experiment.

The scrutiny of other polytopic ER-resident transmembrane proteins revealed that the disappearance of EGF is probably not restricted only to iRhom2 overexpression. The inactive mutants of Rhomboid2 and Rhomboid4 had the same effect on EGF levels. It would therefore be useful to repeat the experiment with the polytopic protein Unc93B, unrelated to the rhomboid-like family, or to choose a different topologically similar protein, to see if EGF disappearance is dependent on the overexpression of a proteolytically inactive rhomboid-like family member or on the overexpression of any polytopic ER-resident protein. It might also be interesting to assess if the downregulation of EGF levels in the presence of the mutants of Rhomboid2 and Rhomboid4 is caused by ER stress and the unfolded protein response (UPR) stimulation or whether it is UPR-independent and would persist even upon the UPR inhibition.

The observation that EGF levels in the cell lysates are stabilised or even upregulated by Rhomboid4 overexpression deserves attention. It is possible that EGF is secreted in a non-canonical, metalloprotease-independent pathway, just as has been reported for TGFα (Wunderle *et al.*, 2016). Other EGFR ligands, namely HB-EGF and AREG, were shown to be secreted in microvesicles (termed exosomes) in their membrane-tethered forms (Higginbotham *et al.*, 2011). It might be interesting to explore if this phenomenon applies to other EGFR ligands including EGF. If true, the active Rhomboid4 could therefore be considered a novel component of EGFR signalling regulation through ligand production, supporting the hypothesis about the evolutionarily conserved relationship between the rhomboid-like family of proteins and EGFR signalling.

The experiments where the impact of iRhom2 overexpression on non-EGFR ligand type I transmembrane proteins was studied suggest that the disappearance of iRhom2 clients is not restricted to EGFR ligands. However, at the same time, this effect is not general for any type I transmembrane protein, as shown in **Figure 4.8**. To get a better idea about the spectrum of iRhom2-influenced proteins, other potential clients should be tested. Based on such experiments, the proteins whose levels were negatively influenced by iRhom2 overexpression could be divided into functional groups and suggestions about iRhom2 impact on processes others than EGFR signalling could be made.

Our assessment of how ADAM17, the most well studied iRhom2 interactor, might influence the observed disappearance of EGF caused by iRhom2 overexpression, gave ambiguous results. To rule out the impact of the clonal effect, iRhom1 and 2 double knock-out cell lines originating from other clones should be tested. To corroborate the suggestion that the different results are due to high endogenous background in the WT HEKs,

iRhom1 and 2 could be targeted by shRNAs in the wild-type cell line. If this treatment led to the rescue of EGF levels, it could mean that the effect is dependent on the ratio of iRhom2 and ADAM17. If true, it would also implicate iRhom2 as a nexus in which both the negative regulation of EGFR signalling by preventing EGFR ligand production and the positive regulation by trafficking and activation of ADAM17 coalesce. To shed more light on this possible EGFR regulation network, other ligands of EGF receptor should be scrutinised. In the work of Zettl *et al.*, 2011, the negative effect of iRhom2 on betacellulin, amphiregulin, epiregulin and neuregulin 4 was reported. It would be interesting to repeat the experiments and to test if ADAM17 overexpression would rescue the disappearance of these proteins as well. To complete the list of EGFR ligands, the ones whose susceptibility to the disappearance effect by iRhom2 overexpression is to be tested yet are HB-EGF, epigen and other neuregulins.

The last question to be answered in this thesis was what lies behind the disappearance of EGF in the cells with overexpressed iRhom2. The suggestion that iRhom2 promotes EGF degradation was not corroborated, for neither lysosomal inhibition nor ERAD pathway reversed the effect. To enhance the data credibility, other lysosomal and ERAD inhibitors, for example chloroquine and Eeyarestatin I, respectively, should be tested as well. However, the last missing piece of the mosaic is an experiment where the proteasomal degradation would be inhibited. I performed a preliminary kill curve experiment with the proteasomal inhibitor Carfilzomib, but observed no substantial accumulation of polyubiquitinylated proteins (data not shown). Hence I decided to try another inhibitor in the future. Unfortunately, I did not manage to do it before the thesis completion. In the Zettl *et al.*, 2011 study, proteasomal inhibitors MG-132 and lactacystin were shown to rescue the disappearance of EGF in the cells with overexpressed iRhom1. How this could be linked to iRhom1 presence remains unclear. On the one hand, iRhom1 was implicated in the ER-stress response by facilitating PAC1/2 protein dimerisation and hence the recruitment of proteasomes to the ER membrane (Lee *et al.*, 2015). Although the study mentions only iRhom1, it can not be ruled out that iRhom2 may be involved in the ER stress mitigation and in proteasome recruitment as well. The suggestion that mammalian iRhoms might play a role in the ER-resident protein degradation is further supported by the fact that their fruit fly homologue is involved in the degradation of EGFR ligand precursors (Zettl *et al.*, 2011). However, this potential iRhom1 and/or 2 function might not be necessarily associated with ER-stress conditions. There are some studies suggesting that in addition to the clearance of ER-resident misfolded proteins, the ERAD pathway also acts on properly folded proteins, regulating their proteostasis (reviewed in Hampton and Garza, 2009). This seems to be the case for TGFα, whose levels are regulated by constitutive proteasome-dependent degradation in the early secretory pathway (Wunderle *et al.*, 2016). If iRhoms are involved in the process and if the other EGFR ligands are subject to similar regulation remains to be explored.

However, based on the data shown in this thesis, a role for iRhom2 in the ERAD pathway seems not to be probable. In fact, the results presented here do not even corroborate the fact that the disappearance of iRhom2 clients can be explained by their enhanced degradation. Several suggestions about this phenomenon can be proposed. Firstly, based on the enhanced iRhom2 client degradation model, it might be possible that iRhom2

indeed promotes a proteasome-dependent degradation of EGF, which is, however, independent of the VCP. Such cases were described in the literature, where an intramembrane protease cleaves the protein to be degraded inside the phospholipid bilayer, facilitating its dislocation from the membrane (Boname *et al.*, 2014). Secondly, iRhom2 might act on its clients even before they reach the ER. Hypothetically, iRhom2 could influence the rate of cotranslational transport of the nascent polypeptide into the ER lumen. Following the line of purely hypothetical speculations, the cytoplasm-facing iRhom2 N-terminal domain could also influence the effectiveness of the mRNA:ribosome:nascent polypeptide complex delivery to the translocons on the ER membrane. Interestingly, the iRhom1 N-terminal domain is known to be cleaved off, raising questions about its potential function (Nakagawa *et al.*, 2005). However, based on the data presented in the same study, it appears that the soluble iRhom1 N-terminal domain is rapidly degraded. According to the PEST sequence predictor (http://emboss.bioinformatics.nl/cgi-bin/emboss/epestfind), the N-terminal domain of iRhom1 contains two potential PEST motives, which might account for its rapid disappearance. In the iRhom2 N-terminal domain, however, only one potential PEST sequence was predicted. It therefore might be speculated that the soluble N-terminal domains of the two iRhoms have different stability. Interestingly, my observation that C-terminally tagged iRhom2 is detected as two species, one of nearly 100 kDa and the other of approximately 50 kDa (data not shown), are consistent with the immunoblots presented in Künzel *et al.*, 2018 and with the hypothesis that, similarly to iRhom1, also the N-terminal domain of iRhom2 undergoes cleavage. Once liberated from the membrane tether, the N-terminal domain of iRhom2 could influence the rate of client protein synthesis or even mRNA processing as well as the rate of transcription, although this scenario is very speculative. To rule out the possibility that iRhom2 acts through mRNA level regulation, a real time qPCR of the client mRNA should be performed. In Zettl *et al.*, 2011, it was shown that this hypothesis does not apply to iRhom1. However, given that the N-terminal domain is the least conserved part of iRhom1 and 2 and that the roles of two mammalian iRhoms were shown to be only partially redundant, it would be interesting to explore if iRhom2 has any effect on its client protein mRNAs. Also, to elucidate whether the N-terminal domain is required for the iRhom clients depletion, a deletion mutant lacking the N-terminal domain could be tested in future assays.

6 Conclusion

To summarise, overexpressed iRhom2 has been confirmed as a negative regulator of protein levels of EGF receptor ligands precursors. However, this effect is not restricted to EGFR ligands, for other type I transmembrane proteins are affected in a similar way. The effect can not be explained merely as an artefact of a polytopic transmembrane protein overexpression, for the intramembrane protease Rhomboid4 overexpression does not diminish iRhom2 client protein levels. On the other hand, the overexpression of catalytically inactive mutants of rhomboid proteases seem to have the same effect as iRhom2, raising questions about the potential role of ER-stress in the process. Overexpression of iRhom2 interactor ADAM17 does not counteract the iRhom2-triggered disappearance of EGF in wild-type HEKs, but in iRhom1/2 double knock-out HEKs overexpressed ADAM17 rescues the levels of EGF. Neither ERAD nor lysosomal inhibition led to EGF protein levels rescue. Therefore, if the effect of iRhom2 overexpression is indeed caused by enhanced degradation of its client proteins, it most likely occurs via a hitherto undescribed pathway.

7 References

*secondary citation

Adrain, C. *et al.* (2011) 'Mammalian EGF receptor activation by the rhomboid protease RHBDL2.', *EMBO reports*, 12(5), pp. 421–7. doi: 10.1038/embor.2011.50.

Adrain, C. *et al.* (2012) 'Tumor necrosis factor signaling requires iRhom2 to promote trafficking and activation of TACE', *Science (New York, N.Y.)*. Europe PMC Funders, 335(6065), p. 225. doi: 10.1126/SCIENCE.1214400.

Adrain, C. and Freeman, M. (2012) 'New lives for old: evolution of pseudoenzyme function illustrated by iRhoms', *Nature Reviews Molecular Cell Biology*. Nature Publishing Group, 13(8), pp. 489–498. doi: 10.1038/nrm3392.

Alvarez, E. *et al.* (1991) 'Pro-Leu-Ser/Thr-Pro is a consensus primary sequence for substrate protein phosphorylation. Characterization of the phosphorylation of c-Myc and c-Jun proteins by an epidermal growth factor receptor threonine 669 protein kinase.', *The Journal of biological chemistry*, 266(23), pp. 15277–85. Available at: http://www.ncbi.nlm.nih.gov/pubmed/1651323

Arribas, J., Bech-Serra, J. J. and Santiago-Josefat, B. (2006) 'ADAMs, cell migration and cancer', *Cancer and Metastasis Reviews*, 25(1), pp. 57–68. doi: 10.1007/s10555-006-7889-6.

Arteaga, C. L. and Engelman, J. A. (2014) 'ERBB receptors: from oncogene discovery to basic science to mechanism-based cancer therapeutics.', *Cancer cell*. NIH Public Access, 25(3), pp. 282–303. doi: 10.1016/j.ccr.2014.02.025.

Ballar, P., Pabuccuoglu, A. and Kose, F. A. (2011) 'Different p97/VCP complexes function in retrotranslocation step of mammalian ER-associated degradation (ERAD)', *The International Journal of Biochemistry & Cell Biology*, 43(4), pp. 613–621. doi: 10.1016/j.biocel.2010.12.021.

Banerjee, A. *et al.* (2010) 'Neuregulin 1–ErbB4 pathway in schizophrenia: From genes to an interactome', *Brain Research Bulletin*, 83(3–4), pp. 132–139. doi: 10.1016/j.brainresbull.2010.04.011.

Barnette, D. N. *et al.* (2018) 'iRhom2-mediated proinflammatory signalling regulates heart repair following myocardial infarction.', *JCI insight*. American Society for Clinical Investigation, 3(3). doi: 10.1172/jci.insight.98268.

Bax, D. V *et al.* (2004) 'Integrin alpha5beta1 and ADAM-17 interact in vitro and co-localize in migrating HeLa cells.', *The Journal of biological chemistry*, 279(21), pp. 22377–86. doi: 10.1074/jbc.M400180200.

Beard, H. A. *et al.* (2019) 'Discovery of Cellular Roles of Intramembrane Proteases', *ACS Chemical Biology*. American Chemical Society, p. acschembio.9b00404. doi: 10.1021/acschembio.9b00404.

Ben-Shem, A., Fass, D. and Bibi, E. (2007) 'Structural basis for intramembrane proteolysis by rhomboid serine proteases.', *Proceedings of the National Academy of Sciences of the United States of America*. National Academy of Sciences, 104(2), pp. 462–6. doi: 10.1073/pnas.0609773104.

Bertics, P. J. and Gill, G. N. (1985) 'Self-phosphorylation enhances the protein-tyrosine kinase activity of the epidermal growth factor receptor.', *The Journal of biological chemistry*, 260(27), pp. 14642–7. Available at: http://www.ncbi.nlm.nih.gov/pubmed/2997217

Black, R. A. *et al.* (1997) 'A metalloproteinase disintegrin that releases tumour-necrosis factor-α from cells', *Nature*. Nature Publishing Group, 385(6618), pp. 729–733. doi: 10.1038/385729a0.

Black, R. A. and White, J. M. (1998) 'ADAMs: focus on the protease domain', *Current Opinion in Cell Biology*. Elsevier Current Trends, 10(5), pp. 654–659. doi: 10.1016/S0955-0674(98)80042-2.

Blaydon, D. C. *et al.* (2012) 'RHBDF2 mutations are associated with tylosis, a familial esophageal cancer syndrome.', *American journal of human genetics*. Elsevier, 90(2), pp. 340–6. doi: 10.1016/j.ajhg.2011.12.008.

Bode, W., Gomis-Rüth, F.-X. and Stöckler, W. (1993) 'Astacins, serralysins, snake venom and matrix metalloproteinases exhibit identical zinc-binding environments (HEXXHXXGXXH and Met-turn) and topologies and should be grouped into a common family, the "metzincins"', *FEBS Letters*, 331(1–2), pp. 134–140. doi: 10.1016/0014-5793(93)80312-I.

Boname, J. M. *et al.* (2014) 'Cleavage by signal peptide peptidase is required for the degradation of selected tail-anchored proteins.', *The Journal of cell biology*, 205(6), pp. 847–62. doi: 10.1083/jcb.201312009.

Brooke, M. A. *et al.* (2014) 'iRHOM2-dependent regulation of ADAM17 in cutaneous disease and epidermal barrier function.', *Human molecular genetics*. Oxford University Press, 23(15), pp. 4064–76. doi: 10.1093/hmg/ddu120.

Buxbaum, J. D. *et al.* (1998) 'Evidence that tumor necrosis factor alpha converting enzyme is involved in regulated alpha-secretase cleavage of the Alzheimer amyloid protein precursor.', *The Journal of biological chemistry*, 273(43), pp. 27765–7. doi: 10.1074/jbc.273.43.27765.

Cabron, A.-S. *et al.* (2018) 'Structural and Functional Analyses of the Shedding Protease ADAM17 in HoxB8-Immortalized Macrophages and Dendritic-like Cells', *The Journal of Immunology*, 201(10), pp. 3106–3118. doi: 10.4049/jimmunol.1701556.

Cavadas, M. *et al.* (2017) 'Phosphorylation of iRhom2 Controls Stimulated Proteolytic Shedding by the Metalloprotease ADAM17/TACE.', *Cell reports*. Elsevier, 21(3), pp. 745–757. doi: 10.1016/j.celrep.2017.09.074.

De Cesare, D. *et al.* (1998) 'Rsk-2 activity is necessary for epidermal growth factor-induced phosphorylation of CREB protein and transcription of c-fos gene', *Proceedings of the National Academy of Sciences*, 95(21), pp. 12202–12207. doi: 10.1073/pnas.95.21.12202.

Chalaris, A. *et al.* (2007) 'Apoptosis is a natural stimulus of IL6R shedding and contributes to the proinflammatory trans-signaling function of neutrophils.', *Blood*, 110(6), pp. 1748–55. doi: 10.1182/blood-2007-01-067918.

Chanthaphavong, R. S. *et al.* (2012) 'A role for cGMP in inducible nitric-oxide synthase (iNOS)-induced tumor necrosis factor (TNF) α-converting enzyme (TACE/ADAM17) activation, translocation, and TNF receptor 1 (TNFR1) shedding in hepatocytes.', *The Journal of biological chemistry*. American Society for Biochemistry and Molecular Biology, 287(43), pp. 35887–98. doi: 10.1074/jbc.M112.365171.

Cho, C. *et al.* (1998) 'Fertilization Defects in Sperm from Mice Lacking Fertilin;';, *Science*, 281(5384), pp. 1857–1859. doi: 10.1126/science.281.5384.1857.

Christianson, J. C. *et al.* (2011) 'Defining human ERAD networks through an integrative mapping strategy.', *Nature cell biology*. NIH Public Access, 14(1), pp. 93–105. doi: 10.1038/ncb2383.

Christova, Y. *et al.* (2013) 'Mammalian iRhoms have distinct physiological functions including an essential role in TACE regulation.', *EMBO reports*. European Molecular Biology Organization, 14(10), pp. 884–90. doi: 10.1038/embor.2013.128.

Citri, A. and Yarden, Y. (2006) 'EGF–ERBB signalling: towards the systems level', *Nature Reviews Molecular Cell Biology*, 7(7), pp. 505–516. doi: 10.1038/nrm1962.

Daub, H. *et al.* (1996) 'Role of transactivation of the EGF receptor in signalling by G-protein-coupled receptors.', *Nature*, 379(6565), pp. 557–60. doi: 10.1038/379557a0.

Dong, J. *et al.* (1999) 'Metalloprotease-mediated ligand release regulates autocrine signaling through the epidermal growth factor receptor.', *Proceedings of the National Academy of Sciences of the United States of America*, 96(11), pp. 6235–40. doi: 10.1073/pnas.96.11.6235.

Duffy, M. J. *et al.* (2009) 'Role of ADAMs in cancer formation and progression.', *Clinical cancer research : an official journal of the American Association for Cancer Research*, 15(4), pp. 1140–4. doi: 10.1158/1078-0432.CCR-08-1585.

Dulloo, I., Muliyil, S. and Freeman, M. (2019) 'The molecular, cellular and pathophysiological roles of iRhom pseudoproteases.', *Open biology*. The Royal Society, 9(3), p. 190003. doi: 10.1098/rsob.190003.

Düsterhoft, S. *et al.* (2013) 'Membrane-proximal domain of a disintegrin and metalloprotease-17 represents the putative molecular switch of its shedding activity operated by protein-disulfide isomerase.', *J.Am.Chem.Soc.*, 135, pp. 5776–5781. doi: 10.2210/PDB2M2F/PDB.

Düsterhöft, S. *et al.* (2014) 'A disintegrin and metalloprotease 17 dynamic interaction sequence, the sweet tooth for the human interleukin 6 receptor.', *The Journal of biological chemistry*, 289(23), pp. 16336–48. doi: 10.1074/jbc.M114.557322.

Düsterhöft, S. *et al.* (2015) 'Extracellular Juxtamembrane Segment of ADAM17 Interacts with Membranes and Is Essential for Its Shedding Activity', *Biochemistry*, 54(38), pp. 5791–5801. doi: 10.1021/acs.biochem.5b00497.

Düsterhöft, S. *et al.* (2019) 'Status update on iRhom and ADAM17: It's still complicated.', *Biochimica et biophysica acta. Molecular cell research*. doi: 10.1016/j.bbamcr.2019.06.017.

Dutt, A. *et al.* (2004) 'EGF signal propagation during C. elegans vulval development mediated by ROM-1 rhomboid.', *PLoS biology*. Edited by Julie Ahringer, 2(11), p. e334. doi: 10.1371/journal.pbio.0020334.

Edwards, D. R., Handsley, M. M. and Pennington, C. J. (2008) 'The ADAM metalloproteinases.', *Molecular aspects of medicine*, 29(5), pp. 258–89. doi: 10.1016/j.mam.2008.08.001.

Ellis, A. *et al.* (1994) 'Tylosis associated with carcinoma of the oesophagus and oral leukoplakia in a large Liverpool family—A review of six generations', *European Journal of Cancer Part B: Oral Oncology*. Pergamon, 30(2), pp. 102–112. doi: 10.1016/0964-1955(94)90061-2.

Ellis, A. *et al.* (2015) 'Tylosis with oesophageal cancer: Diagnosis, management and molecular mechanisms.', *Orphanet journal of rare diseases*. BioMed Central, 10, p. 126. doi: 10.1186/s13023-015-0346-2.

Ferguson, K. M. *et al.* (2003) 'EGF Activates Its Receptor by Removing Interactions that Autoinhibit Ectodomain Dimerization', *Molecular Cell*. Elsevier, 11(2), pp. 507–517. doi: 10.1016/S1097-2765(03)00047-9.

Fischer, O. M. *et al.* (2003) 'EGFR signal transactivation in cancer cells', *Biochemical Society Transactions*, 31(6), pp. 1203–1208. doi: 10.1042/bst0311203.

Fleig, L. *et al.* (2012) 'Ubiquitin-Dependent Intramembrane Rhomboid Protease Promotes ERAD of Membrane Proteins', *Molecular Cell*, 47(4), pp. 558–569. doi: 10.1016/j.molcel.2012.06.008.

Fonseca, D. and Carvalho, P. (2019) 'EGAD ! There is an ERAD doppelganger in the Golgi', *The EMBO Journal*, p. e102679. doi: 10.15252/embj.2019102679.

Freeman, M. (1996) 'Reiterative use of the EGF receptor triggers differentiation of all cell types in the Drosophila eye.', *Cell*. Elsevier, 87(4), pp. 651–60. doi: 10.1016/s0092-8674(00)81385-9.

Le Gall, S. M. *et al.* (2010) 'ADAM17 is regulated by a rapid and reversible mechanism that controls access to its catalytic site.', *Journal of cell science*, 123(Pt 22), pp. 3913–22. doi: 10.1242/jcs.069997.

Gooz, M. (2010) 'ADAM-17: the enzyme that does it all', *Critical Reviews in Biochemistry and Molecular Biology*, 45(2), pp. 146–169. doi: 10.3109/10409231003628015.

Gooz, P. *et al.* (2012) 'A disintegrin and metalloenzyme (ADAM) 17 activation is regulated by α5β1 integrin in kidney mesangial cells.', *PloS one*. Edited by E. C. Tsilibary, 7(3), p. e33350. doi: 10.1371/journal.pone.0033350.

Grieve, A. G. *et al.* (2017) 'Phosphorylation of iRhom2 at the plasma membrane controls mammalian TACE-dependent inflammatory and growth factor signalling.', *eLife*. eLife Sciences Publications, Ltd, 6. doi: 10.7554/eLife.23968.

Groth, E. *et al.* (2016) 'Stimulated release and functional activity of surface expressed metalloproteinase ADAM17 in exosomes.', *Biochimica et biophysica acta*, 1863(11), pp. 2795–2808. doi: 10.1016/j.bbamcr.2016.09.002.

Gutiérrez-López, M. D. *et al.* (2011) 'The sheddase activity of ADAM17/TACE is regulated by the tetraspanin CD9', *Cellular and Molecular Life Sciences*, 68(19), pp. 3275–3292. doi: 10.1007/s00018-011-0639-0.

Hampton, R. Y. and Garza, R. M. (2009) 'Protein Quality Control as a Strategy for Cellular Regulation: Lessons from Ubiquitin-Mediated Regulation of the Sterol Pathway', *Chemical Reviews*. American Chemical Society, 109(4), pp. 1561–1574. doi: 10.1021/cr800544v.

Harper, M. T. and Poole, A. W. (2011) 'PKC inhibition markedly enhances Ca^{2+} signaling and phosphatidylserine exposure downstream of protease-activated receptor-1 but not protease-activated receptor-4 in human platelets.', *Journal of thrombosis and haemostasis : JTH*, 9(8), pp. 1599–607. doi: 10.1111/j.1538-7836.2011.04393.x.

Harris, R. C., Chung, E. and Coffey, R. J. (2003) 'EGF receptor ligands', *Experimental Cell Research*. Academic Press, 284(1), pp. 2–13. doi: 10.1016/S0014-4827(02)00105-2.

Hart, S. *et al.* (2005) 'GPCR-induced migration of breast carcinoma cells depends on both EGFR signal transactivation and EGFR-independent pathways.', *Biological chemistry*, 386(9), pp. 845–55. doi: 10.1515/BC.2005.099.

Haxaire, C. *et al.* (2018) 'Blood-induced bone loss in murine hemophilic arthropathy is prevented by blocking the iRhom2/ADAM17/TNF-α pathway', *Blood*. American Society of Hematology, 132(10), pp. 1064–1074. doi: 10.1182/BLOOD-2017-12-820571.

Hayashida, K. *et al.* (2010) 'Molecular and cellular mechanisms of ectodomain shedding.', *Anatomical record (Hoboken, N.J. : 2007)*. NIH Public Access, 293(6), pp. 925–37. doi: 10.1002/ar.20757.

Higginbotham, J. N. *et al.* (2011) 'Amphiregulin exosomes increase cancer cell invasion.', *Current biology : CB*. NIH Public Access, 21(9), pp. 779–86. doi: 10.1016/j.cub.2011.03.043.

Higy, M., Junne, T. and Spiess, M. (2004) 'Topogenesis of Membrane Proteins at the Endoplasmic Reticulum', *Biochemistry*, 43(40), pp. 12716–12722. doi: 10.1021/bi048368m.

Holmes, W. E. *et al.* (1992) 'Identification of Heregulin, a Specific Activator of p185erbB2', *Science*. American Association for the Advancement of Science, 256(5060), pp. 1205–1210. doi: 10.1126/SCIENCE.256.5060.1205.

Horiuchi, K., Miyamoto, T., *et al.* (2007) 'Cell Surface Colony-Stimulating Factor 1 Can Be Cleaved by TNFα Converting Enzyme or Endocytosed in a Clathrin-Dependent Manner', *The Journal of Immunology*, 179(10), pp. 6715–6724. doi: 10.4049/jimmunol.179.10.6715.

Horiuchi, K., Kimura, T., *et al.* (2007) 'Cutting edge: TNF-alpha-converting enzyme (TACE/ADAM17) inactivation in mouse myeloid cells prevents lethality from endotoxin shock.', *Journal of immunology (Baltimore, Md. : 1950)*, 179(5), pp. 2686–9. doi: 10.4049/jimmunol.179.5.2686.

Hosur, V. *et al.* (2014) 'Rhbdf2 mutations increase its protein stability and drive EGFR hyperactivation through enhanced secretion of amphiregulin.', *Proceedings of the National Academy of Sciences of the United States of America*, 111(21), pp. E2200-9. doi: 10.1073/pnas.1323908111.

Hou, F. *et al.* (2011) 'MAVS forms functional prion-like aggregates to activate and propagate antiviral innate immune response.', *Cell*. Elsevier, 146(3), pp. 448–61. doi: 10.1016/j.cell.2011.06.041.

Huang, J., Bridges, L. C. and White, J. M. (2005) 'Selective modulation of integrin-mediated cell migration by distinct ADAM family members.', *Molecular biology of the cell*, 16(10), pp. 4982–91. doi: 10.1091/mbc.e05-03-0258.

Huxley-Jones, J. *et al.* (2007) 'The evolution of the vertebrate metzincins; insights from *Ciona intestinalis* and *Danio rerio*.', *BMC evolutionary biology*. BioMed Central, 7, p. 63. doi: 10.1186/1471-2148-7-63.

Ingram, R. N. *et al.* (2006) 'Stabilization of the autoproteolysis of TNF-alpha converting enzyme (TACE) results in a novel crystal form suitable for structure-based drug design studies.', *Protein Eng.Des.Sel.*, 19, pp. 155–161. doi: 10.2210/PDB2DDF/PDB.

Ishimoto, T. *et al.* (2017) 'Activation of Transforming Growth Factor Beta 1 Signaling in Gastric Cancer-associated Fibroblasts Increases Their Motility, via Expression of Rhomboid 5 Homolog 2, and Ability to Induce Invasiveness of Gastric Cancer Cells.', *Gastroenterology*. Elsevier, 153(1), pp. 191-204.e16. doi: 10.1053/j.gastro.2017.03.046.

Issuree, P. D. A. *et al.* (2013) 'iRHOM2 is a critical pathogenic mediator of inflammatory arthritis.', *The Journal of clinical investigation*. American Society for Clinical Investigation, 123(2), pp. 928–32. doi: 10.1172/JCI66168.

Itzhak, D. N. *et al.* (2016) 'Global, quantitative and dynamic mapping of protein subcellular localization.', *eLife*. eLife Sciences Publications, Ltd, 5. doi: 10.7554/eLife.16950.

De Jager, P. L. *et al.* (2014) 'Alzheimer's disease: early alterations in brain DNA methylation at ANK1, BIN1, RHBDF2 and other loci', *Nature Neuroscience*. Nature Publishing Group, 17(9), pp. 1156–1163. doi: 10.1038/nn.3786.

Janes, P. W. *et al.* (2005) 'Adam meets Eph: an ADAM substrate recognition module acts as a molecular switch for ephrin cleavage in trans.', *Cell*, 123(2), pp. 291–304. doi: 10.1016/j.cell.2005.08.014.

Jiang, H.-S. and Wu, Y.-C. (2014) 'LIN-3/EGF promotes the programmed cell death of specific cells in Caenorhabditis elegans by transcriptional activation of the pro-apoptotic gene egl-1.', *PLoS genetics*. Edited by A. Gartner, 10(8), p. e1004513. doi: 10.1371/journal.pgen.1004513.

Johnson, K. R. *et al.* (2003) 'Curly bare (cub), a new mouse mutation on chromosome 11 causing skin and hair abnormalities, and a modifier gene (mcub) on chromosome 5', *Genomics*. Academic Press, 81(1), pp. 6–14. doi: 10.1016/S0888-7543(02)00013-7.

Johnson, N. *et al.* (2017) 'Quantitative proteomics screen identifies a substrate repertoire of rhomboid protease RHBDL2 in human cells and implicates it in epithelial homeostasis.', *Scientific reports*, 7(1), p. 7283. doi: 10.1038/s41598-017-07556-3.

de Jong, K. *et al.* (2002) 'Protein Kinase C Activation Induces Phosphatidylserine Exposure on Red Blood Cells', *Biochemistry*, 41(41), pp. 12562–12567. doi: 10.1021/bi025882o.

Kawaguchi, M., Mitsuhashi, Y. and Kondo, S. (2005) 'Overexpression of tumour necrosis factor-alpha-converting enzyme in psoriasis.', *The British journal of dermatology*, 152(5), pp. 915–9. doi: 10.1111/j.1365-2133.2005.06440.x.

Kini, R. M. and Evans, H. J. (1992) 'Structural domains in venom proteins: evidence that metalloproteinases and nonenzymatic platelet aggregation cc (disintegrins) from snake venoms are derived by proteolysis from a common precursor.', *Toxicon : official journal of the International Society on Toxinology*, 30(3), pp. 265–93. Available at: http://www.ncbi.nlm.nih.gov/pubmed/1529462

Koonin, E. V *et al.* (2003) 'The rhomboids: a nearly ubiquitous family of intramembrane serine proteases that probably evolved by multiple ancient horizontal gene transfers.', *Genome biology*, 4(3), p. R19. doi: 10.1186/gb-2003-4-3-r19.

Künzel, U. *et al.* (2018) 'FRMD8 promotes inflammatory and growth factor signalling by stabilising the iRhom/ADAM17 sheddase complex.', *eLife*. eLife Sciences Publications, Ltd, 7. doi: 10.7554/eLife.35012.

Lee, J. R. *et al.* (2001) 'Regulated intracellular ligand transport and proteolysis control EGF signal activation in Drosophila.', *Cell*, 107(2), pp. 161–71. doi: 10.1016/s0092-8674(01)00526-8.

Lee, W. *et al.* (2015) 'iRhom1 regulates proteasome activity via PAC1/2 under ER stress.', *Scientific reports*. Nature Publishing Group, 5, p. 11559. doi: 10.1038/srep11559.

Lemberg, M. K. and Freeman, M. (2007) 'Functional and evolutionary implications of enhanced genomic analysis of rhomboid intramembrane proteases.', *Genome research*. Cold Spring Harbor Laboratory Press, 17(11), pp. 1634–46. doi: 10.1101/gr.6425307.

Lemmens, K., Doggen, K. and De Keulenaer, G. W. (2007) 'Role of Neuregulin-1/ErbB Signaling in Cardiovascular Physiology and Disease', *Circulation*, 116(8), pp. 954–960. doi: 10.1161/CIRCULATIONAHA.107.690487.

Leonard, J. D., Lin, F. and Milla, M. E. (2005) ‘Chaperone-like properties of the prodomain of TNFalpha-converting enzyme (TACE) and the functional role of its cysteine switch.’, *The Biochemical journal*, 387(Pt 3), pp. 797–805. doi: 10.1042/BJ20041727.

Li, X. *et al.* (2009) ‘The regulation of TACE catalytic function by its prodomain.’, *Molecular biology reports*, 36(4), pp. 641–51. doi: 10.1007/s11033-008-9224-5.

Li, X. *et al.* (2015) ‘iRhoms 1 and 2 are essential upstream regulators of ADAM17-dependent EGFR signaling.’, *Proceedings of the National Academy of Sciences of the United States of America*. National Academy of Sciences, 112(19), pp. 6080–5. doi: 10.1073/pnas.1505649112.

Li, X. *et al.* (2017) ‘Structural modeling defines transmembrane residues in ADAM17 that are crucial for Rhbdf2-ADAM17-dependent proteolysis.’, *Journal of cell science*. Company of Biologists, 130(5), pp. 868–878. doi: 10.1242/jcs.196436.

Li, Z., Liu, S. and Cai, Y. (2015) ‘EGFR/MAPK signaling regulates the proliferation of Drosophila renal and nephric stem cells.’, *Journal of genetics and genomics = Yi chuan xue bao*, 42(1), pp. 9–20. doi: 10.1016/j.jgg.2014.11.007.

Liu, C. *et al.* (2009) ‘TACE-Mediated Ectodomain Shedding of the Type I TGF-β Receptor Downregulates TGF-β Signaling’, *Molecular Cell*, 35(1), pp. 26–36. doi: 10.1016/j.molcel.2009.06.018.

Lorenzen, I. *et al.* (2016) ‘Control of ADAM17 activity by regulation of its cellular localisation’, *Scientific Reports*, 6(1), p. 35067. doi: 10.1038/srep35067.

Lu, X.-L. *et al.* (2017) ‘iRhom2 is involved in lipopolysaccharide-induced cardiac injury in vivo and in vitro through regulating inflammation response’, *Biomedicine & Pharmacotherapy*. Elsevier Masson, 86, pp. 645–653. doi: 10.1016/J.BIOPHA.2016.11.075.

Luo, W.-W. *et al.* (2016) ‘iRhom2 is essential for innate immunity to DNA viruses by mediating trafficking and stability of the adaptor STING’, *Nature Immunology*. Nature Publishing Group, 17(9), pp. 1057–1066. doi: 10.1038/ni.3510.

Luo, W.-W. *et al.* (2017) ‘iRhom2 is essential for innate immunity to RNA virus by antagonizing ER- and mitochondria-associated degradation of VISA.’, *PLoS pathogens*. Public Library of Science, 13(11), p. e1006693. doi: 10.1371/journal.ppat.1006693.

Maney, S. K. *et al.* (2015) ‘Deletions in the cytoplasmic domain of iRhom1 and iRhom2 promote shedding of the TNF receptor by the protease ADAM17’, *Science Signaling*. American Association for the Advancement of Science, 8(401), pp. ra109–ra109. doi: 10.1126/SCISIGNAL.AAC5356.

Maretzky, T. *et al.* (2011) ‘Migration of growth factor-stimulated epithelial and endothelial cells depends on EGFR transactivation by ADAM17.’, *Nature communications*, 2(1), p. 229. doi: 10.1038/ncomms1232.

Maretzky, T. *et al.* (2013) ‘iRhom2 controls the substrate selectivity of stimulated ADAM17-dependent

ectodomain shedding.', *Proceedings of the National Academy of Sciences of the United States of America*. National Academy of Sciences, 110(28), pp. 11433–8. doi: 10.1073/pnas.1302553110.

Margolis, B. L. *et al.* (1989) 'All autophosphorylation sites of epidermal growth factor (EGF) receptor and HER2/neu are located in their carboxyl-terminal tails. Identification of a novel site in EGF receptor.', *The Journal of biological chemistry*, 264(18), pp. 10667–71. Available at: http://www.ncbi.nlm.nih.gov/pubmed/2543678

Matsukawa, S. *et al.* (2012) 'KDEL tagging: a method for generating dominant-negative inhibitors of the secretion of TGF-beta superfamily proteins.', *The International journal of developmental biology*, 56(5), pp. 351–6. doi: 10.1387/ijdb.123514sm.

Matthews, V. *et al.* (2003) 'Cellular cholesterol depletion triggers shedding of the human interleukin-6 receptor by ADAM10 and ADAM17 (TACE).', *The Journal of biological chemistry*, 278(40), pp. 38829–39. doi: 10.1074/jbc.M210584200.

McIlwain, D. R. *et al.* (2012) 'iRhom2 regulation of TACE controls TNF-mediated protection against Listeria and responses to LPS.', *Science (New York, N.Y.)*. NIH Public Access, 335(6065), pp. 229–32. doi: 10.1126/science.1214448.

Mehnert, M., Sommer, T. and Jarosch, E. (2014) 'Der1 promotes movement of misfolded proteins through the endoplasmic reticulum membrane.', *Nature cell biology*, 16(1), pp. 77–86. doi: 10.1038/ncb2882.

Milla, M. E. *et al.* (1999) 'Specific sequence elements are required for the expression of functional tumor necrosis factor-alpha-converting enzyme (TACE).', *The Journal of biological chemistry*, 274(43), pp. 30563–70. doi: 10.1074/jbc.274.43.30563.

Mishra, R., Hanker, A. B. and Garrett, J. T. (2017) 'Genomic alterations of ERBB receptors in cancer: clinical implications.', *Oncotarget*. Impact Journals, LLC, 8(69), pp. 114371–114392. doi: 10.18632/oncotarget.22825.

Moss, M. L. *et al.* (1997) 'Structural features and biochemical properties of TNF-alpha converting enzyme (TACE).', *Journal of neuroimmunology*, 72(2), pp. 127–9. Available at: http://www.ncbi.nlm.nih.gov/pubmed/9042103

Musiwaro, P. *et al.* (2013) 'Characteristics and requirements of basal autophagy in HEK 293 cells.', *Autophagy*, 9(9), pp. 1407–17. doi: 10.4161/auto.25455.

Nakagawa, T. *et al.* (2005) 'Characterization of a human Rhomboid homolog, p100hRho/RHBDF1, which interacts with TGF-α family ligands', *Developmental Dynamics*, 233(4), pp. 1315–1331. doi: 10.1002/dvdy.20450.

Neal, S. *et al.* (2018) 'The Dfm1 Derlin Is Required for ERAD Retrotranslocation of Integral Membrane Proteins', *Molecular Cell*, 69(2), pp. 306-320.e4. doi: 10.1016/j.molcel.2017.12.012.

Oda, K. *et al.* (2005) 'A comprehensive pathway map of epidermal growth factor receptor signaling.', *Molecular systems biology*. European Molecular Biology Organization, 1, p. 2005.0010. doi: 10.1038/msb4100014.

Oda, Y. *et al.* (2006) 'Derlin-2 and Derlin-3 are regulated by the mammalian unfolded protein response and are required for ER-associated degradation.', *The Journal of cell biology*. The Rockefeller University Press, 172(3), pp. 383–93. doi: 10.1083/jcb.200507057.

Ogiso, H. *et al.* (2002) 'Crystal structure of the complex of human epidermal growth factor and receptor extracellular domains.', *Cell*. Elsevier, 110(6), pp. 775–87. doi: 10.1016/s0092-8674(02)00963-7.

Ohtsu, H., Dempsey, P. J. and Eguchi, S. (2006) 'ADAMs as mediators of EGF receptor transactivation by G protein-coupled receptors.', *American journal of physiology. Cell physiology*, 291(1), pp. C1-10. doi: 10.1152/ajpcell.00620.2005.

Oikonomidi, I. *et al.* (2018) 'iTAP, a novel iRhom interactor, controls TNF secretion by policing the stability of iRhom/TACE.', *eLife*, 7. doi: 10.7554/eLife.35032.

Papadakis, K. A. and Targan, S. R. (2000) 'Role of cytokines in the pathogenesis of inflammatory bowel disease.', *Annual review of medicine*, 51(1), pp. 289–98. doi: 10.1146/annurev.med.51.1.289.

Peschon, J. J. *et al.* (1998) 'An Essential Role for Ectodomain Shedding in Mammalian Development', *Science*, 282(5392), pp. 1281–1284. doi: 10.1126/science.282.5392.1281.

Pinkas-Kramarski, R. *et al.* (1996) 'Diversification of Neu differentiation factor and epidermal growth factor signaling by combinatorial receptor interactions.', *The EMBO journal*, 15(10), pp. 2452–67. Available at: http://www.ncbi.nlm.nih.gov/pubmed/8665853

Qing, X. *et al.* (2018) 'iRhom2 promotes lupus nephritis through TNF-α and EGFR signaling.', *The Journal of clinical investigation*. American Society for Clinical Investigation, 128(4), pp. 1397–1412. doi: 10.1172/JCI97650.

Radhakrishnan, S. K., den Besten, W. and Deshaies, R. J. (2014) 'p97-dependent retrotranslocation and proteolytic processing govern formation of active Nrf1 upon proteasome inhibition', *eLife*, 3, p. e01856. doi: 10.7554/eLife.01856.

Richards, W. G. *et al.* (1998) 'Epidermal growth factor receptor activity mediates renal cyst formation in polycystic kidney disease.', *The Journal of clinical investigation*, 101(5), pp. 935–9. doi: 10.1172/JCI2071.

Robertshaw, H. J. and Brennan, F. M. (2005) 'Release of tumour necrosis factor alpha (TNFalpha) by TNFalpha cleaving enzyme (TACE) in response to septic stimuli in vitro.', *British journal of anaesthesia*, 94(2), pp. 222–8. doi: 10.1093/bja/aei021.

Saarinen, S. *et al.* (2012) 'Analysis of a Finnish family confirms RHBDF2 mutations as the underlying factor in tylosis with esophageal cancer', *Familial Cancer*. Springer Netherlands, 11(3), pp. 525–528. doi: 10.1007/s10689-012-9532-8.

Sahin, U. *et al.* (2004) 'Distinct roles for ADAM10 and ADAM17 in ectodomain shedding of six EGFR ligands.', *The Journal of cell biology*, 164(5), pp. 769–79. doi: 10.1083/jcb.200307137.

Sahin, U. and Blobel, C. P. (2007) 'Ectodomain shedding of the EGF-receptor ligand epigen is mediated by ADAM17.', *FEBS letters*, 581(1), pp. 41–4. doi: 10.1016/j.febslet.2006.11.074.

Schlessinger, J. (2000) 'Cell signaling by receptor tyrosine kinases.', *Cell*. Elsevier, 103(2), pp. 211–25. doi: 10.1016/s0092-8674(00)00114-8.

Schlöndorff, J., Becherer, J. D. and Blobel, C. P. (2000) 'Intracellular maturation and localization of the tumour necrosis factor alpha convertase (TACE).', *The Biochemical journal*, 347 Pt 1, pp. 131–8. Available at: http://www.ncbi.nlm.nih.gov/pubmed/10727411

Schmidt, O. *et al.* (2019) 'Endosome and Golgi-associated degradation (EGAD) of membrane proteins regulates sphingolipid metabolism', *The EMBO Journal*. John Wiley & Sons, Ltd, p. e101433. doi: 10.15252/embj.2018101433.

Schulze, W. X., Deng, L. and Mann, M. (2005) 'Phosphotyrosine interactome of the ErbB-receptor kinase family.', *Molecular systems biology*, 1(1), p. 2005.0008. doi: 10.1038/msb4100012.

Seegar, T. C. M. *et al.* (2017) 'Structural Basis for Regulated Proteolysis by the alpha-Secretase ADAM10.', *Cell*, 171, pp. 1638-1648.e7. doi: 10.2210/PDB6BE6/PDB.

Seifert, T. *et al.* (2002) 'TACE mRNA expression in peripheral mononudear cells precedes new lesions on MRI in multiple sclerosis.', *Multiple sclerosis (Houndmills, Basingstoke, England)*, 8(6), pp. 447–51. doi: 10.1191/1352458502ms830oa.

Siggs, O. M. *et al.* (2012) 'iRhom2 is required for the secretion of mouse TNFα', *Blood*. The American Society of Hematology, 119(24), p. 5769. doi: 10.1182/BLOOD-2012-03-417949.

Siggs, O. M. *et al.* (2014) 'Genetic interaction implicates iRhom2 in the regulation of EGF receptor signalling in mice.', *Biology open*. The Company of Biologists Ltd, 3(12), pp. 1151–7. doi: 10.1242/bio.201410116.

Silberberg, G. *et al.* (2006) 'The involvement ofErbB4 with schizophrenia: Association and expression studies', *American Journal of Medical Genetics Part B: Neuropsychiatric Genetics*, 141B(2), pp. 142–148. doi: 10.1002/ajmg.b.30275.

Singh, B. and Coffey, R. J. (2014) 'Trafficking of epidermal growth factor receptor ligands in polarized epithelial cells.', *Annual review of physiology*. NIH Public Access, 76, pp. 275–300. doi: 10.1146/annurev-physiol-021113-170406.

Stevens, H. P. *et al.* (1996) ‘Linkage of an American Pedigree With Palmoplantar Keratoderma and Malignancy (Palmoplantar Ectodermal Dysplasia Type III) to 17q24’, *Archives of Dermatology*. American Medical Association, 132(6), p. 640. doi: 10.1001/archderm.1996.03890300056010.

Takeda, S. *et al.* (2006) ‘Crystal structures of VAP1 reveal ADAMs’ MDC domain architecture and its unique C-shaped scaffold’, *The EMBO Journal*. John Wiley & Sons, Ltd, 25(11), pp. 2388–2396. doi: 10.1038/sj.emboj.7601131.

Tellier, E. *et al.* (2006) ‘The shedding activity of ADAM17 is sequestered in lipid rafts’, *Experimental Cell Research*, 312(20), pp. 3969–3980. doi: 10.1016/j.yexcr.2006.08.027.

Tichá, A., Collis, B. and Strisovsky, K. (2018) ‘The Rhomboid Superfamily: Structural Mechanisms and Chemical Biology Opportunities’, *Trends in Biochemical Sciences*, 43(9), pp. 726–739. doi: 10.1016/j.tibs.2018.06.009.

Trad, A. *et al.* (2013) ‘The disintegrin domain of ADAM17 antagonises fibroblast-carcinoma cell interactions.’, *International journal of oncology*, 42(5), pp. 1793–800. doi: 10.3892/ijo.2013.1864.

Trávníčková, K. (2017) *Evolution of regulatory mechanisms of EGF receptor activation*. Available at: https://ckis.cuni.cz/F/6X5Q8T7J2I6PFML8CAF7DR9NR684G1SDMTNJGXV72CB9ANI4E6-13223?func=full-set-set&set_number=000197&set_entry=000001&format=999

Tsakadze, N. L. *et al.* (2006) ‘Tumor Necrosis Factor-α-converting Enzyme (TACE/ADAM-17) Mediates the Ectodomain Cleavage of Intercellular Adhesion Molecule-1 (ICAM-1)’, *Journal of Biological Chemistry*, 281(6), pp. 3157–3164. doi: 10.1074/jbc.M510797200.

Tyler, R. E. *et al.* (2012) ‘Unassembled CD147 is an endogenous endoplasmic reticulum-associated degradation substrate.’, *Molecular biology of the cell*, 23(24), pp. 4668–78. doi: 10.1091/mbc.E12-06-0428.

Tzahar, E. *et al.* (1996) ‘A hierarchical network of interreceptor interactions determines signal transduction by Neu differentiation factor/neuregulin and epidermal growth factor.’, *Molecular and cellular biology*, 16(10), pp. 5276–87. doi: 10.1128/mcb.16.10.5276.

Ullrich, A. *et al.* (1984) ‘Human epidermal growth factor receptor cDNA sequence and aberrant expression of the amplified gene in A431 epidermoid carcinoma cells.’, *Nature*, 309(5967), pp. 418–25. doi: 10.1038/309418a0.

Urban, S., Lee, J. R. and Freeman, M. (2001) ‘Drosophila rhomboid-1 defines a family of putative intramembrane serine proteases.’, *Cell*, 107(2), pp. 173–82. doi: 10.1016/s0092-8674(01)00525-6.

Urban, S., Lee, J. R. and Freeman, M. (2002) ‘A family of Rhomboid intramembrane proteases activates all Drosophila membrane-tethered EGF ligands.’, *The EMBO journal*, 21(16), pp. 4277–86. doi: 10.1093/emboj/cdf434.

Varela, A. B. *et al.* (2011) 'Tylosis A with squamous cell carcinoma of the oesophagus in a Spanish family.', *European journal of gastroenterology & hepatology*, 23(3), pp. 286–8. doi: 10.1097/MEG.0b013e328344042d.

Wang, S. *et al.* (2019) 'Recent advances on the roles of epidermal growth factor receptor in psoriasis.', *American journal of translational research*. e-Century Publishing Corporation, 11(2), pp. 520–528. Available at: http://www.ncbi.nlm.nih.gov/pubmed/30899359

Wang, Y., Zhang, Y. and Ha, Y. (2006) 'Crystal structure of a rhomboid family intramembrane protease.', *Nature*, 444(7116), pp. 179–80. doi: 10.1038/nature05255.

Weber, S. and Saftig, P. (2012) 'Ectodomain shedding and ADAMs in development', *Development*, 139(20), pp. 3693–3709. doi: 10.1242/dev.076398.

Wen, C., Metzstein, M. M. and Greenwald, I. (1997) 'SUP-17, a Caenorhabditis elegans ADAM protein related to Drosophila KUZBANIAN, and its role in LIN-12/NOTCH signalling.', *Development (Cambridge, England)*, 124(23), pp. 4759–67. Available at: http://www.ncbi.nlm.nih.gov/pubmed/9428412

Wong, E. *et al.* (2016) 'Harnessing the natural inhibitory domain to control TNFα Converting Enzyme (TACE) activity in vivo.', *Scientific reports*, 6(1), p. 35598. doi: 10.1038/srep35598.

Wunderle, L. *et al.* (2016) 'Rhomboid intramembrane protease RHBDL4 triggers ER-export and non-canonical secretion of membrane-anchored TGFα.', *Scientific reports*. Nature Publishing Group, 6, p. 27342. doi: 10.1038/srep27342.

Xu, P. *et al.* (2012) 'TACE activation by MAPK-mediated regulation of cell surface dimerization and TIMP3 association.', *Science signaling*, 5(222), p. ra34. doi: 10.1126/scisignal.2002689.

Xu, P. and Derynck, R. (2010) 'Direct activation of TACE-mediated ectodomain shedding by p38 MAP kinase regulates EGF receptor-dependent cell proliferation.', *Molecular cell*, 37(4), pp. 551–66. doi: 10.1016/j.molcel.2010.01.034.

Yan, Z. *et al.* (2008) 'Human rhomboid family-1 gene silencing causes apoptosis or autophagy to epithelial cancer cells and inhibits xenograft tumor growth', *Molecular Cancer Therapeutics*. American Association for Cancer Research, 7(6), pp. 1355–1364. doi: 10.1158/1535-7163.MCT-08-0104.

Yang, Leilei *et al.* (2014) 'iRhom2 Mutation Leads to Aberrant Hair Follicle Differentiation in Mice', *PLoS ONE*. Edited by A. T. Slominski. Public Library of Science, 9(12), p. e115114. doi: 10.1371/journal.pone.0115114.

Yarden, Y. and Sliwkowski, M. X. (2001) 'Untangling the ErbB signalling network.', *Nature reviews. Molecular cell biology*, 2(2), pp. 127–37. doi: 10.1038/35052073.

Yuan, H. *et al.* (2018) 'RHBDF1 regulates APC-mediated stimulation of the epithelial-to-mesenchymal transition and proliferation of colorectal cancer cells in part via the Wnt/β-catenin signalling pathway', *Experimental Cell Research*. Academic Press, 368(1), pp. 24–36. doi: 10.1016/J.YEXCR.2018.04.009.

Yuan, R., Primakoff, P. and Myles, D. G. (1997) 'A Role for the Disintegrin Domain of Cyritestin, a Sperm Surface Protein Belonging to the ADAM Family, in Mouse Sperm–Egg Plasma Membrane Adhesion and Fusion', *The Journal of Cell Biology*, 137(1), pp. 105–112. doi: 10.1083/jcb.137.1.105.

Zettl, M. *et al.* (2011) 'Rhomboid family pseudoproteases use the ER quality control machinery to regulate intercellular signaling.', *Cell*. Elsevier, 145(1), pp. 79–91. doi: 10.1016/j.cell.2011.02.047.

Zhang, Y. *et al.* (2018) 'Uev1A-Ubc13 catalyzes K63-linked ubiquitination of RHBDF2 to promote TACE maturation', *Cellular Signalling*. Pergamon, 42, pp. 155–164. doi: 10.1016/J.CELLSIG.2017.10.013.

Zhou, H.-J. *et al.* (2015) 'Discovery of a First-in-Class, Potent, Selective, and Orally Bioavailable Inhibitor of the p97 AAA ATPase (CB-5083)', *Journal of Medicinal Chemistry*, 58(24), pp. 9480–9497. doi: 10.1021/acs.jmedchem.5b01346.

Zou, H. *et al.* (2009) 'Human rhomboid family-1 gene *RHBDF1* participates in GPCR-mediated transactivation of EGFR growth signals in head and neck squamous cancer cells', *The FASEB Journal*. Federation of American Societies for Experimental Biology, 23(2), pp. 425–432. doi: 10.1096/fj.08-112771.

Zunke, F. and Rose-John, S. (2017) 'The shedding protease ADAM17: Physiology and pathophysiology', *Biochimica et Biophysica Acta (BBA) - Molecular Cell Research*, 1864(11), pp. 2059–2070. doi: 10.1016/j.bbamcr.2017.07.001.